JOURNAL OF APPLIED PHYSICS

JULY
1940
Vol. 11 No. 7

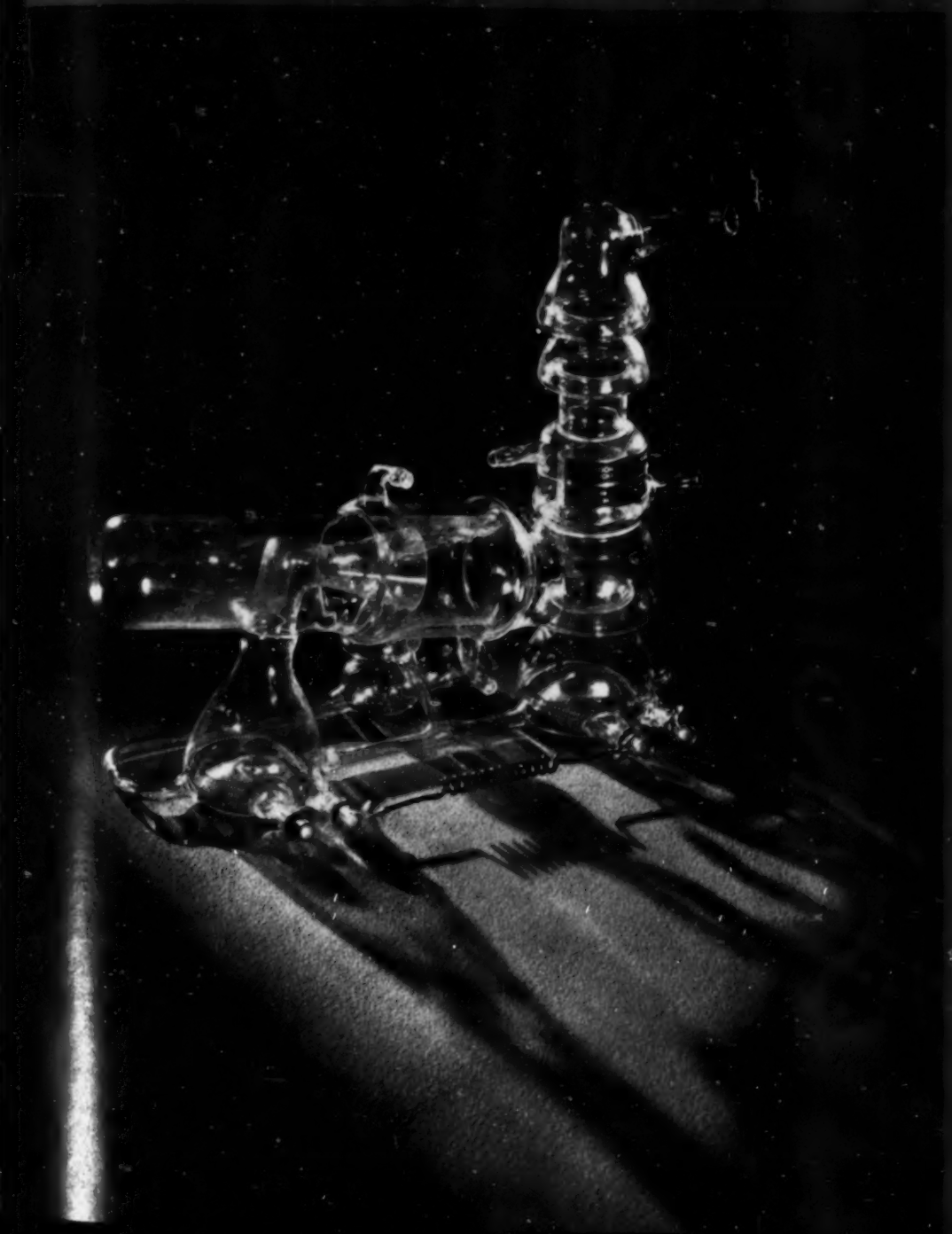

Modern Type
of
Oil Diffusion Pump

Brattleboro Printing, Inc.

JOURNAL OF APPLIED
PHYSICS

JULY, 1940 Vol. 11, No. 7

In This Issue

Page

National Defense and the Physicist 451

Spectrochemical Analysis of Sheet Steel at the Great Lakes Steel Company R. A. Sawyer and H. B. Vincent 452

Mechanism of Spark Discharge in Air at Atmospheric Pressure. II Leonard B. Loeb and J. M. Meek 459

Resumés of Recent Research 475

Contributed Original Research

Correlation Method for the Elimination of Errors Due to Unstable Excitation Conditions in Quantitative Spectrum Analysis Saul Levy 480

Growth Conditions for Single and Optically Mosaic Crystals of Zinc C. A. Cinnamon and Albert B. Martin 487

Experimental Study of Heat Interchange R. B. Jacobs and S. C. Collins 491

Flow of a Gas Through Porous Media J. L. Fowler and K. L. Hertel 496

Electronic Generation of Electromagnetic Oscillations E. U. Condon 502

Letters to the Editor

Backfiring in Mercury Arc Rectifiers John E. White 507

In Every Issue

Here and There 477

Contributors to This Issue 479

Innovations in Instruments 508

Index to Advertisers vi

BOARD OF EDITORS

Elmer Hutchisson,
Editor

Associate Editors

F. Bitter
W. E. Forsythe
L. A. Jones
B. E. Warren
J. B. Whitehead

Publication
of the
American Institute of Physics

ADMINISTRATIVE STAFF

Henry A. Barton,
Director

Madeline M. Mitchell,
Publications Manager

John T. Tate,
Adviser on Publications

GOVERNING BOARD

Paul E. Klopsteg,
Chairman
George B. Pegram,
Secretary
Karl T. Compton
Wheeler P. Davey
Floyd A. Firestone
Harvey Fletcher
R. C. Gibbs
Arthur C. Hardy
George R. Harrison
A. Stuart Hunter
H. R. Lillie
Frederic Palmer, Jr.
George B. Pegram
W. B. Rayton
John T. Tate
Wallace Waterfall

The Journal of Applied Physics, published monthly at Prince and Lemon Sts., Lancaster, Pa., is devoted to physics in its role as the science basic to other natural sciences and to the arts and industries. Previous to 1937 this publication was known as Physics. It aims to be of service not only in physical laboratories, but also in the laboratories of industrial, chemical, geological, geophysical, meteorological, radio, and similar concerns. The Journal of Applied Physics publishes editorials, news of physicists and reviews, as well as technical papers of applied physics.

Manuscripts should be submitted to Elmer Hutchisson, Editor, University of Pittsburgh, Pittsburgh, Pennsylvania.

SUBSCRIPTION PRICE

	U. S., POSS. AND CANADA	FOREIGN
To members of scientific societies	$5.00	$5.70
To all others	7.00	7.70

Single copies are $.70 each.

Changes of address and proofs should be addressed to the Publications Manager.

Subscriptions and orders for back numbers should be addressed to Prince and Lemon Streets, Lancaster, Pa. or to the American Institute of Physics, 175 Fifth Avenue, New York, N. Y.

Advertising rates supplied on request. Orders, advertising copy and cuts should be sent to the American Institute of Physics.

Entered as second class matter at the Post Office at Lancaster, Pennsylvania, under the Act of March 3, 1897.
Accepted for mailing at the special rate of postage provided for in the Act of February 28, 1925, authorized May 2, 1932.

Copyright 1940, by the American Institute of Physics.

L&N Optical Pyrometer Measures Temperature Of Small Objects

Accurate temperature measurements of very small objects are at last possible. Leeds & Northrup's newly redesigned Optical Pyrometer can quickly be adapted to measure temperatures of objects down to 0.01" in diameter and smaller.

In several laboratories, this instrument is unearthing facts about lamps and their manufacture that have never before been available. The relation between filament temperature and lamp life, filament deterioration, light output and other characteristics are studied.

Not only more versatile, the new Optical is faster, easier to operate and more accurate. It

Lamp filament temperature is accurately determined in this laboratory with a new L&N Optical Pyrometer.

weighs a third less than the earlier instrument. The calibration chart is eliminated, as is much of the work involved in measuring temperatures, because the new Optical can be balanced more quickly. See Catalog N-33-D.

Surface resistance of Okolite-Okoprene cable being measured between two metal-foil electrodes, 6 inches apart. Tests with this L&N Insulation Resistance Test Set conform to "ASTM D-257 Standard Methods of Test for Insulation Resistance of Electrical Insulating Materials."

Cable Mfr. Uses ASTM Method

Okonite Measures Insulation Resistance With Leeds & Northrup Test Set

A major advantage of Okonite's Okoprene-sheathed cables is brought out with the help of L&N's accurate Insulation Resistance Test Set. Tests on dry Okoprene-sheathed cables show 805,000 megohms surface resistance per inch, per inch of circumference. *Surface resistance is still up to 604,000 megohms after 24 hours immersion in water.*

Besides this demonstration and routine tests on production samples, the instrument is also used for research into the properties of various rubber compounds, varnished cambric, vinyl resins and the like. Measurements up to 3,000,000 megohms are made at 500 volts; up to 1,500,000 megohms at 200 volts. Specific Insulation Resistances up to 200,000 megohms are measured.

High accuracy is easily maintained with this equipment. A guard circuit eliminates the effects of leakage currents. Humidity has no effect except on the dielectric under observation. Both the instrument and this installation are designed for quick and easy determinations. Write for details.

LEEDS & NORTHRUP COMPANY, 4978 STENTON AVE., PHILA., PA.

LEEDS & NORTHRUP

Measuring Instruments · Telemeters · Automatic Controls · Heat Treating Furnaces

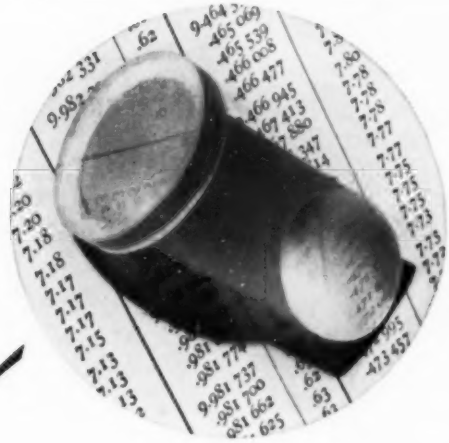

Not for sale

This prism is a *reject*, although the user of the refractometer for which it was designed probably could not detect a single fault in its performance. But, merely "good enough" falls below Bausch & Lomb standards.

These standards, based upon rigid inspection, give no quarter to inaccuracy. This is one of many reasons why you can place your trust in the uniform high quality of B&L instruments.

For your next instrument select one that bears the B&L trade-mark. Write concerning your optical instrument problems, to Bausch & Lomb Optical Company, 670 St. Paul Street, Rochester, N. Y.

BAUSCH & LOMB OPTICAL COMPANY

FOR YOUR EYES, INSIST ON BAUSCH & LOMB EYEWEAR, MADE FROM BAUSCH & LOMB GLASS TO BAUSCH & LOMB HIGH STANDARDS OF PRECISION

Journal of Applied Physics

Volume 11 July, 1940 Number 7

National Defense and the Physicist

HOW can the physicist help in the program for national defense? This question has been raised recently not only by those in charge of national defense but also by the physicist himself. Experience in the early days of our entry into the first world war emphasizes that the effective use of a scientist's services depends upon good organization. Until such organization has been effected, the physicist must, of course, continue with his everyday job. In 1916 the National Research Council was established to assist the Government in organizing the scientific resources of the country. This organization proved so useful that it was continued by executive order of the President even in peace time.

Realizing the urgent need at the present time for additional organization of the physicist's services, the American Institute of Physics has already appointed a committee on national defense to confer with the officers of the National Academy of Sciences and the National Research Council. This committee is also keeping in close touch with President Roosevelt's "National Defense Research Committee" headed by Dr. Vannevar Bush. This new committee has an outstanding personnel. The eight other members are Lyman J. Briggs, Director of the National Bureau of Standards; Conway P. Coe, Commissioner of Patents; Karl T. Compton, President of Massachusetts Institute of Technology; J. B. Conant, President of Harvard University; F. B. Jewett, President of the National Academy of Sciences; Richard C. Tolman, California Institute of Technology; the Secretary of the Navy; and the Secretary of War. One of the early tasks of this committee will probably be the classification of those who have abilities along special lines useful in a defense program.

A conspicuous need in the general defense program is a greater number of well-trained technical men. The place of the physicist in the training of these technical men is evident. Defense requires men who know the fundamentals of interior and exterior ballistics, the principles involved in the flight of airplanes or in streamlining, the use of sound in range finding or submarine detection, the design of optical instruments, infra-red signaling, principles of camouflage, radio communication, and many other types of applied physics. The organization of courses in these subjects is one job that may be done both by those in universities and those in industry. One of the great advantages of such work is that the benefits are permanent and are just as valuable in peace time as in war time.

For August

Graphical Method for Determination of Lattice Constants, by LOUIS A. CARAPELLA;

Plastic Deformation in Lead Under Compression, by W. JAMES LYONS;

Influence of Initial Stress on Elastic Waves, by M. A. BIOT;

Frequency Controlled Oscillators, by SAMUEL SABAROFF;

Torsional Oscillations of Crankshafts, by M. A. BIOT;

Studies in Lubrication, VIII, by F. MORGAN, M. MUSKAT, AND D. W. REED;

Temperature Measurement with Blocking-Layer Photo-Cells, by B. M. LARSEN AND W. E. SHENK;

Rectilinear Electron Flow in Beams, by J. R. PIERCE;

Breakdown Potentials of Gases, by G. W. FOX AND D. O. MCCOY.

Spectrochemical Analysis of Sheet Steel at the Great Lakes Steel Company

By R. A. Sawyer and H. B. Vincent

*University of Michigan, Ann Arbor, Michigan**

Introduction

In an earlier number of this journal,[1] the authors described a spectrographic laboratory at the plant of the Campbell, Wyant and Cannon Foundry Company of Muskegon, Michigan, for the rapid and accurate analysis of alloy cast iron. In this installation and in one at the River Rouge plant of the Ford Motor Company,[2] more recently described, the alloying materials in the irons handled are present in amounts ranging up to 4 percent; the problem was thus one of determining composition rather than of checking purity. The procedure was designed not for high sensitivity and low concentrations, but for speed and precision in composition ranges somewhat higher than is usual in spectrographic analysis.

More recently a spectrographic installation has been completed, for the Great Lakes Steel Corporation of Ecorse, Michigan, to serve a quite different purpose. This company manufactures, among other products, sheet steel for automobile bodies. The sheet is rolled, usually to 20 gauge thickness, from "rimming steel" billets of low alloy content, such content coming chiefly from the scrap steel, which is added to the melt. In the manufacture of automobile-body parts, such as fenders, hoods, or tops, the sheet steel is drawn cold in huge stamping presses. Particularly for fenders, the draw is very deep, and the demands on the properties of the steel consequently severe. Proper heat treatment and mechanical working of the steel can aid greatly in attaining the desired properties. It is believed, however, that the presence of alloy metals in the steel, even in the amounts found, which are as low as a few hundredths of one percent, may have significant and often harmful effects upon the drawing properties of the steel.

Chemical analyses of iron for such small percentages are time-consuming and attain the required precision only with difficulty. It was, therefore, proposed to undertake these analyses spectrographically. The spectrograph seemed ideally suited for such a task, since the sensitivity of arc sources is much greater than the present requirement, and much greater than can ordinarily be attained chemically.

As pointed out, however, in the earlier article, sensitivity is not the only requirement of a light source for quantitative spectrographic analysis. The source must be consistent in operation, so that, in successive spectra from the same sample, the spectral lines of the various constituents of the electrodes shall have the same relative intensities. The problem of the analysis of body sheet steel resolves itself, fundamentally, into the selection of a light source of the requisite sensitivity and reliability.

The Light Source

Studies of light sources for iron analysis have shown that the small arc on 220 volts, though sensitive, is quite unsatisfactory. Surface oxidation, subsurface boiling of the electrodes, and random wandering of the cathode spot result in erratic fluctuations of electrode and arc temperatures, with consequent variable and differential rates of evaporation and of excitation of different components of the electrodes. The accuracy of iron analyses performed with the d.c. arc is therefore poor, although the sensitivity to small concentrations of foreign metals is high. On the other hand, the spark circuit used in the cast iron analysis gives a source of high accuracy but not of sufficient sensitivity for the present application.

After tests of several light sources, a high voltage alternating-current arc was chosen for the present installation. In this type of arc the secondary of a high voltage transformer is connected to the arc through a large ballast resist-

* The work reported here was done in the Department of Physics on a project sponsored through the Department of Engineering Research.

ance, which controls the current. The current is usually 1 to 3 amperes, with potentials of 1100 to 4500 volts, and the gap is made short enough so that the arc can reignite at each half-cycle.

Observations of the arc with an oscilloscope show a nearly sinusoidal variation of the current, while the voltage (Fig. 1) shows peaks at the break, *D*, and at reignition, *C*, of the arc. The reignition voltage must at least equal the minimum sparking voltage for the given ionized gas and electrode material.[3] Furthermore, it depends on the rate at which ions are lost from the discharge gap and on the duration of the quiescent period of the arc. Each new half-cycle starts with a breakdown, usually to a new point on the electrodes, and probably with some explosive release of electrode material. As the current rises, the initial glow discharge changes to an arc discharge, which persists, at the arc maintaining voltage *A*, until almost the end of the cycle, when, with falling current, the glow reappears at the higher voltage, *D*. The wandering of the cathode spot is controlled in that it is forced to reestablish itself at each half-cycle. The fluctuations of electrode and arc temperatures are much less than in a d.c. arc, and experimental results show that the a.c. arc is much more reliable than the d.c. arc for quantitative spectrochemical analysis.

The high voltage a.c. arc has been applied by Duffendack and Thomson and by others[4, 5] to the analysis of fluids and solutions; they used graphite electrodes on the tips of which a sample had been dried. As adapted to metallic electrodes in the present work the a.c. arc has marked advantages for steel analysis. The sensitivity is high and the consumption of material small, while the low current avoids collapse or dripping of the sheet samples. It is found desirable to mount the two sheet electrodes on edge at right angles to one another. The arc is thus localized at the intersection, and burns between two small spots which are cross sections of the sheet. Since the sheets are rolled down from rimming billets which are not uniform in composition throughout their sections, it is desirable to examine such a cross section of the sheet and to obtain its average composition.

The relative intensities of the spectral lines in the a.c. arc are affected by changes in arc current and in gap length. Optimum values must be

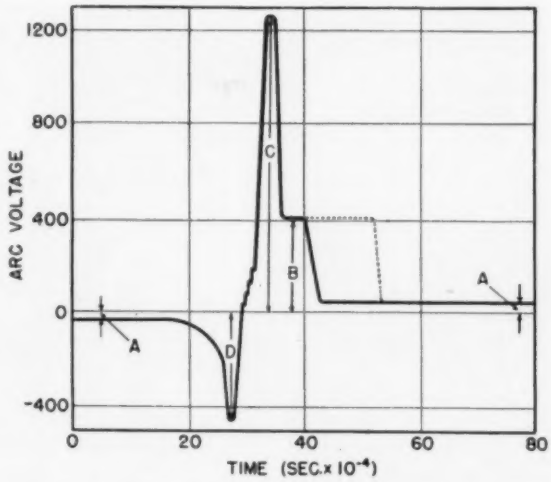

FIG. 1. Variation of voltage with time during one cycle of an a.c. arc. *A*, *A* = arc maintaining voltage, *B* = glow voltage at breakdown, *C* = sparking voltage at reignition, *D* = glow voltage at end of cycle.

determined experimentally and carefully reproduced in each exposure. Furthermore, the current used (1.5 amperes) heats the sheet electrodes sufficiently during an exposure to affect the relative rate of evaporation of the various components of the steel. Control of the sheet temperature by water cooling is essential to accuracy.

Instruments

For the Great Lakes Steel Company installation an arc stand has been developed which allows screw adjustment of the arc gap, and rapid mounting of the samples in water-cooled clamps. Fig. 2 shows two photographs of the stand—in operating position, (a), and with the lower jaw swung open for loading, (b). Wooden end plates connected by three metal rods give a rigid frame. Two of the rods carry the electrode clamps, which are electrically insulated by the wooden end plates. Rubber hose seen in the figure carries the cooling water to the four jaws. For convenience in loading, the lower clamp rotates, as shown in (b), on its supporting sleeve. The rotation is limited at its end of the swing by pin stops. The upper clamp assembly is rigidly fixed in position by set screws.

A sectional drawing of one of the clamps is shown in Fig. 3(a). The jaws are held by the screw, *C*, which is operated by a removable handwheel and are opened by the spring *D*. Two pins, *H*, serve to space the clamps. One of the

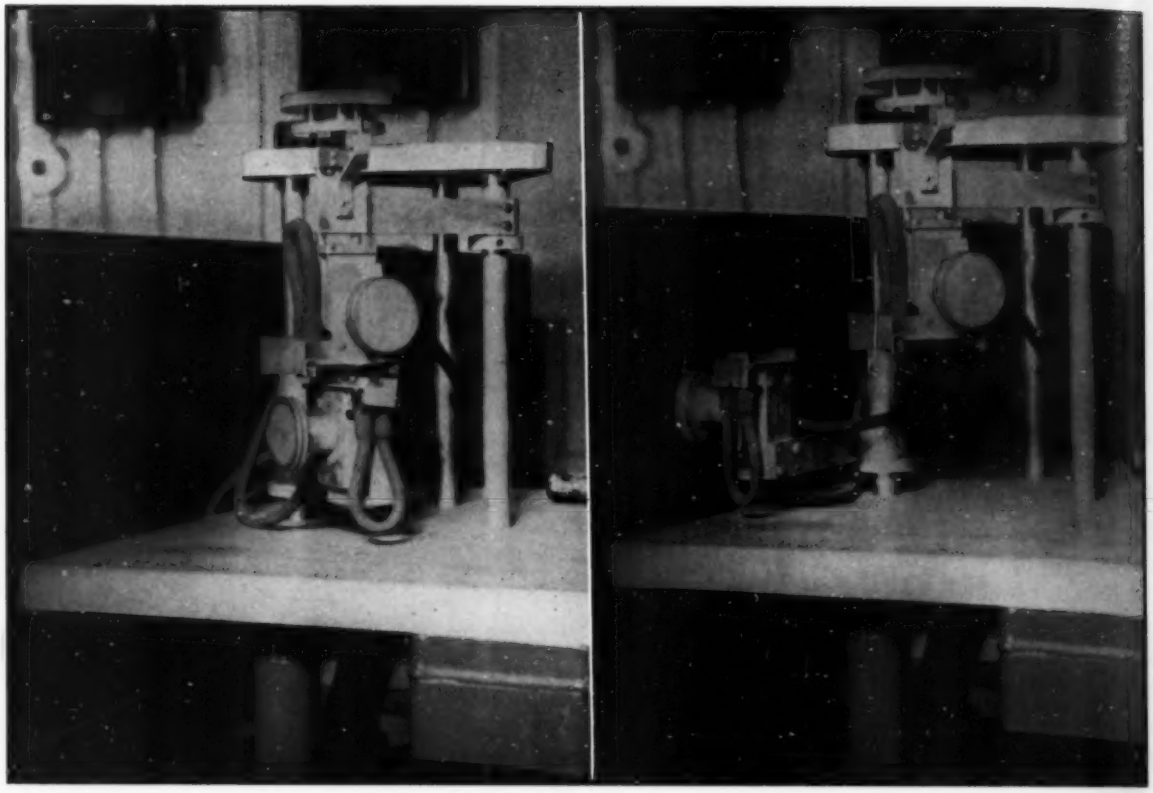

(a) (b)

FIG. 2. Arc stand with water-cooled clamps; (a), in operating position, (b), open for loading.

water-cooled jaws carries at each end a gauge, J, which permits the sheet sample to project $\frac{1}{8}$ inch above the jaw-face. The sample is brought up against these gauges and clamped. Thus regardless of the width of the strip of sheet used, a uniform projection of the sample is assured. This uniform projection together with water-cooling of the jaws and the fixed current, gives the control of the sample temperature which has been found essential to uniform results.

Rapid and accurate setting of the arc gap is accomplished by the micrometer screw and friction clutch shown in Fig. 3(a) and (b). The screw, N, running in the supporting member, K, raises and lowers the bridge, L. The bridge, by friction of the spring, M, carries the two rods, O, which support the upper electrode clamp. A pin in the wheel, P, striking the stop, R, limits the rotation of the screw to that corresponding to the desired electrode gap. When the two clamps are loaded and in position, and the wheel set to lift

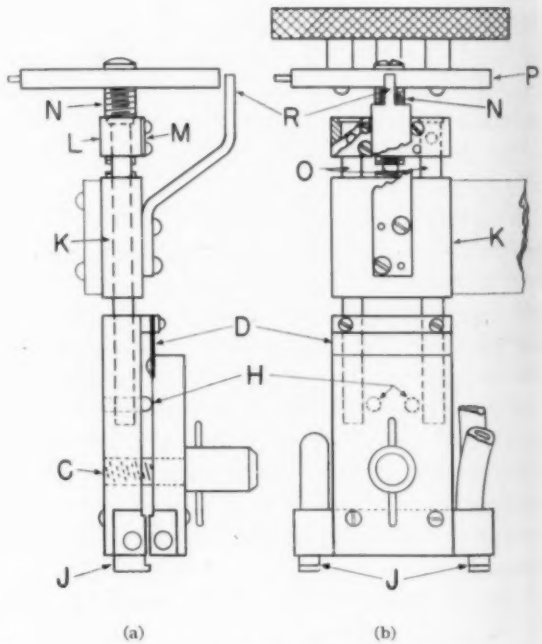

(a) (b)

FIG. 3. Details of clamp assembly.

the clamp to its highest position, the upper clamp is pushed down by hand until the sheets touch. The handwheel is then turned to the other limit of its travel, and back to its former position. As the bridge moves downward, slippage occurs in the friction member; during the upward motion, no slippage occurs, and the electrodes are given a definite separation of $\frac{1}{8}$ inch.

The 4400-volt transformer is connected to the arc through a ballast resistance of about 2800 ohms which fixes the arc current at 1.5 amperes. The resistance is built up of individual units of about 300 ohms, each wound of No. 24 Copel wire on transite cards. The units are mounted on edge in a protecting cage, and the normal air circulation gives adequate cooling.

A general view of the light source is shown in Fig. 4. The ballast resistance is seen behind the arc stand. The arc stand is provided with a protective housing, shown open. This housing must be closed, actuating push switches in the primary circuit, before the transformer current can be turned on.

A Bausch and Lomb quartz spectrograph of the Littrow type is used. The region covered on the plate from 3600A–2800A, contains suitable lines for the analysis of each element handled. The light source is about 25 cm from the slit. It is imaged on the spectrograph optics by a lens placed just in front of the slit. This imaging insures a uniform distribution of light along the spectrum line, since each point of the source contributes light to each point of the slit and of the spectral line image, and, further, each part of the illuminated portion of optics contributes light to each point of the line image.

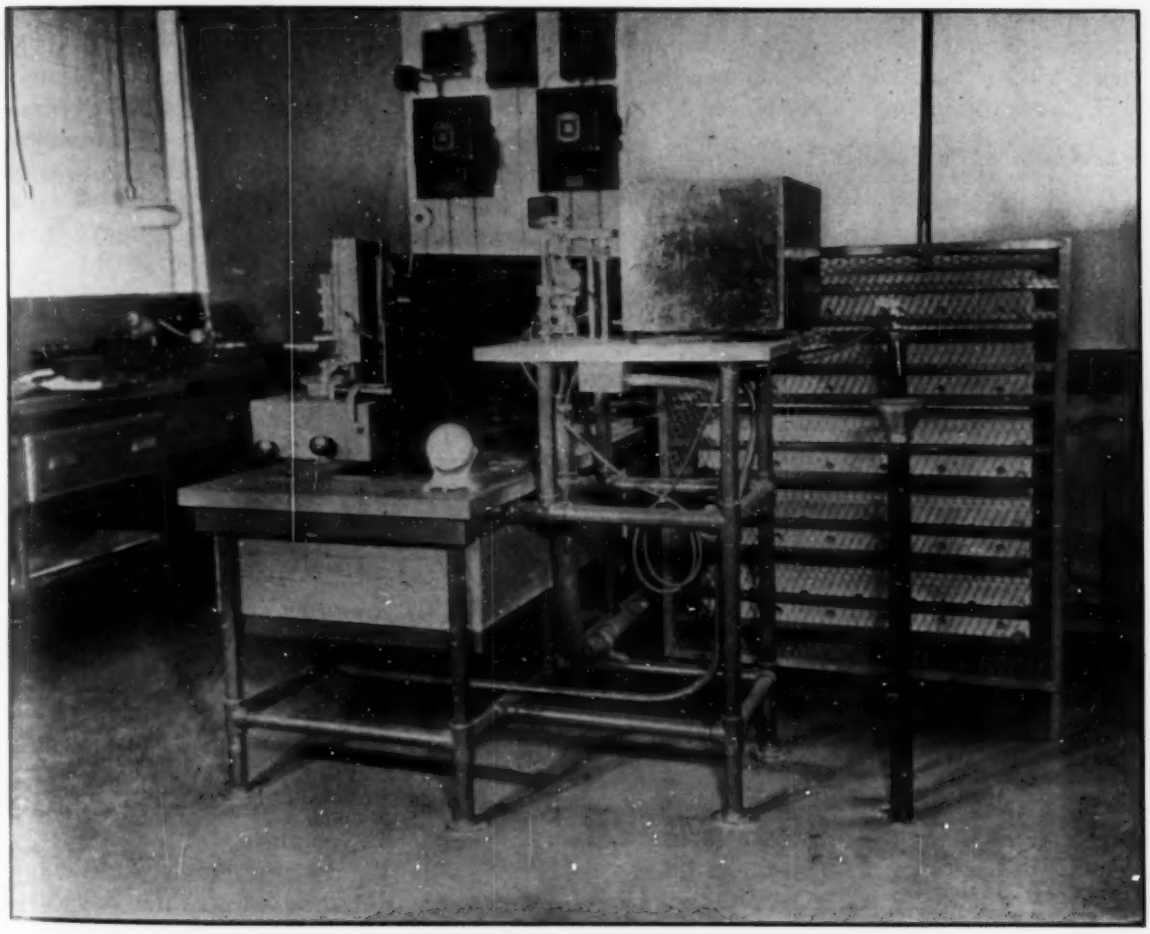

FIG. 4. View of source and spectrograph.

The spectrograph and light source are in the same room, a convenient arrangement for a single operator. If a large volume of work is to be handled by two or more analysts, it is better to place the spectrograph in the dark room with one operator and to place the light source in an adjoining room to be tended by a second operator.[1,2] In the present installation a small adjoining dark room is used. It is equipped with the rocking trays and infra-red dryer described elsewhere[6] for rapid plate processing. A third room contains the microphotometer, a Bausch & Lomb density comparator which has been remodeled as in the previously described installation. In the present work the microphotometer slit is set to cover 25μ of the spectral line width. The spectra taken with a 40μ spectrograph slit are nearly twice this width. Readings are taken by moving the spectral line image slowly across the microphotometer slit and observing the maximum galvanometer reading. Since the galvanometer has a period of 2 seconds a reading on a line may be made readily in 5 or 6 seconds.

Experimental Procedure

Two strips an inch wide by any convenient length, are cut from the sheet steel for analysis, and one strip is mounted in each of the water-cooled clamps. Following a pre-exposure burning of the arc for 30 seconds, the spectrograph shutter is opened and the analysis exposure made. The equipment is at present calibrated for the analysis of chromium, copper, nickel and tin in the ranges of approximately 0.01 percent to 0.10 percent. With the lines of these elements available in the spectrographic region, it is not possible to perform analyses of all four of these elements with one exposure. An exposure of 3 to 5 seconds has been found satisfactory for chromium and copper, twenty seconds for nickel and forty seconds for tin. A spectrographic slit length of 6 mm is used and twelve spectra can be recorded on a plate four inches wide. Thus the spectra for the analysis of all four elements in three samples can be placed on one plate. If a large number of samples were to be handled, time and plates could be saved by making the four exposures on one sample concurrently in one spectrum using three movable diaphragms to cover successively the plate regions of the analytical lines of copper, chromium and nickel, as their exposures were completed, while the tin exposure continued the full forty seconds.

The processing of the photographic plate is carried out in a minimum of time with the help of the dark room accessories mentioned above. Since extreme speed is not required in the work, the most rapid developers are not used. However, processing can be completed in about six minutes. It has been found desirable, even if speed is not essential, to use rocking trays and rapid drying to insure uniform results.

The interpretation of the plates with the help of the microphotometer involves two steps. First, the plate calibration, or relation between plate blackening and exposure, is obtained, as in the cast iron analysis, by reading the galvanometer deflections on the microphotometer for several iron lines whose relative exposures have been determined previously for the equipment used. From these readings, a calibration curve of the plate emulsion is plotted showing the logarithm of the exposure as a function of galvanometer deflection. The relative exposures or intensities of any lines may be determined at once from this curve when their galvanometer deflections are known, since the difference of the logarithms of their exposures is the logarithm of the ratio of their exposures.

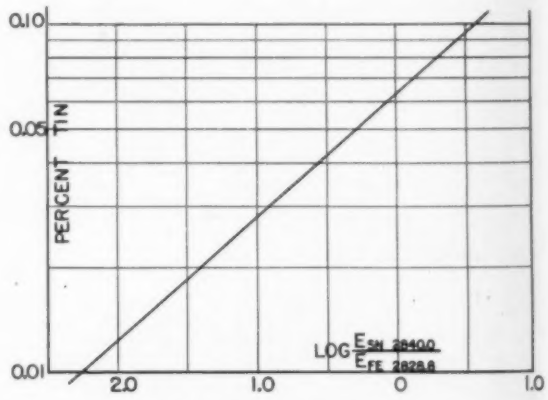

FIG. 5. Analytical curve for tin.

The next step is to determine from the microphotometer readings, by use of the calibration curve the logarithm of the ratio of the relative intensities of a selected line of each element under analysis and of a selected comparison iron line. For each element there has been drawn

previously an analytical curve showing, from measurements on chemically analyzed samples, the variation of this log E ratio with percentage concentration of the element in the sample. Fig. 5 shows such an analytical curve for tin. From this curve the concentration of the element in the sample is read.

The whole process of analysis on a single sample need not consume more than ten or twelve minutes including about two minutes for loading the sample and plate holder, and making the exposure, six minutes for processing the plate, and two or three minutes for the microphotometer readings and transposition to percentage content. Obviously, if several spectra are recorded on a single plate, and two operators are used, the rate at which analyses can be made may be greatly increased.

A major difficulty in the spectrographic analysis of metals at these low concentrations in steel is that of obtaining from chemical analysis satisfactory composition data upon which to base the analytical curves. Since the concentrations in this work are near the limit of sensitivity of the usual wet methods of analysis, it has been found desirable to average the results of several chemical determinations if possible by two or more laboratories. A check on the chemical results is given by the requirement that the analytical curve, plotted from measurements on a series of samples graded by chemical analysis, must be smooth. The curve may thus be better than the individual points, although the question will be left of a possible additive correction factor.

Accuracy and Reliability

In this range of composition an individual spectrographic analysis is more reliable than an individual chemical analysis so that chemical checks of spectrographic results are of little value. Estimates of the reliability of the analyses can be obtained by comparison of repeated measurements on the same sample.

TABLE I.

% Ni	Dev. %	(Dev. %)²	% Cr	Dev. %	(Dev. %)²
0.0315	5.04	25.4	0.0438	2.65	7.0
0.0305	1.70	2.9	0.0489	8.69	75.5
0.0306	2.03	4.1	0.0414	7.98	63.7
0.0291	2.97	8.8	0.0421	6.43	41.4
0.0287	4.30	18.5	0.0465	3.35	11.2
0.0302	0.70	0.5	0.0463	2.91	8.5
0.0295	1.64	2.7	0.0443	1.48	2.2
0.0298	0.64	0.4	0.0460	2.24	5.0
			0.0455	1.13	1.3
Mean 0.02990		Σd^2 63.3	Mean 0.04499		Σd^2 215.8
Standard dev. $=(\Sigma d^2/(n-1))^{\frac{1}{2}}=3.0\%$			Standard dev. $=(\Sigma d^2/(n-1))^{\frac{1}{2}}=5.2\%$		

TABLE II.

Lift	Sample	Cu	Cr	Ni	Sn
693	1	0.071	0.01−	0.025	0.01−
	2	.085	.01−	.018	.011
	3	.082	.01−	.020	.01−
694	1	.086	.013	.022	.014
	2	.085	.01−	.017	.011
	3	.076	.01−	.018	.01−
691	1	.069	.01−	.017	.011
	2	.062	.01−	.017	.011
	3	.077	.01−	.022	.01−
692	1	.073	.01−	.020	.01−
	2	.075	.01−	.023	.01−
	3	.072	.01−	.010	.01−
695	1	.098	.01−	.018	.01−
	2	.10+	.01−	.016	.013
	3	.072	.01−	.018	.010
696	1	.064	.01−	.017	.010
	2	.084	.01−	.018	.011
	3	.059	.010	.018	.012
697	1	.060	.01−	.019	.01−
	2	.062	.01−	.017	.011
	3	.075	.01−	.016	.01−
698	1	.093	.010	.018	.01−
	2	.063	.010	.018	.01−
	3	.063	.010	.023	.01−

Table I gives the results of two typical tests in the University laboratory made to determine how closely determinations on nickel and chromium could be repeated. In each case the individual determinations were made on separate spectra from the same sample recorded on the same photographic plate. The percentage deviation from the mean, and the squared percentage deviation are given; the standard deviation $(\Sigma d^2/(n-1))^{\frac{1}{2}}$ is computed. The standard deviation, sometimes called the mean error of a single observation, should be exceeded in only 31.7 percent of the cases in a series of measurements; and three times this deviation should occur only once in 375 cases. Extensive tests of the equipment and method have shown that at concentrations found in this work standard deviations of from 3 to 6 percent are to be expected. Since the present ranges of analysis are for chromium

0.02–0.10 percent, for copper 0.01–0.04 percent, for nickel 0.01–0.10 percent, and for tin 0.01–0.10 percent, this accuracy represents determination to 0.01 percent or better in concentration.

In the plant laboratory repeated measurements are not ordinarily taken on the same sample. Some data are available of measurements on samples cut from different parts of a strip rolled from the same lift, or part of a billet. Variations between these measurements may be due to the method or to real variations in the sample, or both. The general close agreement is an indication of the uniformity of the product and of the accuracy of the analytical procedure.

Table II shows some typical data from the spectrographic laboratory of the Great Lakes Steel Company. Results from a number of lifts are shown, and for each lift three different samples were tested from widely spaced portions of the resulting strip. The results are given in percent. 0.01-indicates less than 0.01 percent, an amount considered to be of no importance.

It will be seen that the spectrographic method permits determinations of metallic constituents of steel as low as 0.01 percent to be determined to 0.001 percent or 0.002 percent, or with an accuracy of about 10 percent. The sensitivity and accuracy are adequate for the present problem. The speed is much better than that of chemical analysis and the technique is of a simple routine nature.

It is a pleasure to express our appreciation to Mr. L. Selmi and Mr. C. L. Altenburger of the Metallurgical Department of the Great Lakes Steel Company for their assistance and cooperation.

Bibliography

1. R. A. Sawyer and H. B. Vincent, J. App. Phys. **8**, 163 (1937); also Metals and Alloys **9**, 27 (1938).
2. R. A. Sawyer and H. B. Vincent, Metal Progress **36**, 35 (1939).
3. J. Slepian, *Conduction of Electricity in Gases* (Westinghouse Elec. & Mfg. Co., Educational Dept., 1933), p. 115.
4. O. S. Duffendack and K. B. Thomson, Proc. Am. Soc. Test. Mat. **36**, II, 310 (1936).
5. J. S. Owens, Ind. Eng. Chem. **11**, 59 (1939); O. S. Duffendack and R. A. Wolfe, Ind. Eng. Chem. **10**, 161 (1938).
6. H. B. Vincent and R. A. Sawyer, Spectrochimica Acta **1**, 131 (1939).

Calendar of Meetings

July

24–26 American Society of Civil Engineers, Denver, Colorado

August

27–30 American Institute of Electrical Engineers, Los Angeles, California

September

9–13 American Chemical Society, Detroit, Michigan

October

2– 4 Optical Society of America, Rochester, New York
7–11 National Safety Council, Chicago, Illinois
18–19 Society of Rheology, New York, New York
21–26 American Welding Society, Cleveland, Ohio
21–25 American Society for Metals, Cleveland, Ohio
28–30 National Academy of Sciences, Philadelphia, Pennsylvania
28–Nov. 2 Conference on Applied Nuclear Physics, Massachusetts Institute of Technology, Cambridge, Massachusetts

The Mechanism of Spark Discharge in Air at Atmospheric Pressure. II*

BY LEONARD B. LOEB AND J. M. MEEK

Department of Physics, University of California, Berkeley, California

4. *Quantitative Criterion for Streamer Formation.*

WITH this qualitative picture in mind we turn to Meek's application of the quantitative criterion for streamer formation. He pointed out that the condition for streamer advance is that the *tip field of the streamer must be great enough to draw into the tip the photoelectrons created near the tip* so that they are not lost to the anode directly. He assumed for streamer propagation that the tip field X_1 of the positive space charge in the streamer must equal the impressed field X.

It has been shown in Eq. (2) that

$$X_1=4\epsilon\alpha e^{\alpha x}\Big/3\left(\frac{2D}{k}\frac{x}{X}\right)^{\frac{1}{2}},$$

and here we set $X_1=X$ at $x=x_1$ in order that a streamer form at some distance x_1.

The ratio of D/k for electrons in a field has been shown by Townsend[34] to be expressed as $D/k=(P/N\epsilon)(c_1^2/c^2)$. Here P is the gas pressure in dynes/cm² where there are N molecules per cm³, so that $P/N\epsilon$ is the gas pressure in dynes/cm² divided by the Faraday constant per cm³. c_1^2/c^2 is the ratio of the *average* energy of the electrons to the average energy of the gas molecules defining P, the ratio of electron temperature T_e to that of the gas T. Townsend has shown how to evaluate $T_e/T=c_1^2/c^2$ when fields are so low that ionization and excitation by electron impact do not occur. Druyvesteyn[35] and Smit[36] have shown how to evaluate c_1^2 or T_e when elastic or elastic and inelastic impacts occur. In the high energy region, however, the problem is extremely difficult and data needed for molecular gases are missing, so that the solution has never been worked out. K. T. Compton[37] gives an approximate equation for c_1^2.

$$c_1^2=1010\frac{\epsilon}{m}\cdot\frac{X}{p}\cdot\frac{\lambda_0}{\sqrt{f}}.$$

Here λ_0 is the electron free path at 760 mm, f is the average fraction of energy lost per impact, and p is the pressure in mm of Hg. Below the ionization and excitation potentials in inert gases, $f=2.66\ m/M$. For molecular gases, and above excitation energies, f is greater but unknown. λ_0 can be obtained from Ramsauer's curves if the electron energy is roughly known. The expression for X_1 becomes

$$X_1=\frac{(4/3)\epsilon\alpha e^{\alpha x}}{\left(\frac{2P}{N\epsilon}\cdot\frac{c_1^2}{c^2}\frac{x}{X}\right)^{\frac{1}{2}}}=\frac{(4/3)\epsilon\alpha e^{\alpha x}}{\left(1010\frac{2x}{3p}\frac{\lambda_0}{\sqrt{f}}\right)^{\frac{1}{2}}}. \quad (3)$$

As is known from studies of electron mobility, the electron velocity

$$v=0.815(\epsilon/m)\cdot(\lambda_0/c_1)\cdot(X/p). \quad (3A)$$

Since c_1 is given in terms of $\lambda_0/\sqrt{f}$, an experimental evaluation of v under sparking conditions such as made by White[18] or Raether[19] will give $\lambda_0\sqrt{f}$. Using the value of $v=1.25\times10^7$ cm/sec. as given by Raether at $X/p=41$, one finds $\lambda_0\sqrt{f}=5.7\times10^{-6}$. Brose and Saayman[38] give the electron free path in air at about 3 volts energy as $\lambda_0=3.6\times10^{-5}$ cm. This makes $f=0.025$ and

$$\lambda_0/\sqrt{f}=3.6\times10^{-5}/(0.025)^{\frac{1}{2}}=2.28\times10^{-4}.$$

Actually, both λ_0 and f are functions of electron energy so that $\lambda_0/\sqrt{f}$ will change somewhat with electron energy. Therefore the use of a constant value of $\lambda_0/\sqrt{f}$ over an extended range of X/p is not exact. However, it will *not* change by more than a factor of 2 or 3 in the range of X/p for high pressure sparks, from 20 to 45. Thus we

* Part I of this paper appeared in the June issue.

write approximately

$$X_1=\frac{(4/3)\epsilon\alpha e^{\alpha x}}{\left(0.133\frac{x}{p}\right)^{\frac{1}{2}}}\leqq\frac{1.76\times10^{-9}\alpha e^{\alpha x}}{\left(\frac{x}{p}\right)^{\frac{1}{2}}}\text{ e.s.u.}$$

or

$$X_1\leqq5.27\times10^{-7}\frac{\alpha e^{\alpha x}}{\left(\frac{x}{p}\right)^{\frac{1}{2}}}\text{ volts per cm.}\qquad(4)$$

5. The Meek Equation for Spark Breakdown at Atmospheric Pressure

Now if $x=\delta$, the gap length for a plane parallel gap, the condition for the sparking *threshold* is that $X_1=X_s$ the sparking field, for this insures a streamer crossing the gap and giving a spark. Then

$$X_s\left(\frac{\delta}{p}\right)^{\frac{1}{2}}=5.27\times10^{-7}\alpha e^{\alpha\delta},$$

$$\frac{X_s}{p}\left(\frac{\delta}{p}\right)^{\frac{1}{2}}=5.27\times10^{-7}\frac{\alpha}{p}e^{\alpha(p\delta)/p},$$

so that

$$\frac{\alpha}{p}(p\delta)+\log_e\frac{\alpha}{p}=14.46+\log_e\frac{X_s}{p}-\tfrac{1}{2}\log_e p\delta+\log_e\delta.\qquad(5)$$

For an overvolted gap at $X_1=X_s+\Delta X_s$, $x=x_0<\delta$. Here midgap streamers form and breakdown proceeds rapidly and effectively.

For any other field distribution, streamer formation will follow when for $X_1=X_s$ the starting field, the electron avalanche has traversed a length x_s such that

$$X_1=X_s=\frac{(4/3)\epsilon\alpha_{x_s}e^{\int_0^{x_s}\alpha dx}}{\left(1010\cdot\frac{2}{3}\frac{x_s}{p}\frac{\lambda_0}{\sqrt{f}}\right)^{\frac{1}{2}}}=1.63\times10^{-9}\frac{\alpha_{x_s}e^{\int_0^{x_s}\alpha dx}}{\left(\frac{x_s}{p}\right)^{\frac{1}{2}}},\qquad(6)$$

provided that enough density of ionization is achieved to insure photoelectrons. Here, since the field and thus X/p varies with x, α depends on x and α_{x_s} is the value of α at the end of the avalanche x_s where great multiplication occurs. This permits a more general application of streamer formation to breakdown as will later be seen.

Consider again the plane parallel gap at the sparking threshold. Since we have values for α/p as a $f(X/p)$ it is clear that, given x and p, X_s/p can be determined by the values of X/p and α/p which satisfy the above equation. A solution by Meek[17] gave $X_s/p=42.2$, $(\alpha=18.6)$ for the spark in air. This makes $X=32.2$ which is close to the conventional value of 31.6. However, *the criterion that $X_1=X_s$ is in itself only very rough*, and it may be any factor times X_s, e.g., 0.8, 1, 1.2, etc. This makes the sparking *threshold* somewhat indefinite which it is not unlikely is the case. In fact, to set a threshold, the photo-current from the cathode and the time lag allowed for in measurement must be fixed before we can set the value of a in $X_1=aX_s$. Observationally, however, the values of V_s seem fairly definite as the equation is insensitive to variations in X_1 owing to the cumulative character of ionization. For instance, setting $X_1=X_s$ makes $X_s=32{,}200$ volts/cm, while setting $X_1=0.2X_s$ makes $X_s=31{,}800$ at 760 mm with $\delta=1$ cm.

6. Meek's Theory and Paschen's Law

Equation (5) expresses X_s/p as a function of α/p and of $p\delta$, except for the term $\log_e\delta$. Except for this term X_s/p is a function of $p\delta$. The experimentally observed relation that X_s/p, and hence the sparking potential V_s, varied with the value not of δ or p independently, but with the product $p\delta$, is called Paschen's law.[39] It has been tested extensively and verified at lower pressures. It is usually assumed to hold at higher pressures, though no careful test has been made of it for large values of δ at atmospheric pressure. Such a study should be made, since on its result the proof of this theory depends.

Paschen's law has been deduced by numerous workers in a general way on the mechanism assumed by Townsend.[40] Its validity rests not on Townsend's mechanism in detail but on the circumstance that in the theory the coefficients α/p and γ are both assumed to be functions of X/p. The physical meaning of the law is that the sparking potential and the value of X_s/p are determined by the total *number of molecules* which an electron encounters in a linear path

across the gap, i.e., on the number of ions created. We are now, however, dealing with a *new mechanism*. In this we picture as the essential criterion not the total *number* of ions formed in a linear succession of processes, but the *density* of ions. If there are gases in which when $X=X_s$ photo-ionization is not adequate, the theory must be modified as will later be seen. It is probable, however, that in all gases at the value of X_s operative for sparks up to $\delta=10$ cm, enough photoelectrons will be produced. Under these conditions, as pointed out by Varney[41,42] who studied spark breakdown as a result of ionization by collision in a gas with positive ion space charge production by ion movement, the use of ion *densities* instead of *numbers* of ions formed leads to a small deviation from Paschen's law.

At low values of $p\delta$, where the Townsend-Holst theory applies, Paschen's law is strictly obeyed as numerous investigators have found.[43] The deviations from Paschen's law due to the space charge factor in Meek's theory is shown in Table I. The sparking potentials V_s in kilovolts are calculated for various values of $p\delta$ and δ. If Paschen's law held, then the values of V_s would be constant for a given $p\delta$. The computed deviations are within the limits of uncertainty of the existing observed sparking potentials.

7. *Comparison of Meek's Theory with Experiment*

The equation has been tested in a preliminary fashion in gases like H_2 and appears to hold. The curve of sparking potential V_s in air against $p\delta$ plotted to logarithmic scale is shown in Fig. 11(a) using Sander's[44] values of α/p as a $f(X/p)$ up to $X/p=160$ in air and for higher values Posin's[45] data on N_2 are used. The experimental curve shown as dotted is that given by Whitehead[46] as the mean of the data of a number of workers. The theory and experiment agree from $p\delta=10^4$ down to nearly $p\delta=10^2$ mm×cm. For values of

TABLE I.

$p\delta$ mm×cm	V_s in kv		
	$\delta=0.1$	$\delta=1.0$	$\delta=10.0$
7600	245	248	249
760	31.5	32.2	32.9
380	18.0	18.6	18.9

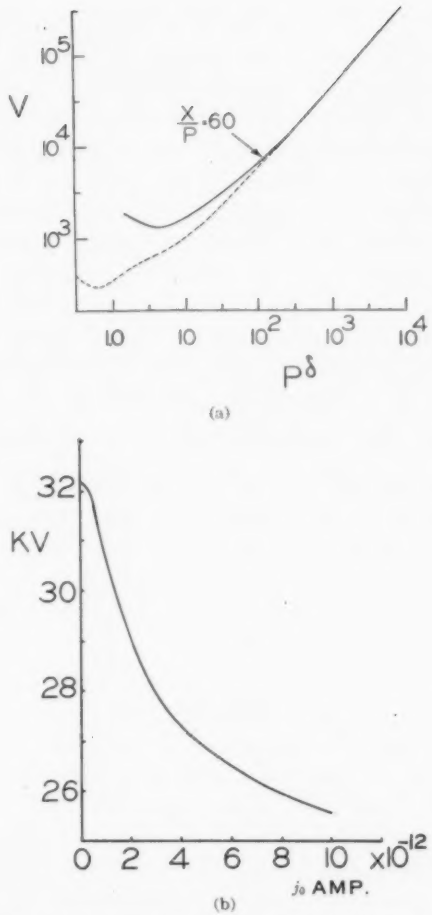

FIG. 11. (a) Curves plotted on logarithmic scale to show the relation between the minimum potential for breakdown (in volts) and the product of $p\delta$ of pressure times gap length (mm Hg×cm). The calculated curve (continuous) and the experimental curve (dashed) are both shown. Note that the two curves coincide down to a value of $p\delta\sim100$. Below this the observed sparking potential is lower, indicating the presence of the Townsend-Holst mechanism. (b) Theoretical curve for sparking potential as a function of photoelectric current density at equilibrium.

$p\delta\sim100$, the calculated values are higher than those observed and the deviation increases steadily with decreasing $p\delta$ and thus with increasing X/p. The deviation becomes notable at the values of X/p where the abrupt termination of the curves giving an α *without* a γ are being replaced by curves with a measurable value of γ. Deviation of the theoretical V_s from experiment on the new theory occurs at just the values of $p\delta$ where streamer formation ceases to be possible and the Townsend-Holst theory of the mechanism of low pressure sparks becomes applicable. This means that as $p\delta$ becomes very low the

space charge densities of positive ions in avalanches, become less efficient in causing spark breakdown than the mechanism of Townsend, *probably because of inadequate photo-ionization in the gas*. At this point, the formative time lags of sparking should be materially higher than is the case with high pressure sparks.[30] It has also been observed in low pressure sparks by Tamm and Rogowski[47] and Tamm.[48] In the low pressure regions the instability indicated by the Townsend mechanism appears at first as a glow which breaks down as a spark with time lags of the order 5×10^{-6} sec. using values of $p\delta\sim100$ to 200 in air. This is studied in detail by Schade.[30]

8. *Characteristics of Breakdown Streamers*

The streamer radius must be at least that of the tip of the positive space charge in the avalanche which initiates it. It may well be somewhat larger since the ionization by the incoming electrons feeding the tip will tend to enlarge it. It is not materially enlarged by diffusion and the positive space charge exerts a conservative action in this regard. The cloud tracks of Raether in Figs. 2, 3, 7 and 9 show the size relative to that of the avalanche. The ion density in these streamers is probably distinctly higher than the space charge in the tip of the avalanche for it is created by the superposed tip field and impressed field of the gap. It is sufficiently intense in the case of midgap streamers so that it can be photographed as shown by Dunnington and White. Streamers are also observed visually in corona, and Kip[23] has shown the ion density to be of the order of 2×10^{13} ions/cm^3. Individual corona streamers are just below the threshold of photographic recording while spark streamers can be photographed. The ion density may thus well exceed 10^{14} ions/cm^3. What the field gradients in these streamers are cannot be told. Whether they are large enough to create further ions by collision before the streamer bridges the gap is doubtful. Of this more will be said when the longer gaps are considered. During their life in the shorter gaps, there is little electron attachment or recombination of ions.

9. *Cathode Illumination and Sparking Potential*

The discovery by H. J. White[15] of the lowering of the sparking potential in air at atmospheric pressure for air gaps of $\delta\sim1$ cm by intense ultraviolet illumination of the cathode has presented some theoretical difficulties. It has been discussed by Loeb.[49] Rogowski[15, 50] and his associates, who independently discovered the phenomenon, have presented an extensive theory along the Townsend lines. This explanation is based on assumptions to which the writers cannot subscribe, and one can consider the problem as still an open one. It is not impossible that the influence of photoelectric current density j_0 on sparking potential at lower values of p can be satisfactorily accounted for along the lines suggested by Schade.[30] On the other hand, at higher $p\delta$ the streamer mechanism should not be influenced by j_0 except in the measure that the statistical time lags are reduced. This circumstance thus appeared to present a definite obstacle to the acceptance of the streamer mechanism despite its obvious advantages. The difficulty, however, is only an apparent one. All the measurements made on the lowering have been made with possible formative lags of the order of 10^{-5} sec. Hence, as Meek has shown, irrespective of any theory of spark mechanism with large j_0 a considerable space charge distortion of the gap due to positive ion motion has been built up. Meek[51] using the streamer theory of the spark discharge has computed the lowering of V_s by j_0. In one case he used the rigorous theory set up by Varney, White, Loeb and Posin[41] for the equilibrium space charge distortion with a photocurrent j_0. The resultant variation of V_s as plotted against j_0 is shown in Fig. 11(b). Using

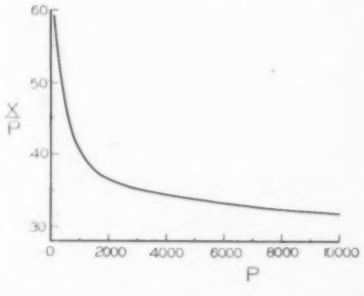

FIG. 12. Curve to show the relation between X_s/p and p, following from Meek's theory, for a 1.0-cm gap. This is in fair agreement with the experimental observations within the range. The curve is analogous to the relation which has been observed between X/p and δ, the gap length up to about 10.0 cm at 760 mm Hg. It is important to note the apparent flattening of the curve at high p

approximate theory, he also computed the effect for the case where the ion movement in 10^{-5} sec. only is considered. The computed results for the equilibrium case differ from observation in two respects; 1, The lowering of V_s by j_0 is almost double that observed; and 2, The lowering becomes significant at lower values of j_0 than those observed. The greater lowering is to be expected from a theory using the *equilibrium* field for in practice the fields develop only for 10^{-5} second. The rough values of V_s computed using 10^{-5} second are in good agreement with those observed. The experiments were all carried out using spark illumination of the cathode. Since the effective "duration" of the spark is not known, the value of j_0 cannot properly be evaluated from a measurement of the electrons liberated. Thus j_0 as given by the observers is possibly in error by as much as a factor of ten or more. What is needed at present are accurate equilibrium values of V_s as a function of j_0 at high values of j_0. In any case, it is clear that the lowering of V_s by high values of j_0 is not a stumbling block to the streamer theory.

10. Conclusions Relative to Shorter Gaps

Thus there are at least two mechanisms of sparking active, which replace each other under appropriate conditions, the Townsend-Holst mechanism occurring from below the minimum sparking potential to values of $p\delta$ of the order of 100 and the Meek mechanism based on positive streamer formation dominating from values of $p\delta$ of about 100 up.

One may now ask as to how far up in values of $p\delta$ this mechanism holds, whether in very long sparks Meek's mechanism still holds. There is a reason for this question since observations of long sparks in air and studies of lightning discharge show positive streamer formation and advance from the anode to be active in a measure but accompanied by breakdown streamers extending from the negative electrode well beyond the middle of the gap as well. These negative streamers in long sparks appear at first sight to be incompatible with what has been said of the progress of electron avalanches, but they are not, as we will see, although the question requires additional analysis.

11. The Problem of Spark Breakdown in Long Gaps

Experimental study of V_s as a function of $p\delta$ thus far gives meager data for plane parallel gaps much above $p\delta = 10^4$ cm $\times$ mm pressure. The high potentials needed as well as plate dimensions have precluded much study beyond 10-cm gaps and pressures in excess of 20 atmospheres. The data fulfill Paschen's law to within three percent at $p\delta \sim 10^4$ (using $\rho\delta$ in place of $p\delta$ when density ρ is no longer directly proportional to p). The apparent linear relation between V_s and $p\delta$ does not accurately hold, V_s increasing somewhat more slowly than in proportion to $p\delta$. The relation is such that if we divide the sparking *field strength* by pressure the important parameter X_s/p decreases with increasing $p\delta$. This is shown in the curve of Fig. 12. It is seen that X_s/p decreases at first rapidly and then more slowly, *appearing* to approach a constant value of $X_s/p \sim 30$. The Townsend-Holst equation, with the proper form of α/p as a function of X/p inserted, leads to a similar curve in agreement with observation. This agreement must be largely ascribed to the cumulative character of ionization by electrons and to the form of the relation between α/p as a function of X/p since in neither case does the secondary process (γ or photo-ionization) as used in the equations play an important role.

Beyond $p\delta \sim 10^4$ there is no satisfactory information. It is known, however, that with larger gap distances using spheres even in the absence of corona or prebreakdown discharges at the electrodes, i.e., with surge impulse breakdown, the *average* field between electrodes is very much below the 25,000 volts per cm which suffices for 10-cm gaps at atmospheric pressure. For a small negative electrode with a large positive electrode, the *average* field is of the order of 9000 volts/cm and with small positive electrodes it is of the order of 4400 volts per cm. In the case of lightning discharge the average fields may be even smaller although this is not known with certainty.

In such cases the fields are not only far from uniform but the fields at the electrodes are very high and thus must locally suffice to initiate streamers and avalanches. Thus the *average* field strengths have not much significance. Since breakdown occurs under these conditions, it is essential to examine more closely the conditions

under which streamers and avalanches propagate. One may start such a study by looking at the limitations placed by values of X, p and δ not only on the initiation of streamers and avalanches, but also on their continued propagation.

12. *Conditions Essential to Streamer and Avalanche Propagation*

For any given value of X/p and pressure p there is a certain length of electron avalanche path required to initiate a streamer formation. When this length is equal to or *less* than the gap length δ a spark is produced. Where it is less than the gap length the development of a midgap streamer leads to an efficient form of breakdown. If it is longer than δ then no streamers could form and one could have no spark. Thus X_s depends on the achievement of an adequate space charge density by an avalanche less than or equal to δ long. The length of an avalanche for such breakdown depends on: (1) The space charge density needed to give the field X_1 required and (2) the production of enough photoelectrons by such a density to insure propagation of the streamer. This in turn must depend somewhat on the character of the gas and the gaseous density.

Since ionization is cumulative, it might be expected that given a long enough path length the space charge density must eventually yield any field desired. At low X/p with low α this may require a long distance of travel. However, the electron diffusion in the avalanche tip is tending to reduce the density as the path length increases. From the condition given by Eq. (4) that

$$\frac{X_1}{p} = 5.27\times10^{-7}\frac{\alpha}{p}e^{\alpha\delta}\Big/\left(\frac{\delta}{p}\right)^{\frac{1}{2}}$$

and from the form of the relation of α/p as a function of X/p one might be able to determine this limit. It seems possible to satisfy the condition down to the lowest values of α if δ be sufficiently great. Before such path lengths are achieved, the low rate of ion production will lead to intensities of photon emission which are incapable of permitting streamer advance. Hence, the limitations on streamer growth and thus on the values of X_s will depend essentially on the ion density needed at the head of an avalanche to permit streamer growth.

13. *Ion Densities Necessary for Streamer Propagation*

As we have no data about the quantitative aspects of photo-ionization in the case of electron avalanche production it is difficult to estimate the ion density needed. We do, however, have some data on the ion densities in propagating pre-onset streamers in positive corona. In one cm of length of such streamers Kip[23] estimated the number of ions from the pulse current as about 5×10^9. These were estimated to lie in a cylinder of radius of about 0.01 cm which gives the ion density as 1.6×10^{13} per cm^3. It is doubtful whether the density is as high as this in the tip, and it is also doubtful whether this represents the minimum necessary for development. From other evidence, as we shall see, one might place the density in the neighborhood of 7×10^{11} ions/cm^3. From Eq. (4) Meek has calculated that at a $p\delta$ of about 200 where streamers begin to be replaced by the Townsend-Holst mechanism, the ion density at the end of the avalanche of one cm length is 6.9×10^{11} per cm^3. At 760 mm in a gap of 10 cm length where Meek's equation still gives correct results, the ion density is 8.8×10^{11} ions/cm^3. For a 15-cm gap length at 760 mm the ion density is 7.2×10^{11} ions/cm^3 which is probably near the limit at which streamers will propagate successfully. Thus we will assume that there is a definite lower ion density limit, N_0, required for streamer formation which at atmospheric pressure and below we will tentatively set as about 7×10^{11} ions/cm^3. It is possible that this limiting density may not be the same at all pressures. At very low p and at a very high $p\delta$ the ion densities in avalanche formation are so low that streamer propagation does not occur due to inadequate photo-ionization. At low $p\delta$ this results in an alternative sparking mechanism. At high $p\delta$ it must again alter the sparking mechanism and lead to a new condition for the spark.

14. *Sparking Criterion for Long Sparks*

To establish the sparking criterion one may proceed as follows. It will be assumed that sparking in long gaps still depends on streamer formation. However for large values of δ it is clear that the ion densities at the head of the avalanche will fall below the critical value N_0 adopted for air near atmospheric pressure as

$N_0 = 7 \times 10^{11}$ ions/cm^3. Hence the condition that the avalanche *cross the gap* and produce a positive space charge field $X_1 = X_s$ at δ cannot be applied. Thus the sparking field strength cannot be calculated from Meek's Eq. (4). What must take place as one reaches such gap lengths is that the spark will require values of X_s greater than those computed by Eq. (4). Assuming that streamer formation requires a minimum concentration N_0 we can compute a field strength X_{s0} and path length δ_0 which satisfy Eq. (3) for a given p and when applied to Eq. (1) give a concentration $N = N_0 = 7 \times 10^{11}$ ions. The calculation of the values of X_{s0} and δ_0 satisfying these conditions can only be achieved by trial and error. Thus one selects a value of δ at a fixed p and from Eq. (3) and α/p as a $f(X/p)$ evaluates X_s. From these data, α, $x = \delta$ and r in Eq. (1) can be fixed and N evaluated. One may then plot N as a $f(\delta)$ and evaluate the point δ_0 for which $N = N_0$. From δ_0 one can then evaluate X_{s0}.

With this information it is clear that at p, for values of δ greater than δ_0 a streamer cannot form unless $X_s = X_{s0}$. In this case the avalanche will progress to δ_0, a streamer will form in the gap and progress back to the cathode allowing the avalanche to proceed anew as will be seen in detail later. Hence for gaps longer than δ_0 the value of X_s will not decrease for increasing δ as before but will assume a higher value X_{s0} adequate for streamer propagation. The value of X_{s0} and δ_0 will change with p. The sparking potential V_s will then no longer be given by $X_s\delta$ but instead will be given by $V_s = X_{s0}\delta$.

The effect of this change on the characteristic curve for sparking will then be as follows. At low

TABLE II.

p IN MM	X_{s0} VOLTS/CM	δ_0 CM	$\frac{X_{s0}}{p}$	$V_{s0} = X_{s0}\delta_0$
1520	38,000	88	25.0	3,340,000
760	24,200	15	31.8	363,000
380	15,050	3.3	39.6	49,700

values of δ for a constant p the slope of the sparking curve $dV_s/d\delta$ is greater than X_{s0} as is well known. The slope gradually decreases until in conformity with Meek's theory in a limited range it is slightly less than X_{s0} for air. As the gap length approaches δ_0 the slope must again *increase* up to X_{s0} and then remain constant. The new values of V_s above δ_0 must lie on a line of slope $(dV_s/d\delta)_0 = V_s/\delta = X_{s0}$, and this line must pass through the origin.

This change in the slope of the curve near δ_0 will doubtless be gradual. So far no curves of this character have been observed.* The difficulty of obtaining long gaps with uniform fields has in the past precluded the necessary measurements in regions where the change could be observed. That this is so can be seen by computing the values of X_{s0} and δ_0 at a few values of p. They are shown in Table II. It is to be noted that the values depend somewhat critically on the value of N_0 chosen and are not to be regarded as more than orienting magnitudes.

It is seen that above atmospheric pressure Meek's theory is applicable to almost any measurements we are able to make. At atmospheric pressure it is applicable beyond any measurements made to date. Below atmospheric pressure the change in the curves is open to experimental study. This has not until now been undertaken as no one thought it worth while to study long gaps at lower pressure.

The influence of the new sparking criterion on Paschen's law is to introduce a further deviation beyond that inherent in Meek's theory. This deviation is one which increases V_s by an increase in δ more than by an increase in p at such values of δ that Meek's law holds at the higher p and not at lower p. The deviation in any case will not exceed a few percent.

It will thus in what follows be assumed that for gaps in excess of δ_0 in length, at any pressure, the Meek criterion is no longer applicable; that sparks progress by avalanche advance and retrograde streamers; and that the sparking potential is given by $V_s = X_{s0}\delta$. With this assumption one must now analyze the retrograde streamer mechanism.

15. The Mechanism of Avalanche-Streamer Advance in Long Gaps

At atmospheric pressure, if X is less than X_{s0} or if $X = X_{i0}$ but δ is less than δ_0 avalanches will leave the cathode and cross the gap. No streamers will form and the gap will *not* break down. If

* The a.c. sparking potential curves obtained for virtually uniform gaps between large spheres show this behavior when the gap length exceeds about 15 cm.

$X = X_{s0}$ and $\delta = \delta_0$ avalanches cross the gap, streamers form at the anode and breakdown is possible. If $X = X_{s0}$ and δ is greater than δ_0 breakdown will occur. The sparking potential will be fixed by $X_{s0}\delta$ but the avalanche will not cross the gap at once. What will happen is that the avalanche will advance to δ_0. At this time a streamer will propagate in the *retrograde* direction back to the cathode at a speed of some 10^8 cm/sec. Before it is well advanced, the positive space charge at δ_0 will exhibit some retarding action on the advance of the electron cloud until the incoming electrons up the streamer channel reduce the positive space charge field. Once the streamer tip reaches the cathode and the supply of electrons runs up the channel making it a conducting filament of plasma the negative electrode will have extended itself to the distance δ_0 in the midgap. In the meanwhile the avalanche has again begun to proceed at its normal velocity until it reaches a distance $\delta_0+\delta_1$ from the cathode.

The condition for streamer formation is that with X_{s0} fixed, the electron avalanche or *avalanches* proceeding from δ_0 must advance a distance δ_1 such that the combined space charge density at the end of δ_1 is $N_0 = 7\times10^{11}$ ions/cm^3. Now at the cathode there was *one* electron initiating the avalanche. Hence the value of $\delta_1 = \delta_0$. After the first advance of δ_0 there may be more than one electron in the electron space charge so placed that it progresses in the field X_{s0} to multiply effectively and thus lead to the density N_0 needed for a streamer. In this case with n such electrons the distance δ_1 traversed before the second streamer completes this channel will be fixed by $N_0 = nae^{a\delta_1}/\pi r^2$. Hence the later distances of avalanche travel before retrograde streamer formation will not of necessity be δ_0 but distances δ_1. This circumstance will merely have the effect of making the distances of avalanche progress between streamers shorter, thus only reducing the value of r. After advancing $\delta_0+\delta_1$ the avalanche again suffers some retardation while a new streamer advances towards the cathode from $\delta_0+\delta_1$ to join the filament of plasma with its tip at δ_0. This continues until the avalanche approaches the anode when, as is the case in the overvolted gap, the anode streamer finally closes the gap giving breakdown. If in such a long gap an electron is initially created in midgap, as is usually the case for long sparks, then after traversing the distance δ_0 towards the anode the avalanche pauses while the streamer not only propagates backward the distance δ_0 but *proceeds all the way* back to the cathode; from then on it proceeds as before. Hence in long sparks midgap streamers may be of frequent occurrence.

The mechanism is essentially an avalanche process based on the mechanisms assumed. It yields, however, a different value of the sparking potential than that given by Meek's theory in that it applies only to a stage of the process because of the decreased ion densities involved and thus requires one to compute the sparking potential on a different basis. The streamer propagates in a retrograde direction with an initial diameter equal to the value of r given by the avalanche cross section at δ_0 or δ_1. It may spread somewhat as a result of the ionization by the incoming electron avalanches. The low diffusion coefficient for positive ions in the 2×10^{-7} sec. of retrograde travel to the cathode, however, keeps the channel relatively narrow. The electron avalanche cloud, however, by its rapid diffusion tends to broaden the channel as it advances. On the other hand, the space charge field of the positive streamer tip exerts a conservative action in reducing the lateral diffusion of the electron cloud, thus tending to keep the avalanche from spreading as it would were it unrestricted. The broadening of the streamer moving towards the cathode relative to the earlier portions of the electron avalanche can be nicely seen in Figs. 2, 3, 7 and 9, showing Raether's cloud-track pictures. Since in such long avalanche-streamer processes there is a slight diffusive loss of electrons from the avalanche tip, one may expect that a small electron current flows from the cathode up the streamer channel to supply the loss.

16. Sparking in Long Gaps with Non-Uniform Fields

In the case of non-uniform fields, however, the minimum value of X/p in the gap may be below the value X_{s0}/p required for a streamer in a plane parallel gap, even though both positive and negative streamers may propagate. The reason for this lies in the fact that once a positive

streamer or an avalanche and its attendant retrograde streamer forms, and begins to propagate, it carries with itself considerable field distortion. This extends the high field region at the electrode from which it originated out into the weak field region enabling the streamer to propagate further. Unless in its travel the streamer or avalanche encounters a field region so weak that even with its own enhanced field it is incapable of insuring further advance, it will continue. Cases where such conditions obtain and breakdown streamer advance is stopped, have been observed both in the positive and negative point-to-plane coronas with relatively high gradients near small electrodes. Here the positive pre-onset streamers are observed to be choked off by positive space charges from either burst pulse corona or by previous streamers. Only at much higher fields where space charges are being dissipated can the positive streamers form and advance across the gap to cause breakdown. In the case of the negative avalanches from small negative points this advance is again inhibited by both the positive ion space charge and by the negative ion space charge in air at atmospheric pressure.

a. Minimum Field Permitting Streamer Advance

It is uncertain what the *minimum* gradients permitting avalanche and streamer formation and advance are. Probe measurements in a 4-cm gap positive point-to-plane corona discharge indicate that near breakdown with an *average* gradient of 5500 volts/cm the minimum field of 4000 volts/cm is low enough to prohibit streamer advance across the electrodes. It is thus likely that positive streamers require fields of the order of 4400 volts per cm to propagate. It is possible that this value may in some measure be dependent on the character of the fields at the electrodes launching the streamers.

b. Fields at Electrodes for Streamer and Avalanche Formation

For streamer formation and propagation the form of the condition set in Eq. (6) applies if we use Meek's criterion, *provided* that the *ion densities are adequate to permit streamer growth.* The high fields required because of the rapid decrease of fields with distance at electrodes of this character in the region of atmospheric pressure probably insure the requisite ion densities. Hence one may write for the starting potential X_s

$$X_1 = X_s = \frac{(4/3)\epsilon\alpha x_s e^{\int_0^{x_s}\alpha dx}}{\left(1010\cdot\frac{2}{3}\frac{x_s}{p}\frac{\lambda_0}{\sqrt{f}}\right)^{\frac{1}{2}}}. \qquad (6)$$

Here x_s is the distance of travel in the divergent field adequate to insure a density of ionic charge in an avalanche tip in excess of the 7×10^{11} ions per cm^3 needed for streamer formation, and to make X_s equal to the field at x_s.

c. Difference Between Action of Positive and Negative Points

In the case of the divergent field there is a significant factor leading to a difference in the action of positive and negative points as regards avalanche formation which was absent in uniform fields. The field is highest at the electrode so that α is greatest at that point, and the effective multiplication should take place at the electrode. In the case of the positive point the electrons form avalanches ionizing cumulatively and in increasing measure, as α increases with increasing field near the point. In addition the electrons produced are at once drawn into the electrode, giving a maximum positive ion space charge formation at the electrode which can initiate a streamer as soon as the density of charge enhances the field beyond the electrode to the value of X at that point. As the streamer builds outward it quickly reaches lower fields but carries its own tip field with it so that the condition for propagation still continues to be met. Thus it occurs that for all but the finest points in positive point-to-plane corona onset streamers appear almost as soon as multiplication in the electrode field can lead to bursts.

With negative electrodes the situation is quite different. While it is true that in the absence of space charges the quantity $e^{\int_0^{x_s}\alpha dx}$ is the same, irrespective of charge, this is not the case when space charges are formed. For as the electron avalanche proceeds outwards even with a high

α the first few ionizing paths do not yield a large multiplication of ions, and the electron avalanche rapidly comes into lower fields. In addition, it *leaves behind it immobile positive ions*. These produce secondary electrons when they

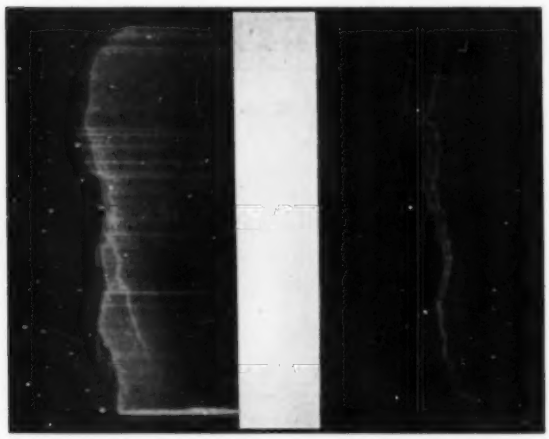

(a) (b)

FIG. 13. Photographs taken with a rotating camera to show the breakdown of a 100-cm gap in air at atmospheric pressure between a positive point and an earthed plane. The voltage source is an impulse generator, which is connected to the discharge gap through a resistance R, where (a) $R=100{,}000$ ohms; (b) $R=1{,}000{,}000$ ohms. The film movement is such that the leader stroke appears on the left, the main stroke on the right. The point electrode is at the upper end of the photograph. The discharge progresses along the trace at the left to strike the ground and then returns as a brilliant flash depicted by the right-hand trace, which follows in general contour the leader stroke. The speed of the main stroke is much greater than that of the leader stroke, so that the distance between the two traces at any position in the gap enables the time of passage of the leader stroke, and thus its velocity, to be determined. In (b) the very faint parallel lines to the left probably represent the first two steps of the leader stroke advance. Note the downward branching, particularly in (a).

strike the electrode with high energy; these electrons again move outward and form more positive ions near the cathode. The ions enhance the field between positive ion cloud and negative electrode. The enhanced field is, however, never of a great length. In an equal measure, the positive ions *reduce* the field acting on the electron avalanche as it recedes from the cathode. This means that in order that the avalanche achieve enough ions to make a retrograde streamer possible the electrons must travel to a greater x_a to make $X_1=X_a$; or, which amounts to the same thing, they require a higher field at the electrode surface. In the extreme case of very small points, ~ 0.2 mm diameter and less, the action is so confined that cumulative ionization as a result of positive ion impact on the electrode furnishes an action more like the Townsend-Holst mechanism at low pressures. In such a discharge, as Trichel[52] has shown, we see the characteristic manifestations of low pressure breakdown with Crookes dark space, negative glow, Faraday dark space and positive column appearing. In addition, the negative ion accumulation even breaks off the discharge periodically leading to the relaxation oscillator-like pulses observed by Trichel.[52] As the point becomes larger and the higher field values of X_a extend further outward such action is minimized and negative avalanche-streamers may form, but at *higher electrode potentials than with the positive point*. Observation shows that while the *onset* for the positive and negative point *corona* occurs at nearly the same potential the positive corona already exhibits streamers, while for smaller electrodes the negative corona shows only the glow discharge characteristics. Larger negative electrodes exhibit avalanche formation but only short or abortive streamers.[53]

If spark breakdown be studied with both these coronas, it will be observed that the fields must be materially increased in order to exhibit positive streamer or negative avalanche-retrograde streamer mechanisms, for at low fields all points are surrounded by space charges which choke off streamer advance. When, however, the positive streamers can propagate again they do so, and breakdown follows shortly.

d. Breakdown with Simultaneous Streamers from Both Electrodes

In the case of negative streamers, as the potential increases, the current increases and the space charge accumulations begin to build up considerable fields at the *anode*. When the fields become high enough to propagate the avalanche-streamer mechanisms from the cathode, the anode space charge gradients reach values where *anode streamers* can start. Then, depending on current density and field conditions, a spark breakdown will result either from the anode streamer progressing most of the way across the gap to the tips of the avalances; or a simultaneous propagation of negative avalanches and

positive streamers across the gap effecting junction anywhere from near the anode to well towards the cathode from the midgap region. Such breakdowns have been observed and photographed by Allibone and Meek[54] for long gaps, using moving film cameras and are shown in Figs. 13(a) and (b) and 14. That fields of such magnitude as to make positive streamer propagation from the anode possible for negative point-to-plane corona exist can be simply shown in terms of data on a negative point-to-plane gap of 4 cm length just before breakdown at atmospheric pressure. The current is then 15 microamperes. In a time of t seconds the current i gives a charge $q=3\times10^9it$ e.s.u. of negative charge in the gap in transit, where t is the time of transit of the ions across the gap. Now the field strength X at the anode will be $X_a=4\pi\sigma$, where σ is the surface density of *induced* positive ions at the anode. If the current to the anode is uniformly distributed over its area A the value of X_a can be computed as follows: if, as is the case for the negative point, the point is effectively screened by the positive space charge

$$X_a=\frac{4\pi\times3\times10^9it}{A}\times300=1.13\times10^{13}\frac{it}{A}\text{ volts per cm.} \quad (8)$$

Now t has been measured by Kip for the positive ions and is not essentially different from that for negative ions. Hence in Eq. (8) $t=2\times10^{-3}$ sec. and $A=10$ cm². Thus $X_A=34{,}000$ volts/cm. With the concentration of the discharge at the center of the anode the field will be materially higher and will thus enable the positive streamer to propagate from the anode. Such fields have recently been observed at the anode by probe measurements in negative point corona.[55]

e. Impulse Breakdown with Negative Point

In the case of impulse breakdown with the negative point, the situation is somewhat different. The time is too short for the effective building up of the negative space charge in the gap. However, a negative avalanche is projected into the gap at once and thus introduces a charge of Q coulombs into the gap at the negative point, before it has propagated across the gap. Now Jeans[56] shows that the field induced at a conducting plane electrode a distance l directly below a quantity of Q coulombs at a point is given by

$$X_a=\frac{2Q\times3\times10^9}{l^2}\text{e.s.u.}=1.8\times10^{12}\frac{Q}{l^2}\text{ volts per cm.} \quad (9)$$

Fig. 14. Photograph of the breakdown between a negative point and an earthed plane. Conditions as in Fig. 13 but with $R=600{,}000$ ohms. The negative point is at the upper end of the photograph. Note first the stepped character of the negative discharge which proceeds downward from the point about one-third of the gap. It is met at this point by an upward-moving positive streamer whose advance can be seen at the extreme left in the lower two-thirds of the picture. The subsequent bright channel represents a potential wave energizing the ionized channel and probably traveling downward. Note also that the potential gradient at the earthed plate is sufficient to initiate a second streamer which had not advanced far enough to make a junction with the negative leader when the first channel closed the circuit. Note also the absence of stepping in the positive streamer in contrast to the progress of the negative streamer.

To make $X_a = 3\times10^4$ volts/cm, Q must equal $1.67\times10^{-8}\ l^2$ coulomb. Thus $\int_0^t i dt$ must equal $1.67\times10^{-8}\ l^2$ coulomb in the time t of streamer formation at a current i. For $l=3$ cm, $Q=1.5\times10^{-7}$ coulomb, which means that the avalanche in its time of growth t must give 9.4×10^{11} ions. This is just about the number of positive ions and therefore of electrons in the avalanche to permit streamer formation. Hence, for this gap where streamer formation is just beginning a positive streamer may start. This picture is perhaps oversimplified. For there are periods before the streamer elements reach the cathode where there is a dipole acting instead of the volume charge Q. There will, however, be times when Q alone acts, and this with the *advance of Q into the gap* can give adequate fields at the anode. For longer gaps l^2 is increased. This means that $\int_0^t i dt$ must be larger. This requires merely that the time t must be greater, which has the consequence that the negative streamer *must* advance *further* into the gap decreasing l and increase Q. This explains clearly why with impulse breakdown for small negative electrodes and long gaps the observed negative streamer advance into the gap is longer and meets the positive streamer more nearly in midgap.

17. Mechanism of Lightning Discharge

When one considers the case of the longest discharges observed, namely the lightning discharge, it is clear that the mechanism concerned will again be based on the propagation of streamers or, where conditions warrant, an avalanche advance and retrograde streamer formation. Observations on lightning discharges have shown that wherever it is possible for positive streamers to form and propagate[57] this mechanism will predominate. However, the observations of Schonland and others on lightning discharges from cloud to ground indicate that since in the majority of the thunder storms the negative cloud predominates, a considerable fraction of the discharges propagate from highly localized concentrations of negative charge in the cloud and move towards the ground.[58] The exact nature of the way in which the electrification leading to a stroke accumulates and concentrates is not known. The excellent studies of Simpson and Scrase[59] made on gradients at the ground, in the air and in the clouds by means of balloons indicate either mild field gradients of 300 volts/cm or less or else gradients that caused a spark to pass in their apparatus. They correctly conclude that either the gradients leading to strokes are exceedingly localized in space or else that they arise very suddenly as a result of turbulent convection in localized areas. Doubtless both effects are present. But when such an accumulation in a negative cloud yields gradients capable of giving avalanches or streamers a breakdown begins, much as is the case for smaller negative electrodes.

a. Progress of a Typical Lightning Discharge

The typical lightning discharge has been extensively studied by Schonland and Collens by means of the Boys camera.[58] It is illustrated by Fig. 15, where the steps in the leader stroke are seen at the right, the time axis going from right to left.[60] Schonland has analyzed the progress as follows.[61] The discharge from the negative cloud is preceded by an invisible pilot streamer advancing into virgin air at the rate of about 1×10^7 cm/sec.* After an advance of some 5 m, or in on the average 50 microseconds of advance, a *stepped* leader stroke traveling at the speed of 2×10^9 cm/sec. advances from the cloud to the tip of the pilot streamer down the pre-ionized pilot streamer and slows down to the pilot streamer speed. Then after another interval of 50μ sec., if the stroke is long enough, it is caught by a second stepped leader and so on. For strokes in excess of 2 km as many as 2 stepped leaders may be proceeding down the channel at once. As the pilot streamer approaches the ground, field distortions such as those calculated in Section 16e lead to the initiation of one or more positive streamers from appropriate conductors. These, as in Allibone and Meek's long sparks, eventually join the pilot streamer. Then

* Schonland finds that for the majority of pilot streamers the velocity lies between 1.0×10^7 and 5×10^7 cm per sec., though higher velocities, up to 2×10^8 cm per sec. are observed. The higher velocities occur for streamers whose behavior indicates that they may be traveling in fields of abnormal strength. In his calculations Meek uses the value of 2×10^7 cm per sec. for the velocity. However, since we are considering here the minimum fields necessary for streamer advance, we will use the lowest value for the velocity as observed by Schonland, *viz.* 1.0×10^7 cm per sec.

over the pre-ionized streamer channel the brilliant return stroke operating through ionization by a potential wave traveling up an ionized channel, follows at a speed of 10^{10} cm per second completing the discharge. Later successive strokes (up to 40 have been observed) from the cloud follow down the first spark channel, with its ionization decaying as a result of recombination, as the more distant elements of the cloud release their charge. These discharges consist of what Schonland terms *dart* leaders proceeding from cloud to ground at the rate of 2×10^{8} cm/sec., through the decayed ionization in the old channel, followed by a rapid return stroke from the ground.

b. Meek's Theory of the Stepped Leader Stroke

Meek has investigated the details of the progress of the pilot streamer and shown the origin of the stepped leader without considering the mechanism of the pilot streamer.[62]

In order that the pilot streamer could advance continuously, he assumed that there must be a minimum current, i, flowing into the streamer tip to provide the charge. To calculate this current he also assumed that the field at the streamer tip was 30,000 volts per cm, a field capable of giving streamers with 1 cm of travel of the avalanche. If the pilot streamer channel has a radius of r cm, then the current according to Schonland, $i=\frac{1}{2}Xvr$. Now r was chosen as the diffusion radius of the electron-avalanche in 5 to 10 m of advance, or in 50 microseconds time of travel. This was calculated to be about 0.3 cm from Raether's equation, giving the current i as 0.1 ampere, a not unlikely value. The ion density at the tip is then $\rho=i/(\pi r^2\epsilon v)$ per cm^3 $=1.1\times10^{11}$ with $v=2\times10^{7}$ cm/sec. The values were not quite properly chosen since the ion density is too small to cause streamer formation. Of this more will be said later.

Having determined these conditions, Meek showed that in the 50 microseconds of travel the initial density of ions at the cloud end of the channel had decayed to 10^{10} ions per cm^3 by recombination. With a resistance, R, of the spark path channel calculated from the ion mobilities of 4.6×10^{5} ohms per cm, the iR drop

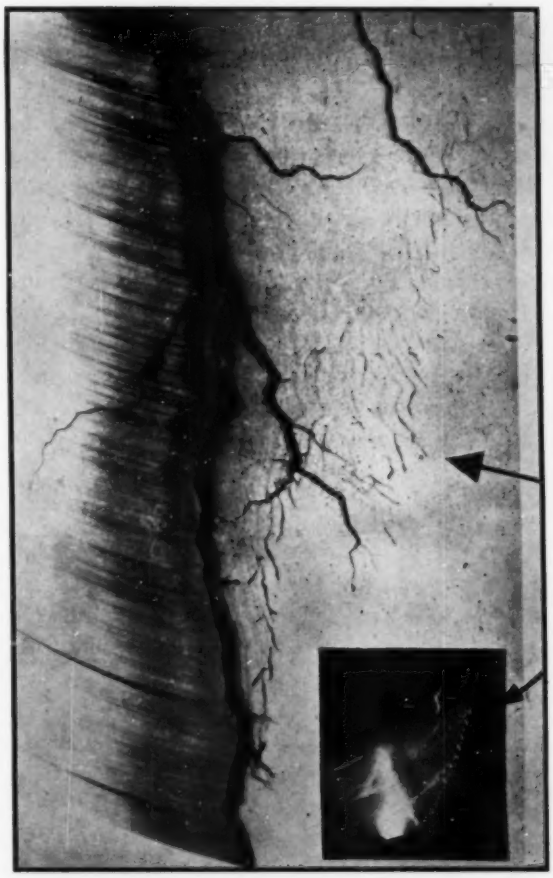

Fig. 15. Photograph taken with a Boys camera to show the development of the stepped leader stroke for the lightning discharge. The direction of motion of the lens which recorded the stroke is from right to left, as shown by the arrow, so that the steps are seen on the right of the subsequent brilliant return stroke. The time interval between each of the steps represents approximately 50μsec. Notice also that the leader stroke corresponding to the branch on the right is well to the right near the arrow while the leader stroke corresponding to the main stroke can be discerned more to the left.

of 4.6×10^{4} volts is sufficient to launch a stepped leader stroke from cloud to pilot streamer tip at the speed of 5×10^{9} cm/sec. This increases the ion density to 10^{14} ions/cm^3 in the channel and reestablishes the conductivity. In the next 50 microseconds the density has by recombination again fallen to 10^{10} ions and a new stepped leader proceeds. The calculations are consistent with the observed data on lightning discharge propagation. The high velocity of the return stroke comes from the density of 10^{14} ions per cm^3 in the stepped leader stroke process which on the Schonland-Loeb and Cravath[61] mechanism

makes such velocities possible. The fact that the decay of ionization by recombination in 50 microseconds to 10^{10} ions/cm^3 is so insensitive to the initial ion density N_0 above 10^{11} ions/cm^3 comes from the recombination equation $N=N_0/(1+N_0\alpha_1 t)$. It lies in the fact that with the coefficient of recombination α_1 in air $=2\times10^{-6}$, $N_0\alpha_1 t=2\times10^{-6}\times5\times10^{-5}\times10^{11}=10$ is greater than 1, and thus N is nearly independent of N_0 but depends on time only.

c. Modification of Meek's Theory in Conformity with Avalanche-Streamer Mechanism

One must now consider the mechanism of the pilot streamer advance. In the light of the mechanism of long sparks one can assume that, when a gradient due to the cloud of 25,000 volts/cm or more is created over a length of some 15 or more cm, a chance electron at the cloud starts an avalanche which proceeds towards the ground at a speed of about 1×10^7 cm/sec. After 15 cm travel this avalanche has built up a density of positive ions of 7×10^{11} charges per cm^3. At this point a retrograde streamer moves to the cloud establishing a conducting channel at its arrival in some 5×10^{-8} sec. or thereabouts. This conducting path is somewhat increased in radius beyond the radius of the avalanche tip which in 15 cm travel is $r=0.052$ cm, owing to the character of the progress of streamer formation as shown in Raether's photographs. The avalanche then forges ahead again for a distance of δ_1 cm and a new streamer propagates backward lengthening the channel of conducting plasma to $15+\delta_1$ cm from the cloud. This process of advance continues for some 50 microseconds until a stepped leader starts and reaches the end of the pilot streamer. The arrival of the stepped leader doubtless increases the tip field of the pilot streamer which forges ahead with a somewhat enhanced speed and perhaps shorter steps before retrograde streamers form, but eventually settles down to the initial procedure. It is possible that the high fields caused by the arrival of the stepped leader at the tip leads to some of the branching observed in lightning discharge.

If then this picture is the correct one for the mechanism of advance of a pilot streamer, the reasoning and figures given above must be altered in detail but not in principle. In principle, Meek's theory assumes that there must be a current i flowing down the streamer channel and that, owing to decay of ionization, the resistance of the streamer channel must decline to a value such that after 50 microseconds the potential gradient caused by the iR drop in the channel reaches values leading to a stepped leader proceeding down a pre-ionized channel having a density of 10^{10} *electrons* per cm^3. It is now necessary in view of the mechanism of streamer advance developed to reconsider the conditions existing. The first of these lies in the criterion for the propagation of the stepped leader. Since recombination is taking place in the channel the negative carriers present must in a large measure be *negative ions*, otherwise the density would not fall to 10^{10} ions/cm^3 in 50 microseconds. While the energy of the electrons and the field strengths in the channel are not known, one can make certain statements. During the early part of the travel of the streamer, it is clear that the fields in the channel will be low as the iR drop is small. If decay by recombination is to proceed the potential gradients must furthermore be well below that corresponding to an $X/p=20$ at which electrons can ionize by impact. Just before the potential wave starts down as a stepped leader, however, both ionization by collision and high electron energies must begin to occur. Under these conditions it is probable that in the early stages electrons will be attaching to molecules to give negative O_2 ions, and the data on rate of attachment indicates that possibly 0.9 of the negative carriers are ions and the rest electrons. Before, however, the step can advance, all the negative ions must suffer electron detachment which requires an X/p of from 70 to 90.[63] Thus in the channel as the ion density falls the carriers are mostly ionic, the iR drop increases and gradients build up leading to ionization by collision, with an attendant sudden increase of gradient between that section and the adjacent region at the avalanche end. In this way quite suddenly fields of the order of 53,000 to 65,000 volts per cm appear at the cloud end of the streamer channel, and the stepped leader starts its advance at a velocity of 2×10^9 cm/sec.

It now becomes essential to consider the value of the current needed in the streamer channel which gives the iR drop. It is at first obvious that the general equation used by Meek and Schonland has no significance in this particular mechanism. One must consider the character and nature of the mechanism in the ionized column set up by streamer formation. As a result of the field X_{s0} which must in the region of advance equal 25,000 volts/cm over the δ_1 cm of avalanche travel, the avalanches create $e^{\alpha\delta_1}$ ions for each of the electrons which advance a distance δ_1. At the end of the $\delta_0=15$ cm of travel if only one avalanche starts, that one electron avalanche has created an ion density of 7×10^{11} ions/cm^3 and a retrograde streamer forms making a plasma in the channel of radius $r\sim5.2\times10^{-2}$ cm with about 10^{13} or more ions/cm^3. Now such a mechanism does not require a current of electrons to maintain itself. All it requires is a potential pulse or wave which moves at about 1×10^7 cm/sec. towards the ground. The plasma must have equal numbers of positive ions and electrons plus negative ions. Hence no current other than a displacement current is needed. This does not contribute to the iR drop as it advances with the tip. If, however, in the advance of the electron avalanche tip there is a loss of electrons as a result of the radial field and lateral diffusion so that the electrons do not remain in the channel later to be occupied by the streamer, negative charges are lost. *These charges must be replenished* to give a neutral plasma and can only do so if they follow down the streamer channel as a current i from the cloud. It is this current that provides the iR drop and leads to the stepped leader mechanism. Thus to calculate i we must calculate the $n=n_1e^{\alpha\delta_1}$ electrons created in the travel of δ_1 before the streamer propagates and from this calculate the electron current i_0 of which a fraction f are lost by diffusion such that $i=fi_0$.

Now it is difficult to evaluate the quantity n_1 which represents the electrons in the avalanche tip which are moving in the field so that they multiply and form the avalanche. Owing to the space charge of the electron avalanche cloud but few of these electrons will be in such a position to produce the avalanche. For the sake of simplicity assume that *only one* electron has the good fortune to form the avalanche.* Setting $n_1=1$, $X_s=24{,}200$ volts/cm, $X_s/p=31.85$, $\alpha=1.47$, $\delta_0=15$ cm, $\alpha\delta_0=22.05$. Hence $n=3.86\times10^9$. This charge is produced in $t=15/v=15/10^7=1.5\times10^{-6}$ sec. Hence $i_0=3.86\times10^9\times4.8\times10^{-10}/1.5\times10^{-6}=1.24\times10^6$ e.s.u., and $i=1.24\times10^6\,f$ e.s.u., where $f\ll1$. To get the potential gradient down the channel we can proceed as follows. The current $i=\pi r^2N_e\epsilon v$, where r is the streamer radius, N_e the electron density, and v the electron velocity. The value of N_+ the *positive* ion density is given by recombination as $N_+=N_0/(1+N_0\alpha_1t)$, with $\alpha_1=2\times10^{-6}$, and t the time of advance of the streamer before stepping, i.e., ~50 μsec. Now again owing to the electron attachment and the required rate of recombination $N_+=N_-+N_e$, with N_- several times (about 9) N_e. Hence if we take N_e as a fraction f_e of N_+, we have

$$i=fi_0=\pi r^2f_eN_+\epsilon v. \tag{10}$$

The value of v is, however, fixed by the electron mobility equation which reads $v=1.23\times10^6\sqrt{X}$ cm/sec. per e.s.u./cm for air at 760 mm as given in conformity with data in Eq. (3A). Inserting this for v in the Eq. (10) and evaluating the constants, the field $X=8.73\times10^7(fi_0)^2/((f_eN_+)^2r^4)$ volts/cm. Inserting the values for $i_0=1.24\times10^6$, $r=5.1\times10^{-2}$ cm, $N_+=10^{10}$, we find $X=2.01\times10^5(f/f_e)^2$. If $f=0.05$ and $f_e=0.1$, the gradient in the channel for streamer advance is $X=50{,}250$ volts/cm. This makes the loss of electrons by diffusion from the avalanche small. It is, however, not inconceivable that this is the case in view of the fields existing. In any case these data are sufficient to indicate the character of the changes needed to bring Meek's theory of the stepped leader stroke into conformity with the present discharge mechanism.

18. Conclusion

We see that the process of spark breakdown is not the simple process originally pictured by the theory of Townsend. It is a complicated group of mechanisms. In the region of low $p\delta$, the

* In conformity with what has been said before, the effect of the n_1 electrons is merely to shorten δ_0 to δ_1 before the next streamer forms. It will increase i_0 in the measure that a shorter δ_1 gives a shorter time of travel to give the needed ion density $N_0=7\times10^{11}$ ions/cm^3. It will also reduce r for the streamer somewhat if $\delta_1<\delta_0$. However with smaller r the value of n to give N_0 is less, so that for convenience one avalanche may be used.

Townsend-Holst mechanism occurs and explains sparking. Above $p\delta \sim 100$ mm×cm, the mechanism is probably one of positive ion space charge streamer propagation with photo-ionization in the gas. Under circumstances where this mechanism is not effective a negative streamer process occurs which requires for its propagation retrograde positive streamers within the negative avalanche which act to conserve the streamer and permit its advance. In very long gaps depending on field conditions breakdown may proceed by either one or both of the streamer mechanisms, but certainly *not* by the Townsend mechanism. What has been said indicates the character of the processes to guide the future study of spark breakdown along more fruitful channels than the classically conceived mechanism has made possible.

The writers desire to acknowledge their gratitude to Dr. E. U. Condon for his careful reading and editing of the paper before submission to publication.

Bibliography

34. L. B. Loeb, *Fundamental Processes of Electrical Discharges in Gases* (Wiley & Sons, 1939), p. 169, 170, 179.
35. M. J. Druyvesteyn, Physica **10**, 69 (1930); **3**, 65 (1936).
36. J. A. Smit, Physica **3**, 543 (1937).
37. Reference 34, p. 186.
38. H. L. Brose and E. H. Saayman, Ann. d. Physik **5**, 797 (1930).
39. L. B. Loeb, Rev. Mod. Phys. **8**, 276 (1936).
40. J. S. Townsend, *Electricity in Gases* (Oxford, 1914), Chapter 10.
41. R. N. Varney, H. J. White, L. B. Loeb and D. Q. Posin, Phys. Rev. **48**, 818 (1935).
42. L. B. Loeb, Rev. Mod. Phys. **8**, 283 (1936).
43. Slight deviations for gases other than air are said to have been observed by H. Fricke, Zeits. f. Physik **86**, 464 (1933) and H. Büttner, Zeits. f. Physik **111**, 750 (1939).
44. F. H. Sanders, Phys. Rev. **44**, 1020 (1933).
45. D. Q. Posin, Phys. Rev. **50**, 650 (1936).
46. S. Whitehead, *Dielectric Phenomena* (Benn, London, 1927), p. 42.
47. W. Rogowski and R. Tamm, Archiv. f. Elektrotechnik **20**, 625 (1928).
48. R. Tamm, Archiv. f. Elektrotechnik **19**, 235 (1928).
49. L. B. Loeb, *Fundamental Processes in Electrical Discharge in Gases* (John Wiley, 1939), p. 422; Rev. Mod. Phys. **8**, 267 (1936).
50. C. Brinkman, Zeits. f. Physik **111**, 737 (1939); W. Rogowski, Zeits. f. Physik **102**, 183 (1936); **106**, 212 (1937); **108**, 1 (1937).
51. J. M. Meek, Proc. Phys. Soc. London, to be published.
52. G. W. Trichel, Phys. Rev. **54**, 1078 (1938).
53. L. B. Loeb, A. F. Kip and G. G. Hudson, submitted for publication in Phys. Rev.
54. T. E. Allibone and J. M. Meek, Proc. Roy. Soc. **A166**, 97 (1938); **A169**, 246 (1938).
55. Waithman and Baker, Phys. Rev. **57**, 252 (1940).
56. J. Jeans, *Electricity and Magnetism* (Cambridge, 5th edition, 1925), p. 186.
57. K. B. McEachron, J. Frank. Inst. **227**, 149 (1939).
58. B. F. J. Schonland and H. Collens, Proc. Roy. Soc. **A143**, 654 (1934); B. F. J. Schonland, D. J. Malan and H. Collens, Proc. Roy. Soc. **A152**, 595 (1935); **A168**, 455 (1938); D. J. Malan and H. Collens, Proc. Roy. Soc. **A162**, 175 (1937); B. F. J. Schonland, Proc. Roy. Soc. **A164**, 132 (1938); B. F. J. Schonland, D. B. Hodges and H. Collens, Proc. Roy. Soc. **A166**, 56 (1938).
59. G. C. Simpson and F. J. Scrase, Proc. Roy. Soc. **A161**, 309 (1937).
60. B. F. J. Schonland, D. J. Malan and H. Collens, Proc. Roy. Soc. **A152**, 595 (1935).
61. B. F. J. Schonland, Proc. Roy. Soc. **A164**, 132 (1938).
62. J. M. Meek, Phys. Rev. **55**, 972 (1939).
63. L. B. Loeb, Phys. Rev. **48**, 684 (1935).

Resumés of Recent Research

Physics of Stressed Solids

A correlation and interpretation of the various empirical data concerning the phenomena of deformation, "flow" or creep, and rupture of a stressed solid are presented in a recent paper by Roy W. Goranson[1] from a consideration of the internal energy stored in the lattice structure of the material. The elastic or potential component of this internal energy is represented by a function having the characteristics of a Condon-Morse potential energy diagram and, if this were the only operative mechanism, release of the stored-up strain energy occurs as rupture in the direction of greatest extension of the lattice structure. This strain energy may, however, also be released by means of a change-of-phase mechanism, solid to fluid to solid, wherein material is transferred from a region of high stress to a region of low stress. For this effect the work received by the system is converted into an activation energy which is equivalent quantitatively to the heat of melting, and the generalized relations are expressed by the thermodynamic potential functions.

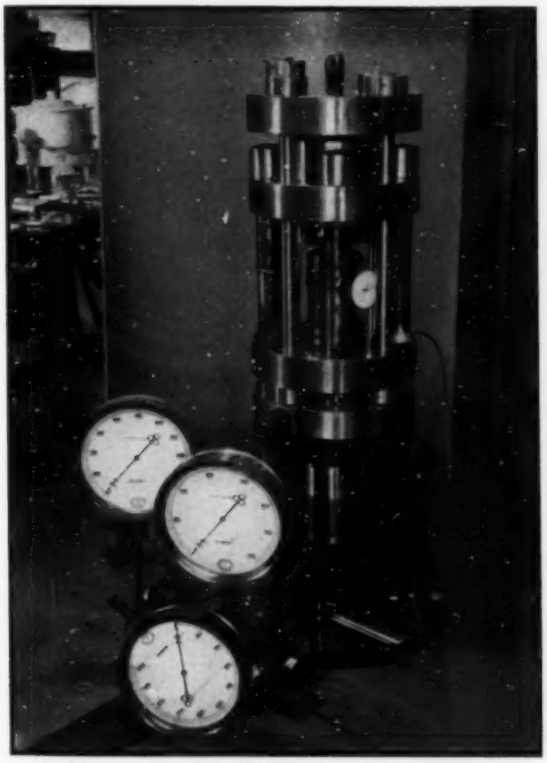

Apparatus designed and used for obtaining very high hydrostatic pressures.

The first type of deformation is an instantaneous effect whereas the latter is a function of time and, in general, these two effects are combined.

If the solid is first compressed under high hydrostatic pressure the elastic strength for a compressive load increases rapidly and eventually becomes infinite. Release of strain energy can then occur only by change of phase—a breakdown by means of a solid-solid transition or by flow.

One of the immediate applications of this hypothesis lies in the experimental attainment of very high hydrostatic pressures by utilizing a cascaded pressure apparatus. With the added stimulus and cooperation of several members of the Department of Terrestrial Magnetism such an apparatus was designed and built at the Geophysical Laboratory of the Carnegie Institution of Washington which has reached pressures consistent with the predictions deduced from this hypothesis.

[1] "Physics of stressed solids," J. Chem. Phys. **8**, 323 (1940).

A New Radiation Pyrometer

A radiation pyrometer recently developed by John Strong[1] makes possible now the measurement of low temperatures of distant objects with an accuracy of 0.1°. The instrument was developed primarily for measuring planetary and lunar temperatures but it can be used, for example, to measure the surface temperature of walls, grass, trees, and the ground.

The infra-red region of the spectrum is involved in the measurement of low temperatures by radiation methods. As a body is heated it becomes "infra-red hot" before it gets "red hot." At ordinary temperatures all bodies are "incandescent" in the region of the spectrum in which the new pyrometer operates.

[1] J. Opt. Soc. Am. **29**, 520 (1939).

The new pyrometer operates on a selected band of radiation centered at 8.8μ. The use of this band avoids variable absorption inherent with the use of a total radiation pyrometer because the 8.8μ band falls in a region of the spectrum where the atmosphere is very transparent.

Spurious results due to stray radiation are avoided by using, instead of a shutter, a hot blackbody at the steam point and a cold blackbody at the ice point.

As auxiliary apparatus, and in addition to the two blackbodies, a sensitive galvanometer is required.

Elastic Moduli of Cu_3Au Through the Order-Disorder Transformation

Theories of the order-disorder transformation based on interactions between nearest neighbor atoms of the lattice have been developed by Bethe and Peierls. The quantum calculations of the elastic constants of single

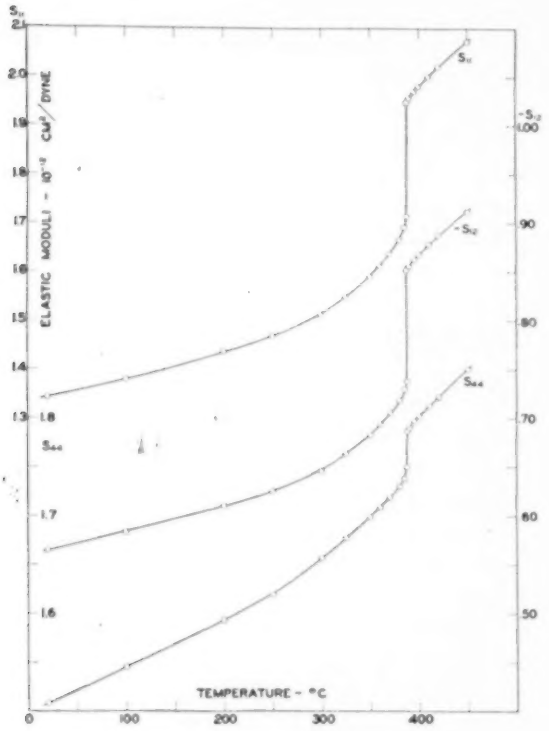

crystals of pure metals are also based in part on such interactions. Support is lent to these theories by the results of some recent experiments* on the elastic moduli of Cu_3Au which were carried out at the Westinghouse Research Laboratories.

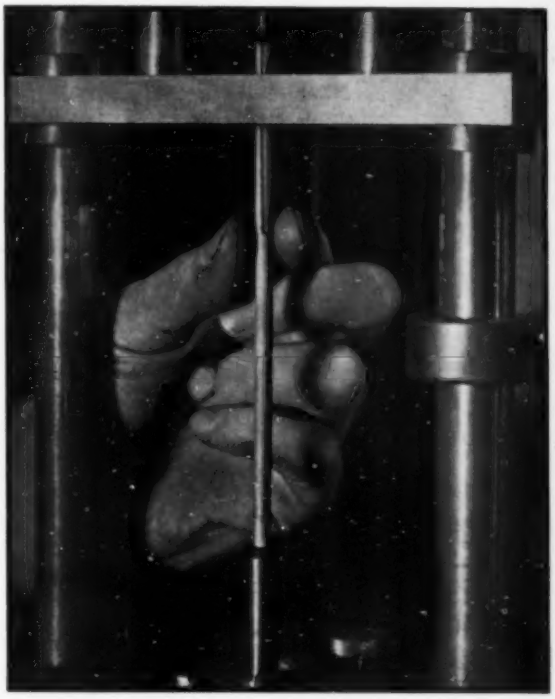

A single crystal rod of Cu_3Au being cemented to a crystalline quartz rod, used to excite mechanical oscillations in the specimen.

Single crystals of the copper-gold alloy Cu_3Au were prepared in a specially designed vacuum furnace, and the principal elastic moduli measured by the composite piezoelectric oscillator method, over the temperature range 20 to 450°C. It is found that at the critical temperature, $T_c = 387.5$°C, where the "degree of order" of the lattice changes abruptly, there is a discontinuous change in all three elastic moduli. Young's modulus in the [100] direction, for example, decreases by about 15 percent due to the change in order at the critical temperature. The shape of the curves above T_c indicates that some degree of local order still persists after the transformation.

Very careful control of the temperature of the specimens is required in the neighborhood of T_c, as the transformation from the ordered to disordered states, and vice versa, is a very sluggish one, requiring several days to go to completion. The experiments seem to indicate that the transformation is of the first kind, and not, as had been supposed, of a higher order.

* Sidney Siegel, Phys. Rev. **57**, 537 (1940).

Here and There

Cover Photograph

The cover photograph shows a two-jet, water-cooled oil diffusion pump of recent design. This model is now in successful operation for the exhaustion of electronic devices. For a detailed discussion of this pump and others of its kind the reader is referred to the article, "Trends in design of fractionating pumps," by Dr. Kenneth C. D. Hickman, which appeared on page 303 of the May, 1940, issue of the *Journal of Applied Physics*.

★

Ohio Science Groups Convene

The fiftieth anniversary of the founding of the Ohio Academy of Science was the occasion of a joint meeting of the Ohio Section of the American Physical Society and the Ohio Academy on May 9–11. The following addresses of particular interest to the physics section were given at the meetings:

Sound Patterns. HARVEY FLETCHER, *Bell Telephone Laboratories, Inc.*
The Development of High Voltage for the Production of Neutrons and Artificial Radioactivity. E. U. CONDON, *Westinghouse Research Laboratories.*
A Comparative Study of Neutron- and X-Radiation Upon Biological Tissues in the Cancer Problem. ISADORE LAMPE, *University of Michigan.*
Industry and Science. CHARLES F. KETTERING, *General Motors Research Corporation.*
Protein Molecule Structure. EDWARD MACK, *Battelle Memorial Institute.*
Cancer-Producing Hydrocarbons. M. S. NEWMAN, *Ohio State University.*
Chemistry Through the Microscope. H. S. BOOTH, *Western Reserve University.*

In addition to the invited papers, a centralized exhibit of ninety-nine projects, numerous fixed exhibits by the various science and engineering departments at Ohio State University, and a tour of a neighboring industrial institution were available to members during the three-day program.

At the annual business meeting of the Ohio Section of the American Physical Society the following officers were elected for the year 1940–1941:

Chairman, PAUL E. MARTIN, Muskingum College, New Concord, Ohio
Vice Chairman, W. E. FORSYTHE, General Electric Company, Nela Park, Cleveland, Ohio
Secretary-Treasurer, RICHARD H. HOWE, Denison University, Granville, Ohio

It was announced by H. P. Knauss, chairman of the program committee, that a symposium on Rubber will be held at Akron, Ohio, on October 12, 1940. This is to be the first symposium of a series upon Ohio's industries, one of which will be sponsored annually by the Ohio Section.

★

Cornell University Medical College

Dr. Detlev W. Bronk, Professor of Biophysics and Director of the Institute of Neurology and of the Johnson Foundation for Medical Physics at the University of Pennsylvania, has been appointed Professor of Physiology and Head of the Department of Physiology and Biophysics at Cornell University Medical College, according to a recent note in *Science*.

Symposium in Theoretical Physics

The annual Symposium in Theoretical physics will be held from June 24 to August 16 at the University of Michigan. Nuclear physics will be stressed, but other subjects will be presented, particularly in the bi-weekly seminars and special lectures. Series of special lectures have been arranged as follows:

Recent developments in the theory of the atomic nucleus, Professor Eugene P. Wigner, Princeton University, throughout the session.
Band spectra, Profes-or David M. Dennison, University of Michigan, throughout the session.
Theoretical aspects of cosmic rays, Professor George E. Uhlenbeck, University of Michigan, throughout the session.
Discussion of recent field theories, especially in connection with the theory of the meson, Assistant Professor Robert Serber, University of Illinois, June 24 to July 7.
Special topics of the theory of radiation and of the theory of radioactivity, Assistant Professor Wendell H. Furry, Harvard University, July 1 to July 14.
Low temperature physics; the properties of liquid helium; superconductivity, Professor Fritz W. London, Duke University, July 7 to July 28.
Recent experimental results in cosmic rays, Professor Bruno Rossi, University of Chicago, July 28 to August 5.

Holders of the Ph.D. degree in any of the physical sciences may attend the lectures as guests of the university without the payment of any fees. Requests for this privilege should be addressed to the President of the University.

★

National Chemical Exposition Planned

The Chicago Section of the American Chemical Society will sponsor the National Chemical Exposition to be held December 11–15 at the Stevens Hotel in Chicago. Eight states and the District of Columbia are represented on the advisory committee of the Exposition.

"It is estimated that approximately 40,000 chemists, chemical engineers, operating engineers, production managers, plant superintendents, buyers and company executives will pass through the exhibits," said Dr. R. C. Newton, Chairman of the Exposition committee. Space application blanks are now available from the Exposition headquarters at 110 North Franklin Street, Chicago.

★

Heating and Ventilating Projects

The American Society of Heating and Ventilating Engineers will actively sponsor a cooperative research project at Rensselaer Polytechnic Institute, Troy, New York, to study sound control problems in air conditioning, according to A. E. Stacey, Jr., chairman of the committee on research.

A. R. Mumford, chairman of the Society's research committee on corrosion, announces that several short lengths of pipe made from different materials and arranged in series are being installed in a number of large New York office buildings for use in a study of corrosion problems. Action of the return condensate from a heating system on the corrosion of the pipe materials is to be observed over a period of time and reported by the committee.

Dr. Isidor Isaac Rabi, Professor of Physics at Columbia University, was recently elected a member of the National Academy of Sciences.

★

Tentative Program

Eighth Summer Conference on Spectroscopy and its Applications at M.I.T.

Monday, July 15, at 9:30 A.M.

Spectroscopic Analysis of Materials

The Physical Basis for Spectrographic Analysis. W. F. MEGGERS, *National Bureau of Standards.*
Visual Methods of Quantitative Analysis. F. H. EMERY, *The Harshaw Chemical Co.*
The Influence of Extraneous Elements in Quantitative Emission Analysis. W. R. BRODE (with E. S. Hodge), *Ohio State University.*
A Precision Method for the Measurement of Diffuse Lines and Its Application to the Spectrum of Tin. W. W. A. JOHNSON (with D. Norman), *New England Spectrochemical Laboratories.*
Temperatures in Spectroscopic Sources Used in Analytical Work. O. S. DUFFENDACK (with J. M. LaRue), *University of Michigan.*

Monday, July 15, at 2:00 P.M.

Spectrographic Apparatus

Specifications and Testing of Spectrochemical Apparatus. R. A. SAWYER (with H. B. Vincent), *University of Michigan.*
New Equipment for Spectrographic Analysis. W. S. BAIRD, *Baird Associates.*
A High Streaming Velocity Arc for Spectrochemistry. M. F. HASLER, *Applied Research Laboratories.*
A New Projection Comparator-Densitometer. J. SCHUCH (with H. W. Dietert), *Harry W. Dietert Co.*
A New Densitometer. W. S. BAIRD, *Baird Associates.*

Tuesday, July 16, at 9:30 A.M.

Applications of Spectrographic Analysis

Spectrochemical Analysis in Agricultural Research. L. H. ROGERS, *University of Florida.*
Some Horticultural Applications of Spectrochemical Analysis. B. C. BRUNSTETTER (with A. T. Myers), *Bureau of Plant Industry, United States Department of Agriculture.*
Geochemical Study of Saratoga Mineral Waters by a Spectrochemical Analysis of Their Trace Elements. L. W. STROCK, *Saratoga Springs Commission.*
A Spectroscopic Study of Central American and Asiatic Jades. D. NORMAN (with W. W. A. Johnson), *New England Spectrochemical Laboratories.*
Determination of the Amount of Mercury Vapor Present in Various Gases. O. S. DUFFENDACK (with R. A. Wolfe and F. Lederer), *University of Michigan.*

Tuesday, July 16, at 2:00 P.M.

Absorption Spectrophotometry

Analysis of the Visible and Ultraviolet Absorption Spectrum of Cytochrome C, with Deductions as to the Electronic Structure of Cytochrome and Hemoglobin Derivatives. D. L. DRABKIN, *University of Pennsylvania.*
Application of Spectrophotometry to the Study of the Hemoglobin Pigments of Cured Meats, with Particular Reference to Variations in the Spectrum of Methemoglobin. W. M. URBAIN, *Swift & Co.*
Measurement of Fast Reactions by Absorption Spectrophotometry. F. KARUSH, *Massachusetts Institute of Technology.*
A Concave Grating-Photoelectric Spectrophotometer. M. N. STATES, (with C. Sheard), *Central Scientific Co.*
A Photoelectric Grating Spectrophotometer. J. L. NICKERSON, *Columbia University.*
A Hydrogen Lamp of High Intensity for Absorption Spectroscopy. A. J. ALLEN, *University of Pittsburgh.*

Wednesday, July 17, at 9:30 A.M.

Spectrographic Measurements on Vitamin A Materials. R. MCFARLAN, *United Drug Company.*
Properties and Use of a High Frequency Spark Discharge for Local Micro-Analysis. S. E. Q. ASHLEY (with W. M. Murray and B. Gettys), *General Electric Co.*
Electrode Concentrations and Total Intensity of Spectral Lines. H. HEMMENDINGER, *Massachusetts Institute of Technology.*
Emission Spectra of the Rare Earth Elements and Their Application in Analysis. W. F. MEGGERS, *National Bureau of Standards.*
Some Future Possibilities of Spectrographic Analysis. G. R. HARRISON, *Massachusetts Institute of Technology.*

Wednesday, July 17, at 2:30 P.M.

Absorption Analysis and Miscellaneous

On the Characteristic Function of the Photographic Plate. J. SHERMAN, *United States Navy Yard, Philadelphia.*
Spectrophotometric Studies by Photoelectric and Spectrographic Methods between λ3000–1500A. E. S. MILLER (with D. M. Kerns, R. Belkengren, and H. Clark), *University of Minnesota.*
Spectroscopic Determination of Atmospheric Ozone. B. O'BRIEN, *University of Rochester.*
Spectroscopic Study and Molecular Constitution of Thionine Solutions. L. F. EPSTEIN (with F. Karush and E. Rabinowitch), *Massachusetts Institute of Technology.*
Comparison of Prism and Sector Photometers for Measurements of Concentration by Absorption. L. HARRIS, *Massachusetts Institute of Technology.*

★

Franklin Institute Awards

The Franklin Institute of the State of Pennsylvania, Philadelphia, announces the following recipients of the 1940 Medal Awards particularly interesting to physicists:

The Edward Longstreth Medal, presented for the purpose of encouraging invention:

Leopold Godowsky, Jr., and Leopold Damrosch Mannes, Eastman Kodak Company, Rochester, New York; developers of the Kodachrome Film;

Games Slayter, Vice President, Owens-Corning Fiberglas Corporation, Newark, Ohio; who devised improved methods and apparatus for making spun and blown glass filaments;

Richard L. Templin, Chief Engineer of Tests, Aluminum Company of America, New Kensington, Pennsylvania; whose application of mechanisms resulted in the development of the Templin Automatic Autographic Deformation Recorder.

The John Price Wetherill Medal, for discovery or invention in the physical sciences, or for new and important combinations of principles or methods already known:

Laurens Hammond, President, Hammond Instrument Company, Chicago, Illinois; developer of the Hammond Organ.

The Louis E. Levy Medal, awarded to the author of a paper of especial merit, published in the *Journal of the Franklin Institute:*

Charles Rosenblum, Instructor in Physical Chemistry, Princeton University; and John R. Flagg, Instructor in Chemistry, University of Rochester; authors of a paper entitled "Artificial Radioactive Indicators."

The Franklin Medal, "to those workers in physical science or technology, without regard to country, whose efforts . . . have done most to advance a knowledge of physical science or its applications":

Arthur Holly Compton, Ryerson Physical Laboratory, University of Chicago; experimenter on various properties of x-rays and discoverer of the Compton effect;

Leo Hendrik Baekeland, President (retired), Bakelite Corporation, New York City; contributor to the industrial arts, and, in particular, inventor and manufacturer of the synthetic product, Bakelite.

★

Dr. George Glockler, Professor of Physical Chemistry at the University of Minnesota and a member of the staff of the School of Chemistry since 1926, has been elected head of the Department of Chemistry of the State University of Iowa, *Science* reports.

Contributors to This Issue

R. B. Jacobs

Robert B. Jacobs received his B.S. and Ph.D. degrees from the California Institute of Technology. He has held the positions of National Research Fellow and instructor in physics at Harvard University, and is at present a Lalor Fellow in Physical Chemistry at Massachusetts Institute of Technology.

Albert B. Martin

Albert B. Martin is doing graduate work at Yale University. He received his B.S. degree from the University of Wyoming in 1937 and his M.S. degree in physics from the same institution in 1939.

J. L. Fowler

Carl A. Cinnamon received his B.A. and M.A. degrees from the University of Wyoming in 1925 and 1930, respectively. He also attended the universities of Colorado, Chicago, and Iowa, and in 1934 received his Ph.D. degree in physics from the State University of Iowa. In 1925 he was appointed Instructor of Physics at the University of Wyoming where he is now Associate Professor of Physics.

C. A. Cinnamon

J. L. Fowler has been since 1938 a research assistant and graduate student at Princeton University. He received his A.B. degree in physics from the University of Tennessee and his M.S. in physics from the same University in 1938.

Kenneth L. Hertel went to the University of Tennessee after receiving his Ph.D. from the University of Chicago in 1926. Since 1935 he has been Head of the Department of Physics and engaged in textile fiber research as physicist for the Agricultural Experiment Station.

S. C. Collins

Saul Levy received his Ph.D. degree in physics from the German University in Prague in 1927. He did research on optics at the University in Prague, at the Kaiser-Wilhelm Institute for Physical Chemistry in Berlin-Dahlem, and at the University of Moscow.

K. L. Hertel

The following contributors have received mention in earlier issues of the *Journal of Applied Physics:*

L. B. Loeb, **8**, No. 7, 491 (1937).
J. M. Meek, **11**, No. 6, 449 (1940).
R. A. Sawyer, **10**, No. 11, 767 (1939).

S. C. Collins, Assistant Professor of Chemistry at the Massachusetts Institute of Technology, received the B.S. and M.S. degrees at the University of Tennessee and the Ph.D. at the University of North Carolina. His research work is concerned with the thermodynamic properties of gases and the development of apparatus for producing low-temperature refrigeration.

Saul Levy

H. B. Vincent has been a member of the Department of Engineering Research at the University of Michigan since 1927 and Research Physicist in that Department since 1930. His work on industrial developments has included such fields as acoustics, elasticity, thermodynamics, and spectroscopy. A photograph of Dr. Vincent appeared on p. 163, Vol. 8, No. 3 (1937).

Contributed Articles

A Correlation Method for the Elimination of Errors Due to Unstable Excitation Conditions in Quantitative Spectrum Analysis

SAUL LEVY*
Perth Amboy, New Jersey
(Received January 10, 1940)

THE quantitative determination of the composition of substances by spectroscopic means (quantitative spectrum analysis) is not very old. Its development required not only the improvement of spectroscopic equipment but also a better understanding of the phenomena which accompany the emission of spectral lines. At the present time, quantitative spectrum analysis has achieved a high degree of perfection as far as speed and accuracy are concerned. The methods employed in this field are finding more and more applications in industrial laboratories and still greater application is to be expected in the future.

Quantitative spectrum analysis, however, is still attended by some difficulties which retard its development and expansion. The difficulties at the present time are not so much in the field of intensity (or density) measurements, the technique of which is near to perfection, but in a certain instability and insufficient reproducibility of line-excitation. In other words, the difficulties lie in the light sources.

Workers in this field have suggested various improvements in equipment to overcome these difficulties, the best known of which is the so-called Feussner[1] method with synchronous interrupted discharge.

Although increasing the stability and improving the standardization of excitation conditions are very desirable, nevertheless improvements in equipment alone can hardly remove the difficulties in a radical way. The reasons for the instability of "burning" of the arc or spark are various. All the electrical parameters: voltage, current, self-inductance, capacitance, and resistance have an essential influence on the intensity relations of spectral lines. But while it is not difficult to maintain the constancy of these parameters, there are many other factors, not so easy to control, which influence the discharge and, therefore, the intensity relations.

Particularly important is the influence of the shape and structure of the electrodes on the discharge. A solid electrode gives a different result than do chips or powder; moreover, with solid electrodes of definite shape, the analysis is not always accurate. Sharp edges or little defects in the electrodes, such as holes or insertions of particles of other metals, can cause a noticeable change in the discharge; in fact a spark discharge can, in this way, be transformed into one similar to an arc discharge. The length of spark or arc, which is not always equal to the distance between the electrodes, has also an influence on the intensity relations. The discharge is moving from one place to another, and its length is changeable. This cannot and should not be avoided, because it is desirable in most cases to make use of a considerable surface for getting a good average.

There are many cases, too, when it is impossible to give a definite shape to the electrodes, as for example when they are very small and cannot be made up in a mechanical way (grain of gold, etc.), or when they are ready-made objects.

The application of standard working curves (relations between concentration and intensity ratio under standard conditions) is in all these cases questionable, for they are obtained usually with electrodes of other shape. On the other hand, the preparation of standard working curves for different shapes of electrodes would be too laborious.

The influence of extraneous impurities has to be mentioned separately. This problem has been

* Formerly member of the Physical Institute of the University of Moscow.
[1] O. Feussner, Archiv. f. Eisenhuettenwesen **6**, 551 (1933).

discussed in the last few years in many papers, and the influence determined in many cases. Twyman, Duffendack, Breckpot, Brode and many others[2] investigated the influence of extraneous metals on relative line intensities. Such influences have to be tested in every given case separately, and if stated, many working curves have to be made for different concentrations of the extraneous impurity. Each working curve, however, requires a series of repeated spectrograms, and takes much time. Besides, one has to know what kind of extraneous impurities there are and in what quantities.

These considerations show that improvements in equipment alone cannot remove some of the difficulties of quantitative spectrum analysis. Therefore an attempt is made in the present paper to indicate another way of eliminating these difficulties. This procedure is essentially the same that was applied by Naedler[3] in the determination of platinum and rhodium in silver where the change of excitation conditions was caused through the various shapes of small electrodes. It is the opinion of the author under whose supervision this method was elaborated (in the laboratory of Professor Landsberg of Moscow University) that it should be useful in many other cases, including the influence of extraneous impurities. Although the method has its greatest application to widely varying excitation conditions, it may also be profitably used under "normal" conditions to improve the accuracy of an analysis.

The method is a simple and natural development of the fundamental principles of quantitative spectrum analysis as given by Gerlach and Schweizer.[4] Let us first outline the method of Gerlach and Schweizer:

1. The concentration of the "impurity" is determined by measurements, in the same spectrogram, of the intensity (or density) ratio of a line of the impurity and one of the main substance. These two lines are chosen to satisfy the condition that they react approximately in the same way when excitation conditions are changed. They were therefore called by Gerlach the "homologous" pair. 2. The constancy of excitation conditions is checked by means of observation (without actual measurement) of a "fixation pair"; i.e., of a pair of lines of the main substance whose intensities are equal under the desired working conditions, but which react in a different way when the conditions change. When the two lines show different intensities, it is a proof that the excitation conditions have deviated from the standard, and the spectrogram is to be rejected. The method of Gerlach and Schweizer is sufficient for an accurate analysis, *if and when it is possible to maintain constant conditions*, but this is not always possible, as we have seen above.

The method which will be described below in detail, consists of a combination of *actual measurements* on two pairs of lines, the working pair and the fixation pair. We choose as the working pair any two arbitrary lines, one from the main substance and one from the impurity, which may or may not react in the same way when excitation conditions are changed. For the fixation pair, two lines from the main substance are chosen which react in a *different* way when excitation conditions are changed. As we shall see, there is a definite correlation between the intensity ratios in both pairs, *which does not depend on that particular factor which has caused the change of excitation;* i.e., on the change of electric parameters, or the shape of electrodes, or the distance between them, or the influence of extraneous elements. This correlation can be easily determined by deliberately changing one of those factors, for instance by varying the self-inductance of the spark circuit. The analysis is then made with the aid of both the correlation curve and the working curve. The method is based on some known facts concerning electrical discharges in gases, which are briefly summarized in the following paragraphs.

Low Pressure Discharge

The investigations of Langmuir[5] and his collaborators have demonstrated that, in the positive column of a discharge, even at relatively low

[2] See W. Brode, *Chemical Spectroscopy* (John Wiley & Son, 1939).

[3] W. W. Naedler, Compte-rendus de l'Acad. des Sciences, U. R. S. S. **4**, 23 (1935); Tech. Phys. U. S. S. R. **4**, 553 (1936).

[4] W. Gerlach and E. Schweizer, *The Foundations and Methods of Chemical Analysis*, etc. (Adam Hilger, London, 1930).

[5] I. Langmuir and E. Mott-Smith, Gen. Elec. Rev. **26**, 731 (1923); Phys. Rev. **28**, 727 (1926).

current densities, an approximately Maxwellian distribution of electron velocities is formed which depends on the gas pressure. Between the quantity T_e, which has in the Maxwell expression the same meaning as the temperature in the corresponding gas kinetic formula, and the average velocity of the electrons $\bar{V}$ (in volts) is the relation:

$$e\bar{V} = \tfrac{3}{2}kT_e,$$

where e is the electronic charge, k is the Boltzmann constant, and T_e is called the electron temperature of the discharge. T_e at low gas pressures is of the order of 20,000°–40,000°K, and decreases when the pressure increases.

The reason for the formation of a Maxwellian distribution of electron velocities is the collisions between the electrons and the atoms. It can be expected, therefore, that the inelastic collisions which excite the atoms will lead to an analogous distribution of the potential (excitation) energy of the atoms. In fact, as Kopfermann and Ladenburg[6] have shown, the numbers of excited atoms in the various energy levels correspond to a Maxwell-Boltzmann distribution, the temperature of which is equal to the electron temperature (about 20,000°K) while the gas temperature of the discharge (from Doppler-effect)[7] is 300–400°K. The measurements were taken in a neon discharge tube at about 1 mm pressure and about 1 amp. per cm² current density. Kopfermann and Ladenburg also deduced theoretically that the assumption of a Maxwellian distribution of electron velocities in conjunction with "collisions of the second kind"[8] leads to a Maxwell-Boltzmann distribution of the atoms among the energy levels.

Let N_k be the number of excited atoms in an upper state k, N_j the number in a lower state j, which may also be an excited state. Then for statistical equilibrium,

$$N_k/N_j = Ae^{-h\nu/kT_e},$$

where $h\nu$ is the energy difference between the two states, T_e is the electron temperature, and A is a constant equal to the ratio of the statistical weights of both states. In other words, the energy levels are occupied by the atoms in the same relative number as in the case of thermal excitation at the corresponding temperature.

Free Arc

Similar conditions exist in the positive column of a free arc discharge (at a pressure of 1 atmos.), as was shown by Mannkoppf.[9] The difference is only that in the arc because of the high pressure, the electron temperature is practically equal to the gas temperature. Therefore we can say that the excitation in that part of the arc is a thermal excitation.

In the cathode layer of the arc the conditions are very different from those of the other part.[10] It is usually accepted[11] that the excitation there corresponds to a high electron temperature, but, as far as the author is aware, no investigations have been made concerning the distribution of the excitation energy of the atoms in that layer. It is possible that there is no statistical equilibrium due to the lack of time (few collisions). Therefore the cathode layer has to be treated separately. However, as Mannkoppf and Peters have shown, the excitation in this layer is remarkably stable—much more so, in fact, than in the positive column.

Free Spark

Photographs by Kaiser and Wallraff,[12] taken with the aid of a rotating mirror in a manner first described by Fessenden, show with particular clarity that the radiation of a spark in air at atmospheric pressure consists essentially of two parts: the radiation of the purely periodic discharge with a lifetime of from 10^{-6} to 10^{-5} sec., and the radiation of the hot vapors with a lifetime up to 10^{-3} sec. This latter part of the radiation is the more important one and represents the greater part of the total light. It is pure temperature radiation. Kaiser and Wallraff demonstrated further by means of an oscillo-

[6] H. Kopfermann and R. Ladenburg, Naturwiss. **19**, 513 (1931); R. Ladenburg, Rev. Mod. Phys. **5**, 243 (1933).
[7] R. Ladenburg and S. Levy, Zeits. f. Physik **65**, 189 (1930).
[8] See A. C. G. Mitchell and M. W. Zemansky, *Resonance Radiation and Excited Atoms* (University Press, Cambridge, 1934), p. 57.
[9] R. Mannkoppf, Zeits. f. Physik **86**, 161 (1933).
[10] R. Mannkoppf and E. Peters, Zeits. f. Physik **70**, 444 (1931).
[11] See W. Rollwagen, Spectrochimica Acta **1**, 66 (1939).
[12] H. Kaiser and A. Wallraff, Ann. d. Physik **34**, 297 (1939).

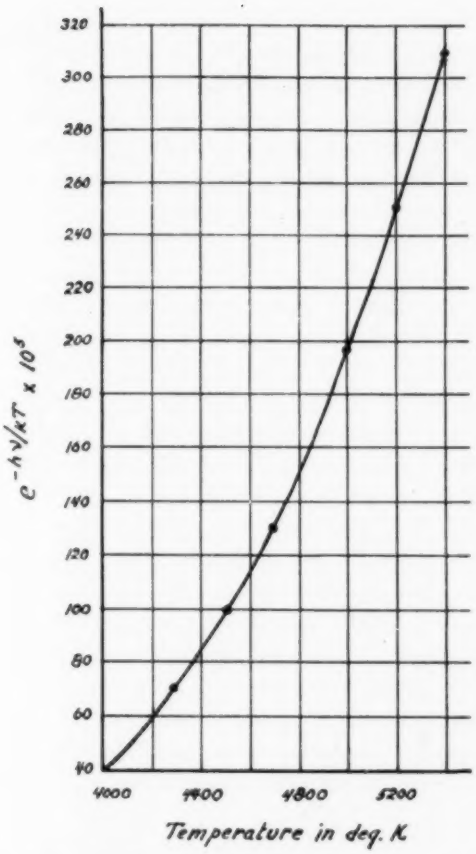

FIG. 1. Graph of $e^{-h\nu/kT}$ against T with $h\nu$ equal to 4.24×10^{-12} erg, corresponding to ν equal to 6.5×10^{14} sec.$^{-1}$.

graph that the spark discharge is really a high frequency arc of low voltage (about 50 v). It is highly probable that the radiation of the first part of the spark discharge is also temperature radiation, like the radiation of a free arc, where the electron temperature is equal to the gas temperature. However, even if it is not so, we can be sure that the excitation energy in the first part of the discharge is also distributed statistically because of the high pressure of the gas.

DEGREE OF IONIZATION

The degree of ionization, as is well known, can be calculated from the equation of Saha,[13] which gives the ionization as a function of the temperature and pressure. Langmuir showed that in a discharge at low pressure there is no one temperature for particles of various kinds, but many "temperatures" for each kind. The ionization therefore cannot be calculated in a simple way, unless complete thermal equilibrium exists. We see now that this calculation is possible in a free spark or arc, and not possible in a Geissler tube at low pressure. Therefore we can say that the neutral and the ionized atoms in a spark or in an arc at atmospheric pressure are in a thermal equilibrium, which may not be true in case of a discharge at a lower pressure.

The curve $e^{-h\nu/kT}$ showing the relative numbers of atoms which occupy two energy levels with energy difference $h\nu = 4.24 \times 10^{-12}$ erg ($\nu = 6.5 \times 10^{14}$ sec.$^{-1}$), as a function of the temperature in the interval between 4000 and 5400°K is shown in Fig. 1. The relative atom number for $T = 4500$°K is 1 : 1000. We see that over a relatively large temperature interval this ratio changes almost linearly with temperature. A change of temperature of 100°K causes a change in the ratio of about 20 percent.[14]

So long as the intensities of spectral lines are proportional to the number of atoms, the intensity ratios are proportional to the Boltzmann factor plotted in Fig. 1. This is true for radiation from a small volume element of the gas in which reabsorption does not take place. Intensity relations are altered when one is dealing with the radiation from a finite volume (large concentration of the atoms in the lower states, great probability of transition). The ratios are not represented by the Boltzmann factor any more, but are still a function of the temperature. The influence of a change in thickness of the emitting layer will be discussed later on. Strictly speaking, there is no one temperature that may be associated with an arc or spark, but rather a distribution of temperature, for the outer parts of the discharge are cooler, and we have in a cross section of the discharge a superposition of many Boltzmann distributions.

Summarizing we can say that the intensity relations of the lines in a spark and in an arc (except maybe for the cathode layer) are determined by the temperature. This is true as well for the radiation of neutral atoms as that of

[13] M. N. Saha, Zeits. f. Physik **6**, 40 (1921).

[14] The change of temperature of 200°K at 9000°K causes only a 4 percent change in the ratio. This is one of the reasons why the spark, whose temperature is much higher than that of the arc, is more stable.

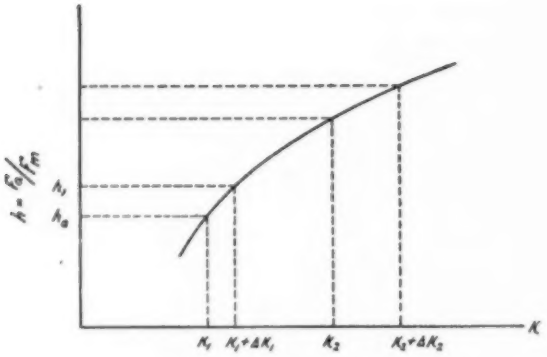

FIG. 2. Concentration of an impurity in percent of the main substance. A typical working curve. Ratio of the impurity line to that of the line of the main substance plotted against concentration of the impurity.

ionized atoms. In a Geissler tube it is true only for the radiation of neutral atoms at high current density.[15] Therefore, *we can change the intensity relations only through variation of the temperature.* Mannkoppf has expressed this very clearly with regard to the influence of an extraneous element on the arc by pointing out that the only influence of an extraneous element is a change of temperature, and that therefore the "sensitized fluorescence," discovered by Franck, i.e., a selective mutual influence of certain energy levels, is impossible in an arc at atmospheric pressure.

We can add now that this is also impossible in a free spark. As to the Geissler tube, the same statement may be made at least with regard to the radiation of the neutral atoms at high current density. *The fluctuations in the light sources caused by any factor are accompanied by the change of temperature.*

These considerations justify the application of the following procedure:

DESCRIPTION OF THE CORRELATION METHOD

The working pair may consist of arbitrarily chosen lines (of the impurity and the main substance) which are convenient for photometric measurements. The choice of the fixation pair is determined only through the condition, that the energy difference of the two excited states should be large enough to cause a noticeable change of intensity ratio while the temperature is changing. This condition can be always satisfied if one of the lines belongs to neutral atoms and the other to ionized atoms, although this is not necessary. In an arc or spark the use of "spark" lines for one of the lines is justified; in a discharge tube at lower pressure it is questionable.

The working curve is to be found in the usual way. Let $h = F_a/F_m$ be the intensity ratio of the working pair (h pair), which is a function of the concentration k of a in m (see a typical working curve in Fig. 2), and $f = F_1/F_2$ the intensity ratio of the fixation pair (f pair). It does not matter whether we work with the actual intensity ratios or with some function of them which is better to measure. The f ratio has to be kept constant while taking the whole series of spectrograms for the working curve: $f = f_0 = \text{const.}$ It is convenient to choose an f_0 value for that purpose which is approximately in the middle of the values corresponding to the extremes of temperature which can be expected.

The determination of the relationship between the intensity ratios in both working and fixation pairs while the temperature is changing has to be made in the following way: Let us vary one (or many) of the parameters which have an influence on the discharge and therefore on its temperature, for instance, the self-inductance of the spark circuit, preserving at the same time the concentration of the impurity in the electrodes, say $k = k_1$. To each value of the varying parameter we will get a pair of values of f and h.

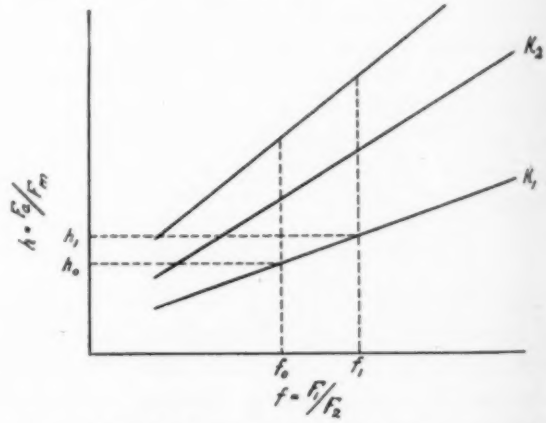

FIG. 3. Correlation curves for various concentrations. Intensity ratio of the working pair plotted against the intensity ratio of the fixation pair under continuous variation of excitation conditions.

[15] The higher the excitation potentials, the higher is the necessary current density. The excitation potentials for neon are about 16-18 volts, whereas, for metallic elements they are 5–10 volts.

We plot the h values against the corresponding f values and get in this way the "correlation curve" for the concentration k_1 (Fig. 3). For other concentrations k_2, k_3, etc. we obtain curves which naturally differ from one another. Then we take from one of the correlation curves, say for the concentration k_1, a pair of corresponding values of f and h, say f_1 and h_1. We see by means of the working curve in Fig. 2 that, because of the change of temperature indicated by f_1, we would obtain the value h_1 instead of h_0. This value of h_1 corresponds to the concentration $k_1+\Delta k_1$ instead of k_1, making a relative error $\Delta k_1/k_1$ which may be positive or negative. Hence, in order to obtain the right result, we have to divide our result by a reduction factor R where $R=1+\Delta k_1/k_1$. Since to each f value (i.e., to each temperature value) belongs a certain R, we can plot $R=1+\Delta k/k$ as a function of f. In this way we get the "reduction curve" (Fig. 4).

It has to be stressed *that the reduction curve for a certain working curve does not depend on that particular concentration by means of which the correlation curve was made* (see section, Discussion of the Method). Nevertheless, in order

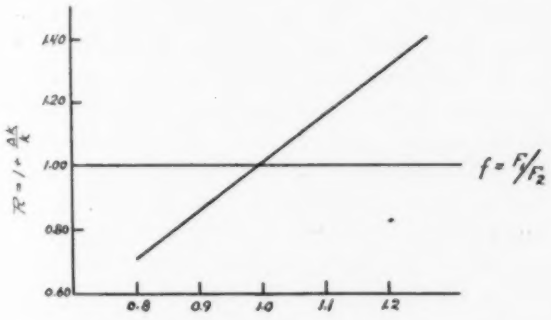

FIG. 4. Example of a reduction curve. Reduction factor $R=1+\Delta k/k$ plotted against the intensity ratio of the fixation pair.

to increase the accuracy of the reduction curve it is useful to plot it by means of many correlation curves. Since the correlation curves are practically straight lines,[16] it is sufficient to take only two points in order to plot the whole curve.

The correct determination of the concentration of an impurity in an unknown sample is made as follows: the h and f ratios are measured on the spectrogram, then the concentration determination k (in the first approximation) is made by means of the h ratio and the working curve in the usual way, and then R is determined by means of the f ratio and the reduction curve. The correct result is k/R.

[16] The ratio of two spectral lines (see Fig. 1) is within certain limits an almost linear function of the temperature, consequently the connection between f and h is also linear.

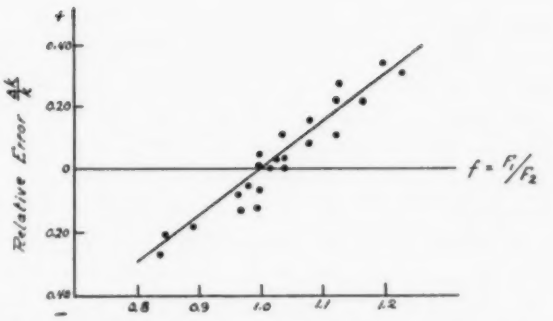

FIG. 5. Correction curve from Naedler's paper. $\Delta k/k$ (equivalent error produced by a change in excitation conditions) plotted against the intensity ratio of the fixation pair. The dots are the actual measurements for plotting the correction curve.

As an example, a typical curve is shown in Fig. 5 taken from Naedler's work on the determination of platinum and rhodium in silver. The light source was a spark and the photometric measurements were made with a logarithmic sector. The silver electrodes were very small and of different shapes. $f=F_1/F_2$ is the intensity ratio of two Ag lines 2744A and 2722A ("fixation pair"), Δk is the corresponding correction to the analysis in percent for platinum. The curve was used in conjunction with the working pair 3043A Pt and 3099A Ag. The mean error of a single determination of Pt before the correction was ± 18 percent; after the correction (using the same spectrogram) ± 9 percent; whereas for Rh, the mean error before correction was ± 21 percent and after correction ± 13 percent.[17]

DISCUSSION OF THE METHOD

The correlation curves obtained at different concentrations have different slopes because of reabsorption, which depends on the concentration. Therefore the change of the relative number of atoms does not cause a proportional change of the intensity ratio. But the slope of the corre-

[17] The remaining rather large error was mostly due to the unsatisfactory quality of the photographic plates and unsufficient accuracy of the measurements with the logarithmic sector.

sponding part of the working curve depends on practically the same reabsorption.[18] If the slope of the correlation curve corresponding to the concentration k_2 is smaller than that corresponding to the concentration k_1, then the corresponding $\Delta k/k$ will still be practically the same, because of the smaller slope of the working curve at k_2. Therefore, the value of $\Delta k/k$ corresponding to a certain f value is the same for all concentrations. This is rigorously true so long as $\Delta k/k$ is small, i.e., so long as the slope of the working curve in the interval Δk does not change very much. A value of $\Delta k/k$ equal to 0.3 or 0.4 can usually be regarded as "small." This is the range of values brought about by the influence of the temperature variation that usually occurs in spectroscopic practice. Otherwise, when $\Delta k/k$ is very large, one reduction curve for all concentrations can no longer be used, and one has to use the corresponding correlation curves.

The intensity ratios are in fact not only a function of the temperature, but also of the "thickness" of the emission layer (because of reabsorption), when one is dealing with a considerable concentration of atoms in the lower states or with great transition probabilities of the lines. Furthermore, a substantial change of the conditions (great variation of current density, etc.) can cause a change in vapor density which also influences the reabsorption. It is important to know the extent to which the correlation curves are affected by a change of reabsorption, in other words, to know the limits of the method. *This question can be answered only through experiment in every doubtful case.* The method is applicable so long as the correlation curves do not change appreciably. In general, the change of the vapor density on the correlation curves will be an effect of the second order.

It is not necessary to measure the intensity of four lines in order to plot and to use the working and the correlation curves. One can avoid the fourth measurement and use only three lines. For instance, F_m can be equal to F_1 or F_2. Moreover, two lines of the impurity can also be used for the "fixation pair."

For the concentration determination one usually uses more than one working pair. An average is usually taken from the results from two or more h pairs from the same spectrum. This procedure is correct, if the divergence of the determination by both pairs is caused only through accidental errors of the measurements. It is not correct, when the divergence is caused by a change of excitation conditions. The correlation curve can be taken in this case with the aid of two lines of the impurity. The average of the results should be taken only after the correction. The advantage of using the lines of the impurity for getting the correlation curves is that no more measurements are required than before.

Application to a "normal" analysis

The correlation method permits one to work under nonstandardized conditions with satisfactory results. It will also diminish the mean error while working under standard conditions by eliminating the fluctuations of the light source. As well known, the mean square error R of the result depends on the partial mean errors $r_1, r_2, r_3, \cdots$ according to the equation

$$R^2 = r_1^2 + r_2^2 + r_3^2 + \cdots.$$

Assuming that the irregularities of the photographic plate cause an error of analysis r_1 of about ± 1.5, and a photometric error r_2 of about ± 1.5, then with a total error $R = \pm 5$ percent,[19] we get for r_3, the error due to irregularity of the source, about ± 4.5 percent. We see therefore that the main error of the analysis in this case is caused by a change of temperature in the source and perhaps through insufficient homogeneity of the sample. The correlation method permits us in this case to eliminate r_3 and separate it from r_4, the error due to inhomogeneity. After r_3 is found as the mean correction from the reduction curve, we determine r_4, which characterizes the influence of the inhomogeneity on the accuracy of the particular method of analysis.

Summary

It is pointed out that some difficulties associated with quantitative spectrum analysis cannot be removed through improvements in equipment only.

A survey of the most important light sources

[18] The temperature influence on the reabsorption is negligible.

[19] See for example J. A. C. McClelland and H. Kenneth Whaley, Spectrochimica Acta **1**, 21 (1939).

for quantitative spectrum analysis shows that the radiation of all of them is determined by only one quantity which is either the gas temperature or the electron temperature, the latter of which is in some cases higher, in others equal to the gas temperature of the discharge. The excitation energy is therefore distributed among the excited states of the atoms statistically, and the number of atoms in the various energy levels is determined uniquely by the electron or gas temperature. Consequently the intensity ratio of two lines is related to the intensity ratio of two others. A "correlation method" is described, which permits one to work at nonstandardized conditions (variation of the shape of the electrodes, influence of extraneous elements, etc.) while reducing the measurements to "normal" (standard) conditions. The method may also be profitably used under standard conditions to improve the accuracy of an analysis while eliminating errors due to accidental fluctuations in the light sources.

In conclusion, the author would like to express his sincerest thanks to Professor Mark W. Zemansky for many helpful discussions and suggestions.

Growth Conditions for Single and Optically Mosaic Crystals of Zinc

C. A. Cinnamon and Albert B. Martin*
Physics Department, University of Wyoming, Laramie, Wyoming
(Received January 30, 1940)

A modified Kapitza method used in the study of conditions favorable to the growth of single crystals of zinc (99.99+ percent pure), shows that the ratio of the temperature gradient (across the interfacial boundary between the liquid and solid phases) to the rate of growth of the crystal must be maintained within an optimum range of values, depending on the angle of orientation. Optically mosaic crystals give no indication of a preferred region of growth and can be obtained over a much wider range of conditions.

Introduction

THE modified Kapitza method of growing single crystals of zinc as described by Cinnamon[1] and used by other investigators[2–4] has met with a fair degree of success. However, a more recent application of this method has resulted in the production of a large number of optically mosaic crystals[5] compared to the number of single crystals.[6] In this respect difficulties arise quite similar to those experienced by investigators[7,8] employing the Czochralski-Gomperz method.

The study of factors influencing the growth of single-crystalline zinc, as initiated by Cinnamon, was but partially completed, in that only the lower limit to the region of favorable growth had been determined. The existence of a lower limit region was later qualitatively confirmed by Poppy[2] and Way,[3] who used the same method and procedure for crystals of approximately the same size and degree of purity. The growth conditions imposed by Jauncey and Bruce[4] also agree reasonably well, considering the difference in cross-sectional area and the possibility of differences in impurities. Poppy, also, found indications of an upper limit to the favorable conditions as predicted by Cinnamon; however, his data were not extensive enough to set a definite

* Now at Yale University, New Haven, Connecticut.
[1] C. A. Cinnamon, Rev. Sci. Inst. **5**, 187 (1934).
[2] W. J. Poppy, Phys. Rev. **46**, 815 (1934).
[3] H. E. Way, Phys. Rev. **50**, 1181 (1936).
[4] G. E. M. Jauncey and W. A. Bruce, Phys. Rev. **50**, 408 (1936).
[5] A description of optically mosaic crystals of zinc and photomicrographs of natural cleavage surfaces are given by H. K. Schilling, Physics **5**, 1 (1934).
[6] A single crystal, when properly cleaved, is characterized by a single, flat and mirror-like cleavage surface in contradistinction to the optically mosaic crystal having a "broken" cleavage surface consisting of discontinuities caused by two or more slightly inclined areas.
[7] H. K. Schilling, Physics **6**, 111 (1935).
[8] J. S. Kellough, "Growth conditions for some zinc-rich alloys," Thesis, University of Iowa, 1937.

boundary line. It therefore appeared significant to investigate the upper limit and to determine as far as possible the complete range of favorable growth for single and mosaic crystals of zinc.

Materials

The material from which the crystal specimens were grown was obtained from two 50-lb. slabs of Horsehead Special zinc (99.99+ percent Zn). A spectrographic analysis of the two lots, made by the New Jersey Zinc Company[9] to determine the relative amounts of the iron and cadmium present, gave the following results: Lot I contained 0.0018 percent cadmium and 0.0017 percent iron; lot II contained 0.0010 percent cadmium and 0.0010 percent iron.

Procedure

The procedure was the same as that used by Cinnamon with the following modifications. It was found more convenient to substitute for the transite cover a thickness of 3 to 4 mm of asbestos paper placed under a thin sheet-iron strip of 0.7 mm thickness. This assembly of the same width and length as the mold could be held firmly thereto by means of a few single turns of fine iron wire. The thermocouples were placed at 5-cm intervals along the mold and stem. On the basis of this length, from preliminary observations, a calculation of the probable error in the measurement of the ratio of temperature gradient to rate of growth gave ± 1.3 percent. With this degree of precision a 5-cm section was considered sufficient to represent the crystal unit under test.

The temperature gradient and rate of growth were controlled over each 5-cm section. These quantities were measured over the section that included the interfacial boundary between the solid and liquid phases. The temperature gradients impressed across different sections extended from 3.4°C/cm to 12°C/cm. The rates of growth imposed on the different sections extended from 0.07 cm/min. to 0.34 cm/min.

The crystals grown were approximately one sq. cm in cross section[10] and varied in length from 5 cm to 60 cm. A 15-cm length required constant attention and control for 8 hours; a 60-cm length required 14 hours.

An improvement in technique was accomplished by etching the specimen in a 10 percent concentrated HCl solution for a period of 2 to $2\frac{1}{2}$ hours. The etching made evident any change in the angle of orientation[11] of the crystal as well as the origin of any superficial mosaic structure. This technique proved very helpful in the location of mosaics in crystals of high orientation. Although the presence of striations on the etched surface could be taken as proof that the specimen was mosaic, the absence of such markings was not conclusive evidence that mosaic structure was lacking. This was found to be the case for the crystals of low orientation, where it became difficult to observe variations in the character of the etch. As a final confirmation, all of the single crystal specimens were cleaved and examined both optically and by the sun test, as described elsewhere.[1] The cleavage technique was improved by first cooling the specimen in a mixture of dry ice and alcohol.

Analysis of Data

In the course of the investigation 81 specimens were grown. Of this number, 39 started growing in the main groove of the mold as good single crystals, while 42 were optically mosaic throughout their length. Four of these 39 crystals experienced an abrupt change in the angle of orientation and continued as single crystals of higher orientation. Four continued as single crystals for the entire length of the groove, while the remaining 31 crystals changed to various types of optically mosaic, as described by Schilling.[5] Occasionally some of these mosaics later changed in orientation. This occurred in approximately 20 percent of all the mosaics grown. Almost invariably the resulting mosaic was of higher orientation.

An analysis of these results was obtained, by taking as the crystal unit, the 5-cm section of the specimen included between the adjacent thermo-

[9] The authors acknowledge with gratitude the kindness of the New Jersey Zinc Company in rendering this service.

[10] During the course of the investigation two molds were used; the first, 0.7 cm² and the second, 1.2 cm². An examination of the data indicated that the effect of such a variation in the cross section of the specimens amounted to less than the scattering of points along the boundary due to the slight variation in the impurities of the materials.

[11] The angle between the normal to the basal plane and the length of the specimen.

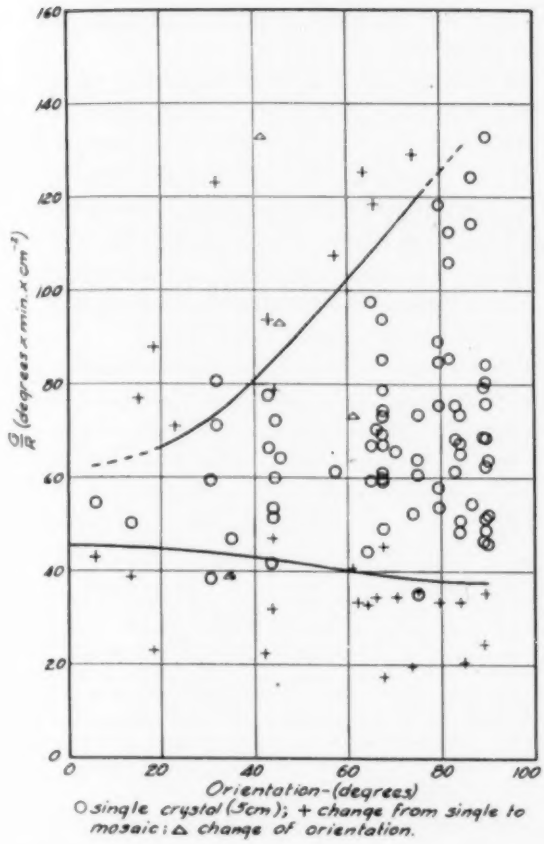

FIG. 1. Graph showing the effect of the temperature gradient (G) and the rate of growth (R), on the propagation of single-crystalline structure.

couple junctions. If the entire 5-cm section resulted in a single crystal, this unit was said to be "good" and the temperature gradient and rate of growth imposed over this length were said to be "favorable." A section in which the single crystal experienced an abrupt change in orientation was said to have "failed." The temperature gradient and rate of growth imposed over this unit were said to be "unfavorable" to the crystal of the original orientation. Such failures were identified as type (1). Also, each section in which a single crystal changed to mosaic was said to have "failed" and the corresponding temperature gradient and rate of growth over this unit were considered "unfavorable." Failures of this kind were identified as type (2).

The effect of the temperature gradient (G) and the rate of growth (R), on the propagation of single-crystalline structure was revealed by plotting different functions of these two variables against the angle of orientation. The most significant function proved to be of the form, G^m/R^n. Plotting the simplest form, G/R, against the angle of orientation for each 5-cm section of "good" single crystal, together with the corresponding data for each section that had failed, there resulted a distinct separation of points. The plot is shown in Fig. 1. Each circle represents a section of "good" single crystal; each triangle, a section in which the crystal experienced a failure of type (1), and each cross, a section wherein the crystal experienced a failure of type (2). The smooth solid lines shown were placed by inspection and indicate the approximate boundaries to the region of successful growth.

Other forms of the function, G^2/R and G/R^2, also gave a distinct region of favorable growth (graphs not shown), but were not markedly distinguishable from the plot of G/R. The first form gave a slightly better definition of boundaries than was obtained for G/R, while the latter gave boundaries slightly less defined. Although the distinction appeared genuine, it is evident that a far greater range in the values of G and R will need be imposed, than were used here, in order to make this difference markedly pronounced and of practical significance. The boundaries to the G/R function are sufficiently exact for practical work and can be readily used as a guide during the process of growing a crystal. Functions that gave no indication of a regional separation of points were (G), (R) and the product (GR).

All the data for the single crystals, together with that of resulting failures, are represented in Fig. 1. The data show that temperature gradient and rate of growth are significant factors in the growth process of single crystals. They also show a region of preferred growth, depending on the angle of orientation. Crystals of high orientation can be grown over a much greater range of values in G/R than those of a lower orientation.

Plotting the corresponding data of G/R for mosaics (crystals that originally started mosaic from the seed nucleus or in the stem and the mosaics originating from the failures of type 2) resulted in no indication of preferred growth conditions (graph not shown). Failures appeared at random, with a maximum frequency of failures for mosaics orientated between 25° and 60°. The results indicate that mosaic crystals are not

restricted by limiting values of G/R, and all orientations can be grown over a wider range than for single crystals. In this respect, mosaics are more similar in behavior to polycrystalline zinc than to monocrystalline zinc. This inconsistency is in agreement with their erratic thermal and electrical resistivity properties.[2,12]

Conclusions

In agreement with the experience of others[7,8,13] the present investigation shows that single crystals must be grown under special conditions. The structure sensitive properties of such crystals are known to be consistent with definite crystallographic relations[2,3,12,14] and thereby indicate that single crystals approach in reality the crystal lattice continuum in agreement with the contention of Buckley.[15] Furthermore, these crystals appear to be free of the lineage structure proposed by Buerger.[16]

It is evident that the factors, effective in propagating the single-crystalline structure, change with the angle of orientation and depend on the relation of the temperature gradient across the solid-liquid phase boundary to the rate of growth of the crystalline formation. For a particular angle of orientation the optimum conditions fall between a definite maximum and minimum value of G/R. Such restrictions on the growth of single-crystalline zinc, as compared to the relatively greater range for mosaics, show definitely that unless the optimum conditions are imposed, the crystals obtained are very likely to be mosaic and thereby lacking in the properties that characterize single crystals.

It is to be understood that the results obtained are for zinc crystals of the size and degree of purity stated and under the conditions imposed by this method of growth. A modification in method, as used by Hasler,[17] apparently yields different limitations on temperature gradient and rate of growth.

An investigation of the scattering of points about the lower and upper boundaries (See Fig. 1) revealed in all cases, with two exceptions,[18] that the crosses falling out of place represented specimens grown from one slab of zinc while the corresponding circles represented crystals grown from the other slab. Apparently, the cause of the scattering is due to the slight differences in the purity of the two slabs of zinc.

The increase in the iron content over that in the zinc used by Cinnamon appears to be responsible for the predominance of mosaics that originated in the stem of the mold where the same technique was used as formerly.[1] It also appears to be responsible for the great number of failures of type (2) compared to the relatively few failures of type (1). The lower boundary in Fig. 1 is entirely determined by failures of type (2), while the lower boundary obtained by Cinnamon was solely determined by failures of type (1). It is interesting to note that the two boundaries fall in approximately the same region of the graph.

Although observations on growth conditions in general are incomplete, the present findings warrant at least two speculations on the probable significance of temperature gradient and rate of growth. (1) The temperature gradient and rate of growth, jointly or separately, must have a direct internal influence on the system of atomic forces at the interfacial boundary between the liquid and solid phases. (2) These factors, jointly or separately, must have an external effect by changing the direction of the temperature gradient across the interfacial boundary. Crystals of low orientation would be more influenced by such changes due to the smaller magnitude of the atomic forces along the direction of growth, while crystals of high orientation would be less influenced due to the greater atomic forces in this direction.

[12] C. A. Cinnamon, Phys. Rev. **46**, 215 (1934).
[13] A. G. Hoyem and E. P. T. Tyndall, Phys. Rev. **33**, 81 (1929).
[14] E. P. T. Tyndall and A. G. Hoyem, Phys. Rev. **38**, 820 (1931); A. G. Hoyem, *ibid.*, **38**, 1357 (1931).
[15] H. E. Buckley, Zeits. f. Krist. **89**, 221 (1934); **93**, 161 (1936).
[16] M. J. Buerger, Zeits. f. Krist. **89**, 195 (1934).
[17] M. F. Hasler, Rev. Sci. Inst. **4**, 656 (1933).

[18] The cross in the upper limit in the proximity of 42° and the triangle in the proximity of 60° constitute two failures that cannot be definitely explained.

An Experimental Study of Heat Interchangers*

R. B. Jacobs† and S. C. Collins
Research Laboratory of Physical Chemistry, Massachusetts Institute of Technology, Cambridge, Massachusetts

(Received January 18, 1940)

Recent developments of engines and turbines for producing low temperatures have emphasized the necessity of improved heat interchangers for further progress in the field. The present report covers an experimental investigation of heat interchanger design and operation intended primarily to cover those applications most likely to occur in the experimental rather than in the commercial laboratory.

Introduction

THE recent successes[1,2] in the application of the adiabatic expansion principle for the liquefaction of gases have been instrumental in arousing considerable activity along similar lines. An investigation of the thermodynamic quantities involved will immediately reveal that the heat-interchanger problem is the bottleneck of the process. The present work is an attempt to clarify some of the problems of, and to suggest some designs for interchangers suitable for expansion machines operating with a relatively high thermodynamic efficiency.

Previous work along these lines is inadequate for two reasons: The first is that the many available engineering treatises[3] are, for the most part, inapplicable due to the differences in the Reynolds numbers which are encountered in engineering and in scientific practice;‡ the second is the impossibility of carrying over into expansion machine design much of the experience which has been gained in Joule-Thomson practice. This is due to a fundamental difference in the operation of the interchangers in the two cases.

The first point requires little elaboration, aside from pointing out that commercial interchangers generally operate with very high Reynolds numbers (i.e., highly turbulent flow) whereas laboratory equipment generally will operate with Reynolds numbers which are somewhat lower, often in the critical region between streamline and turbulent flow.

The second point is very important. The difference in the heat interchanger operation when used in a Joule-Thomson liquefying circuit and when used in an adiabatic expansion cycle in which the gas is made to do useful work is as follows: the Joule-Thomson process consists of sending a stream of highly compressed gas, previously cooled to a point considerably below the inversion temperature, through a heat interchanger and expansion valve. A fraction of the gas is liquefied and the remainder returns through the interchanger. The heat capacity of the low pressure return stream is considerably lower than the high pressure stream partly because of the smaller mass and partly because of the significant difference in specific heat at low and high pressures. Accordingly, for a given change in the temperature of the incoming high pressure stream during its passage through the interchanger there will be a much greater change in the temperature of the outgoing low pressure stream. Since the temperature of both streams is substantially the same at the warm end of the heat interchanger, there must be a wide difference at the cold end, the difference decreasing exponentially along the interchanger. The effectiveness of the interchanger is, therefore, extraordinary near the cold end and the over-all efficiency is very high.[4]

* Contribution No. 422 from the Research Laboratory of Physical Chemistry, Massachusetts Institute of Technology.

† Lalor Fellow in Physical Chemistry.

[1] P. Kapitza, Proc. Roy. Soc. London **A147**, 189 (1934).

[2] P. Kapitza, J. Phys. U. S. S. R. **1**, 1 (1939).

[3] See, for example, W. H. McAdams, *Heat Transmission* (McGraw-Hill, 1933).

‡ Reynolds number is defined as $DV\rho/\mu$, where D is diameter, V is velocity, ρ is density, and μ is viscosity. In engineering work both V and D are generally larger than in scientific work, yielding much higher Reynolds numbers.

[4] That this effect is one of considerable magnitude may be seen from the following illustration. Consider an interchanger which when used in the balanced condition has an inefficiency $(\Delta T/T_2-T_1)_{\text{Bal}}$ of 20 percent. ΔT is the temperature difference between streams, and T_2-T_1 is the temperature difference from top to bottom of the inter-

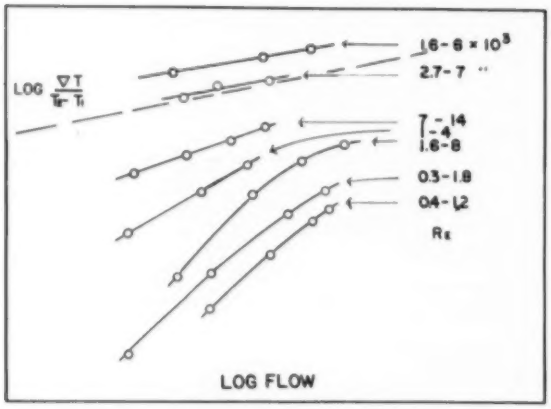

FIG. 1. Flow *vs.* inefficiency. (Dotted line gives slope of curve expected for high *Re.*) For comparison of their relative slopes the curves of Figs. 1, 2 and 3 have been grouped arbitrarily without reference to coordinate scales.

In the case of an adiabatic expansion cycle, however, the pressure range is much smaller because of practical limitations of the working engine. Furthermore, the fraction liquefied is usually zero because the principal application of such a cycle is the production of refrigeration at a certain temperature level. Therefore, the heat capacity of the incoming and outgoing gas will be substantially the same and the heat interchanger will operate with a constant temperature difference, ΔT, between the two gas streams. The interchanger efficiency is much lower, consequently, for this type of service in which there is a balanced flow.

changer on the low pressure side. Now, this inefficiency may be shown (the Joule-Thomson circuit will be described in the near future in a paper by C. Starr) in a first approximation, to be related to the inefficiency of the same interchanger operating under identical conditions in a Joule-Thomson cycle by the following equation:

$$\left(\frac{\Delta T}{T_2-T_1}\right)_{\text{J.T.}} = \left(\frac{\Delta T}{T_2-T_1}\right)_{\text{Bal}} \times e^{-(T_2-T_1/\Delta T)_{\text{Bal}}(\epsilon/1-\epsilon)},$$

where the heat capacity of the outgoing stream is equal to $(1-\epsilon)$ times that of the incoming stream, and $\Delta T_{\text{J.T.}}$ is measured at the hot end of the interchanger. If the Joule-Thomson circuit for hydrogen gas operates between 77° and 23° absolute with an initial pressure of 50 atmospheres, $(1-\epsilon)$ will be found from the Leiden charts (Keesom and Houthoff, Leiden Comm. Supp. 65d, 1928) to be about 0.6. In this case

$$\left(\frac{\Delta T}{T_2-T_1}\right)_{\text{J.T.}} = \left(\frac{\Delta T}{T_2-T_1}\right)_{\text{Bal}} \times e^{-10/3} = 0.0074$$

or in other words, the 80 percent efficient balanced interchanger becomes 99+ percent efficient when used as a Joule-Thomson interchanger under the above conditions. It is understood that the actual Joule Thomson circuit is complicated sometimes by the formation of liquid behind the valve. This effect has not been taken into account in the above calculations.

THE ADIABATIC EXPANSION PROCESS

The adiabatic expansion process makes use of the refrigeration produced when a gas is expanded adiabatically thereby performing external work. For a continuous process there is need for some device (an engine) which will enable the gas to do this work either continuously as in an air-driven turbine or in cycles as in a reciprocating air-driven engine. The refrigeration so produced will reside largely in the exhaust gas. This is used to cool the incoming gas stream in a regenerative process. The device which permits the heat transfer between the two gas streams is the heat interchanger. The efficiency of the process as a whole is affected in a marked way by the heat interchanger efficiency as is illustrated by the following case.

Consider the engine devised by Kapitza for the production of liquid helium. The refrigerative gas is helium. It enters the engine under 30 atmospheres pressure and is exhausted at 2.2 atmospheres. The inlet and exhaust temperatures are 19° and 10°K, respectively. Hence the cooling energy is about 45 calories per mole, or 60 percent of the theoretical refrigeration. The exhaust gas is allowed to interchange with the inlet gas over the range from 19° to 65°K. Thus the quantity of heat to be removed here from the exhaust gas is (65–19) C_p per mole. A certain fraction of this will be lost due to imperfect interchanger action, giving for the net refrigeration a value equal to the total cooling energy minus this loss. A few illustrative cases are given in Table I. Hence, it is clear that the advantageous use of the adiabatic expansion principle is dependent upon a highly efficient interchanger action.

TABLE I.*

Interchanger Efficiency	100%	98%	95%	(Kapitza Interchanger) 92%
Net Refrigeration (cal./per mole)	45	40	33	28

* A similar table applicable for the Joule-Thomson process for hydrogen gas pre-cooled to 63° K at 100 atmospheres pressure is as follows:

Interchanger Efficiency	100%	90%	80%
Fraction Liquefied	0.26	0.22	0.18

from which it is seen that the interchanger effect here is of a different order of magnitude.

Experimental Results

The experimental work was divided into two parts. The object of Part 1 was to obtain sufficient data to predict the behavior of interchangers operating with Reynolds numbers smaller than those required for turbulent flow. The object of Part 2 was to establish by experiment the relative merits of several interchangers of different design.

Part 1

Reynolds number (Re) was varied by changing the flow of gas, the type of gas, and the interchanger cross section, in an effort towards generalization. The inefficiency $(\Delta T/(T_2-T_1))$ {where ΔT represents the temperature difference between the two gas streams at the hot end of the interchanger, and (T_2-T_1) is the temperature drop along its length} was obtained by measuring ΔT and (T_2-T_1) by suitably placed thermocouples. In all of the tests, the interchangers were used in vacuum cases. Volume measurements were made with the aid of a dry-type gas meter manufactured by the American Meter Company. Temperatures ranged from 90° to 373°K.

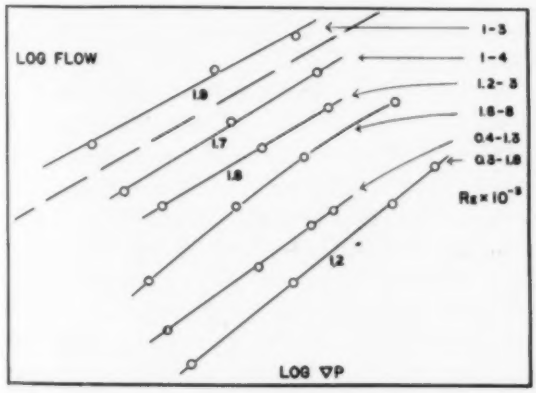

Fig. 2. Pressure drop *vs.* flow. (Dotted line gives slope of curve expected for high Re.)

The results of this section are given in a series of logarithmic plots (Figs. 1–3). On each of these the dotted line indicates the behavior of the system for high Reynolds numbers. Fig. 1 shows that $\Delta T/(T_2-T_1)\sim V^{0.2}$ for high Reynolds numbers (V is the volume of flow per unit time) whereas for lower Reynolds numbers $\Delta T/(T_2-T_1)\sim V^{>0.2}$. Consequently, calculations of $(\Delta T/(T_2-T_1))$, based on engineering data

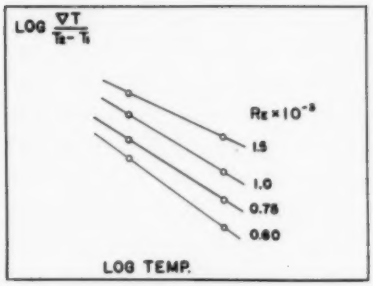

Fig. 3. Temperature—inefficiency plot.

($Re>2\times10^3$) will be too large if $Re<2\times10^3$. The magnitude of this effect can be estimated from the same diagrams.

Figure 2 shows the relation between flow and pressure drop. For high Reynolds numbers the relation is $\Delta P\sim V^{1.8}$, and for lower values of Reynolds number the relation becomes $\Delta P\sim V^{<1.8}$ which indicates that the calculated pressure drops will be too small if applied to flow which is not purely turbulent. As Reynolds number decreases the relation will eventually become $\Delta P\sim V$, which is characteristic of streamline flow. Approximations in the intermediate region can be made from Fig. 2. Fig. 3 illustrates the temperature dependence of $\Delta T/(T_2-T_1)$ as Re is reduced. It appears that the effect of lowering Re is to make $\Delta T/(T_2-T_1)$ a steeper function of T.

Part 2

Many empirical equations[5] have been devised for the calculation of the pressure drop and the heat transfer of a fluid passing through a given channel in turbulent flow. Those equations differ mainly in the values assigned to the constants and exponents. Reduced to their most simple terms all of these relations lead to proportionalities quite similar to the following:

$$\frac{\Delta T}{T_2-T_1}\sim\left(\frac{A}{Pe^{1.2}l}\right), \tag{1}$$

$$\Delta p\sim\left(\frac{Pe^{1.2}l}{A^3}\right)\frac{76}{p}, \tag{2}$$

$$Re\sim 1/Pe, \tag{3}$$

where A is the area of the cross section, Pe is the "wetted" perimeter, l is the length, and p the

[5] Reference 3, p. 168.

pressure in cm. It is understood that these relations hold for different channel cross sections handling the same mass per unit time of the same gas at a given temperature. Furthermore, $\Delta T/(T_2-T_1)$ represents the loss in efficiency in a single channel, due to the temperature gradient which exists between the gas and the walls of that channel. The total interchanger inefficiency is made up of two such terms (one for the high pressure, and one for the low pressure channel) in addition to the losses due to temperature gradients in the interchanger walls.

Since the calculation of the numerical values of Δp and $\Delta T/(T_2-T_1)$ from the properties of the gas is very laborious, we have shortened the procedure somewhat in the following manner. We calculate these two quantities once for a standard reference channel, and then use the relations (1–3) to find the values for any given interchanger. Due account for the deviations mentioned in Part 1 must be taken when the Reynolds numbers fall below 2×10^3.

TABLE II.* *For helium gas at 15 ft.³/min. (7.1 liters/sec.) Computed for standard reference channel. Pressure drops for average p=76 cm.*

	273°K	200°K	100°K	70°K	50°K	30°K
$\frac{\Delta T}{T_2-T_1}$	0.056	0.060	0.069	0.071	0.086	0.090
Re	2.8×10^3	3.4	5.0	6.6	8.7	10.5
ΔP	9.8 cm Hg	7.1	3.3	2.2	1.5	0.9

TABLE III.* *For hydrogen gas (same conditions as Table I).*

	300°K	200°K	100°K	70°K	50°K	30°K
$\frac{\Delta T}{T_2-T_1}$	0.060	0.064	0.078	0.093	0.101	0.117
Re	2.9×10^3	3.8	6.3	7.7	10.4	14.6
ΔP	5.6 cm Hg	3.5	1.6	1.1	0.72	0.41

TABLE IV.*

INTERCHANGER	INEFFICIENCY (CAL.)	INEFFICIENCY (EX.)	Δp (CAL.)	Δp (EX.)	RE
1	0.045	0.043	13.2 cm	25 cm	2.2×10^3
1*a*	.027	.027	105	130	2.8
2	.070	.060	380	420	7.8
		(extra.)		(extra.)	
3	.035	.056	283	360	6.6

* All measurements on helium gas at average temp. =200°K. Flow =15 ft.³/min. Pressure drops are for outlet pressure at 1 atmosphere.

The "reference" channel is chosen to have a cross-sectional area of 1 cm², a perimeter (cross-sectional) of 10 cm² and a length of 300 cm. Tables II and III have been worked out for hydrogen and helium gas for this reference channel. To find the inefficiency of an interchanger the quantity $\Delta T/(T_2-T_1)$ is calculated for each channel from Table II or III in combination with relation (1) or (2) above. The addition of these quantities plus the metal loss gives the inefficiency of the whole interchanger. If the interchanger is used unbalanced, its inefficiency will be affected in the manner mentioned in the introduction. The quantity $\Delta T/(T_2-T_1)$ is practically pressure independent, whereas Δp is inversely proportional to the average pressure. The variations of the quantities in question with flow have been outlined in Part 1.

Our measurements would indicate that the inaccuracy in a computed value of $\Delta T/(T_2-T_1)$ should not in general exceed 10 percent. The error in Δp might be somewhat greater. Since an interchanger is generally over 90 percent efficient, the efficiency itself should be known to within about 1 percent. A frequent source of error lies in the inability to attain in the actual interchanger the exact dimensions and features of the drawing board design.

Table IV gives some experimental results on 15-foot lengths of four different interchangers which might be considered for expansion engine use. Types 1 and 1*a* are illustrated in diagram (1) of Fig. 4. They make use of three annular channels. The intermediate channel carries the high pressure gas, and the inner and outer channels take the return gas. The bore of the central tube is not used. The channel dimensions are maintained by wire spacers which are shown. It is very important that these wires be firmly soldered to the tubes on either side of them, since they should provide a path for heat flow between the two tubes. If the wires are not soldered the innermost and the outermost tube will simply "float," taking no part in the heat transfer. This type of interchanger is expensive and difficult to construct.[6] It is amply justified, however, by its

[6] The authors are indebted to the firm of Cook, Dunbar, Smith Company of Providence, Rhode Island, for cooperation in the construction of these units. This type of interchanger was first described in a paper by S. C. Collins and F. G. Keyes, J. Phys. Chem. **43-1**, 5 (1939).

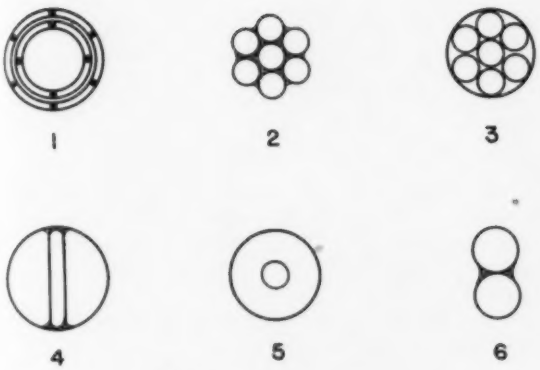

FIG. 4. Interchanger cross sections.

very high efficiency and low pressure drop. Type (2) in Fig. (4) is an interchanger identical in design and dimensions with the lower section of the interchanger used by Kapitza on his expansion machine. Type (3) in the same figure uses all seven tubes for the low pressure gas. The high pressure gas flows down the space between these tubes and is confined by the single outer tube surrounding the ensemble. In type (2) the high pressure gas is fed through the central tube.

Interchanger (3) provided the largest discrepancy between computed and observed values of $\Delta T/(T_2-T_1)$. The reason for this perhaps lies in the imperfection of the interchanger. No provision was made for holding the tubes in place during coiling, and it is possible that they moved considerably from their original position providing a cross section that allows "channeling" of the gas stream. It should be noticed, however, that this interchanger is more effective than type (2) since it has a higher efficiency and a lower resistance, and weighs about the same. As it requires no soldering along its length it is a very simple interchanger to build.

We have constructed several interchangers of the Kapitza type (i.e., No. 2). We find the soldering a very important part of the design, since the efficiency is greatly reduced by imperfect soldering. Our best model was produced by sucking the molten solder through the high side of a type (3) interchanger, and allowing it to solidify in place. This interchanger showed perfectly soldered sections when it was later cut at several places. A 15-foot section proved to be 94 percent efficient as against the computed value of 93 percent. Kapitza used an interchanger which is more than three times as long and obtained an efficiency of only 92 percent against a computed efficiency of at least 96 percent. It is possible that the discrepancy here was due to incomplete soldering.

By far the best interchangers for expansion machine work are those of type (1). They have the highest efficiency and the lowest pressure drop. They weigh about $1\frac{1}{2}$ times as much as types (2) and (3) per unit length but have a much higher ratio of efficiency to weight than the latter. Interchangers of this type may be designed to have almost any desired characteristic since the cross-sectional areas and perimeters may be fixed independently. The lack of this independence in types (2) and (3) make them somewhat more inflexible in design. We have a 30-foot interchanger of type (1) mounted in an expansion machine. Carrying 15 ft.^{3}/min. of helium it operates in the temperature range 20° to 70° absolute with an efficiency higher than 99 percent. A reference to Table I will show that this interchanger would increase by about 50 percent the present yield of the Kapitza machine. (This 30-foot unit perhaps weighs about the same as Kapitza's 48-foot unit.)

Type (5) in Fig. 4 is a commonly used interchanger of rather poor characteristics, since the outer and inner tubes are not in thermal contact. This means that the outer tube just "floats" uselessly and that the whole heat transfer takes place across the walls of the small inner tube. Type (6) is a simple design which is not subject to this defect. It is very useful where the danger of "plugging" is great and a large cross section is imperative. We have found no particular advantage to be gained by interchangers of unusual design such as type (4). Their characteristics are governed by the same equations, i.e., (1–3) and can generally be matched in a simpler design.

In conclusion, the authors take the opportunity to express both their appreciation and indebtedness to Professor F. G. Keyes for his active interest in this work as well as for the many discussions concerning it which they have had with him.

Flow of a Gas Through Porous Media

J. L. Fowler* and K. L. Hertel
University of Tennessee, Knoxville, Tennessee
(Received January 30, 1940)

Kozeny's approximate solution to the problem of fluid flow through porous media is developed and the result is checked by experimental data on air flow through plugs of cotton, wool, rayon, and glass wool fibers. The solution gives

$$\frac{W}{A}=\frac{k\gamma_0}{2\mu}\left(\frac{\tau}{\sigma}\right)^2\frac{(1-c)^2}{c^2}\left(-\frac{\delta p^2}{\delta x}\right)$$

for the isothermal linear flow of a gas. W/A is the macroscopic flux density; μ, the viscosity; γ_0, the density of the gas at unit pressure; τ/σ, the volume of fibers divided by their surface area; c, the fraction of space occupied by fibers; $\delta p^2/\delta x$, the macroscopic gradient of the square of the pressure; and k is a numerical constant which depends on the shape and orientations of the fluid passages. k was found experimentally to be 0.18, which is in approximate agreement with the value found for flow through media made up of spherical particles. The dependence of the flow on the factor c was checked over the approximate range from $c=0.1$ to $c=$ more than 0.5. τ/σ and c have values for fineness and density of samples of fibers in fair agreement with independent determinations.

Introduction

THE textile industry recognizes the need for more accurate information about the physical properties of the raw material it fabricates. The terminology used in the industry may not, however, refer to objective physical properties, but more often to subjective properties, such as staple length, grade, fiber fineness, and character, that have never been defined specifically in terms of physical properties. Before investigating such a quantity as fiber fineness, it is necessary either to discover an accurate definition of fineness or to select an accurately defined physical property that may serve as a substitute. There have been several objective physical properties suggested as approximations to the subjective property of fiber fineness. Linear density and fiber cross section ignore the shape of the fiber cross section, which appears to be an important factor. The ratio of fiber surface area to fiber volume and the equivalent ratio of cross-section perimeter to cross-section area depend upon fiber shape as well as size and should be one factor indicating the potential ability of fibers to cling to each other in spun yarn. Although the resistance offered by fibers to the slipping of fibers among themselves is different from the resistance offered to the flow of air through fibers, both depend upon the amount of exposed fiber surface. The resistance offered to air flow also depends upon the distances between fiber surfaces, and since fibrous materials can be compressed to change these distances uniformly throughout the fiber aggregation, the amount of compression to give a known resistance can be made a convenient measure of the ratio of fiber surface to fiber volume. It is the purpose of this paper to consider the theory of fluid flow through porous media and report the results obtained by varying the porosity of fibrous materials.

For the most part the work on the flow of fluids through porous media has been an experimental verification of Darcy's law, which states that the rate of flow of water through a filter bed is directly proportional to the cross-sectional area of the bed, and to the difference of head between the inlet and outlet, and inversely proportional to the length of the bed. By the method of dimensional analysis Darcy's law has been extended to apply to the general problem of flow of homogeneous fluids through porous media in a linear channel as indicated in the equation

$$v=\text{const.}\,\frac{d^2}{\mu}\left(\frac{dp}{dx}\right). \qquad (1)$$

v is the macroscopic velocity of the fluid, d is the effective diameter of the pore openings in the medium, μ is the coefficient of viscosity of the fluid, and (dp/dx) is the pressure gradient which produces the flow. The constant of proportionality must be a dimensionless quantity which depends on the geometric properties of the medium.[1]

* Now research assistant at Princeton University.

[1] M. Muskat, *The Flow of Homogeneous Fluids Through Porous Media* (McGraw-Hill, New York and London, 1937), p. 69.

Although most of the investigators have determined the permeability factor, constant $\cdot d^2$, experimentally for the media they were studying, a few have attempted to solve for the constant theoretically in terms of the geometric nature of the medium.[2,3] While an exact solution of the hydrodynamic equations satisfying all the boundary conditions in a porous medium would be hopelessly complex, by use of simple arguments introduced by Kozeny it is possible to obtain a reasonable solution in terms of the geometric properties of the medium.[3]

Theory

First, consider the flow of a noncompressible fluid of viscosity μ through a block of medium of constant cross-sectional area A cm^2 and of length X cm. The problem is to determine the volume of fluid which crosses A per second as a function of the macroscopic pressure gradient in the X direction. Thus it is necessary to obtain an estimate of the average value of the X component of the microscopic velocity of the fluid.

The passages of the medium through which the fluid moves will, in general, have very irregular cross sections. It can be shown, however, that when the solutions of the hydrodynamic equations of motion of viscous fluids through linear channels with cross sections of various shapes are used to obtain the average velocity of the fluid, the results, expressed in terms of the ratio of the volume of the channel to the area exposed to the fluid, do not depend critically on the shapes of the channels.[4] That is, the average velocity of a viscous fluid moving with streamline flow in a channel of constant cross section is given by

$$\bar{v}_r=\frac{k'}{\mu}\left(-\frac{dp}{dr}\right)\left(\frac{V}{S}\right)^2, \tag{2}$$

where r is the direction of flow, V is the volume of the channel, S is the exposed area, and k' is a dimensionless shape factor. In Table I, values of k' are given for a number of differently shaped channels. Eq. (2) also should hold for a short section of a passage in a porous medium. It gives the velocity in the direction of the passage. If θ is the angle between this direction and the X axis, the X component of the velocity will be

$$\bar{v}_x=\frac{k^1}{\mu}\left(-\frac{dp}{dr}\right)\left(\frac{V}{S}\right)^2(\cos\theta). \tag{3}$$

It is necessary now to average $\bar{v}_x$ over the free space of the medium. In order to do this it is necessary to break down the factor $(dp/dr)\cos\theta$ into a product of two factors, one of which is independent of θ. However this is done, the result may be expressed in terms of the macroscopic pressure gradient $\delta p/\delta x$ as

$$\langle\bar{v}_x\rangle_{Av}=\frac{k}{\mu}\left(-\frac{\delta p}{\delta x}\right)\left\langle\frac{V}{S}\right\rangle_{Av}^2. \tag{4}$$

In case the flow channels may be regarded as bundles of more or less independent tubes and transverse pressure gradients can be sustained, dp/dr must vary in such a way as to give the same total flux through all sections of a given channel irrespective of the orientation of the channel. dp/dr then will be independent of θ. Expressing δp as the line integral

$$\delta p=\int\frac{dp}{dr}dr=\left\langle\frac{dp}{dr}\right\rangle_{Av}\int\sec\theta dx$$

$$=\left\langle\frac{dp}{dr}\right\rangle_{Av}\langle\sec\theta\rangle_{Av}\delta x \tag{5}$$

it follows that

$$k=k'\frac{\langle\cos\theta\rangle_{Av}}{\langle\sec\theta\rangle_{Av}}. \tag{6}$$

Table I. *Shape factor, k', (Eq. (3)) for flow in channels of various constant cross sections, reference 5.*

Shape of cross section	k'
Circular	0.500
Elliptical	
Major axis = 2 times minor axis	0.476
Major axis = 10 times minor axis	0.414
Rectangular	
Square	0.562
Length = 2 times width	0.515
Length = 10 times width	0.377
Length = ∞ times width (parallel planes)	0.333
Triangular	
Equilateral triangle	0.600

[2] C. S. Slichter, United States Geological Survey, 19th Annual Report, p. 295 (1897–98).
[3] I. J. Kozeny, *Wasserkraft und Wasserwertschaft*, Vol. 1, (1931), p. 67.
[4] A. G. Greenhill, Proc. London Math. Soc. **13**, 43 (1881).

In case no transverse pressure gradients can be sustained, dp/dx must be independent of the orientation of the channel, and so of θ. In this case we may write

$$\frac{dp}{dr}\cos\theta=\frac{dp}{dx}\cos^2\theta$$

and

$$k=k'\langle\cos^2\theta\rangle_{Av}. \tag{7}$$

Let there be c cubic centimeters of solid material per cc of medium. Then $(1-c)$ is the

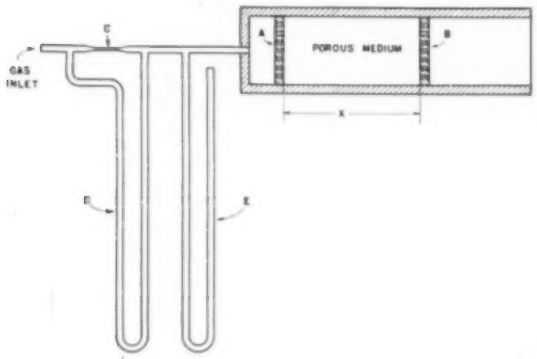

FIG. 1. Apparatus for determining air flow relationships. A and B are perforated plungers between which the samples of fibers are placed; C is a constriction; D is a manometer tube for measuring the quantity of gas flowing into apparatus; E is a manometer tube for measuring the pressure drop across the medium.

fraction of the space open to the fluid. If Q is the volume of fluid which crosses A per second, Q/A is the macroscopic velocity of the fluid and $Q/A(1-c)$ is the average X component of the microscopic velocity. Let there be N particles of average volume τ per cc of the medium; then

$$c=N\tau, \quad \text{or} \quad N=c/\tau. \tag{8}$$

If the average area of each particle is σ, the total area of the particles per cc of medium is $N\sigma=c\sigma/\tau$, Since $(1-c)$ is the free space per cc of medium. $(1-c)/(c\sigma/\tau)$ is the volume of free space per cm³ of surface. In Eq. (4) the average square of the free space per unit area can be approximated by the square of the average free space per unit area, so that the equation becomes

$$\frac{Q}{A}=\frac{k(1-c)^3}{\mu c^2}\left(\frac{\tau}{\sigma}\right)^2\left(-\frac{\delta p}{\delta x}\right). \tag{9}$$

Equation (9) is to be compared with Eq. (1), which was obtained by dimensional analysis from Darcy's law. τ/σ corresponds to d, and $k(1-c)^3/c^2$ corresponds to the constant. Kozeny found that the flow of ground water in sand beds obeys Eq. (9) if k has a value of about 0.3.[3] A critical analysis by Carman of the experimental work of various investigators on flow of fluids through particles (such as: flint sands, steel balls, and glass beads) indicates, when their data is reduced to the form of Eq. (9), that k has a value near 0.20.[5]

Since the fluid will move more or less parallel to the boundaries, one can obtain a theoretical estimate of k by assuming all orientations of the normals to the boundaries to be equally probable. Thus, $\langle\cos\theta\rangle_{Av}=\pi/4$, $\langle\cos^2\theta\rangle_{Av}=\frac{2}{3}$, $\langle\sec\theta\rangle_{Av}=\pi/2$, and k is either $\frac{1}{2}k'$ or $\frac{2}{3}k'$, depending on whether dp/dr or dp/dx is independent of the orientation of the channels. Using the experimental value of k, the value of $\langle k'\rangle_{Av}$ is either 0.40 or 0.30 in the two cases above. From the values of k' given for various cross sections in Table I, it is concluded that the passages in the media on the average have rather elongated cross sections, which is what might be expected.

In the derivation of Eq. (9) a noncompressible fluid was assumed. By use of a simple method, however, the equation can be extended to the case of the isothermal flow of a gas in a porous medium.[6] If both sides of Eq. (9) are multiplied by γ, the density of the gas at any point along the X axis, the expression on the left-hand side becomes equal to the mass of gas flowing per second across one square centimeter of area perpendicular to the X axis at the point. This quantity is a constant.

$$\frac{W}{A}=\frac{Q\gamma}{A}=\frac{k(1-c)^3}{\mu c^2}\left(\frac{\tau}{\sigma}\right)^2\gamma\left(-\frac{\delta p}{\delta x}\right). \tag{10}$$

The density on the right-hand side of Eq. (10) is a function of the pressure of the gas. If the perfect gas law holds in the case of isothermal flow,

$$\gamma=\gamma_0 p; \quad \gamma_0=W/RT, \tag{11}$$

where γ_0 is the density of the gas at unit pressure, W is the molecular weight of the gas, R is the gas constant, and T is the absolute temperature.

[5] P. C. Carman, Trans. Inst. Chem. Eng. **15**, 152 ff. (1937); **16**, 168 ff. (1938).
[6] M. Muskat and H. G. Botset, Physics **1**, 36 (1931).

Finally, Eq. (10) becomes

$$\frac{W}{A}=\frac{k(1-c)^3}{c^2}\left(\frac{\tau}{\sigma}\right)^2\frac{\gamma_0}{2}\left(-\frac{\delta p^2}{\delta x}\right), \qquad (12)$$

which gives the mass flow per second for a gas at a constant temperature in terms of the gradient of the square of the pressure.

Experimental Results

A diagrammatic sketch of the apparatus used to study the flow of air through fibrous media is shown in Fig. 1. The samples of fibers were placed in the tube between the plungers, A and B, which are perforated with small holes. The manometer tube D across the constriction C, which measures the quantity of gas flowing into the apparatus, was calibrated by finding the rate of displacement of water from a vessel connected to the tubes. The manometer tube E measures the pressure drop across the wad of fibers. Before the fibers were used, samples were made into as nearly homogeneous wads as possible on a carding device and were conditioned for several days with compressed air from the tank which supplied the apparatus. After being weighed, the wads were placed in the apparatus and pressed to any desired extent by the movable plunger B. The equipment was arranged so that the length X of the wad could be measured directly.

In the calibration of the constricted tube C the sample tube with the plungers A and B was replaced by a container from which water could be displaced by the air passing through the constriction. It was found that when the pressure difference across the constriction as measured by manometer D was held constant and the outlet pressure as measured by the barometer and manometer E was varied, the volume of water displaced per second varied slightly. Over the range of pressures used in this experiment the mass of air flowing per second was found to be given by the linear equation

$$W=Q_0\gamma_0(p_2+0.74\Delta p), \qquad (13)$$

where p_2 is the atmospheric pressure; Δp is the excess of the outlet pressure above atmospheric pressure; Q_0 is the rate of volume flow in cc per second when the outlet pressure is atmospheric pressure or $\Delta p=0$; and γ_0 is the density of the air at unit pressure. The coefficient of Δp would be unity if the volume flowing through the constriction were independent of the outlet pressure and dependent only upon the pressure drop across the constriction. The gradient of the square of the pressure in Eq. (12) can be written as

$$-\left(\frac{\delta p^2}{\delta x}\right)=\frac{(p_2^2-p_1^2)}{\Delta X}=(2p_2+\Delta p)\frac{\Delta p}{\Delta x}, \qquad (14)$$

where p_1 is the pressure at the inlet to the wad of fibers.

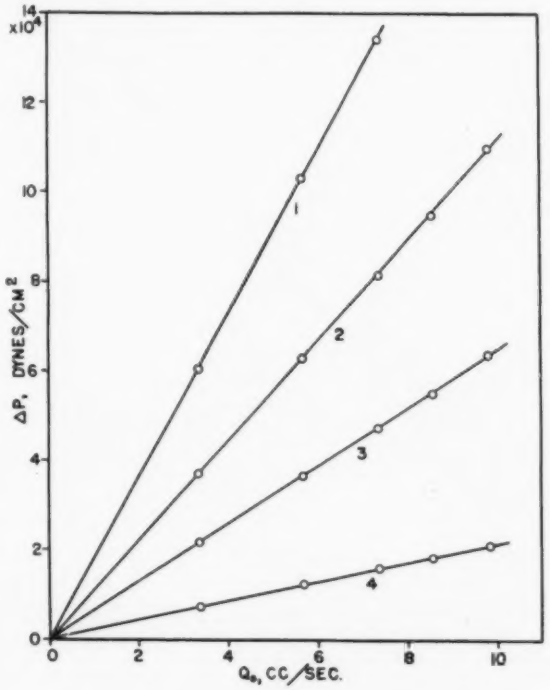

Fig. 2. Pressure drop across samples of fibers as a function of the volume of air entering samples per second. (1) Cotton sample No. 1, weight = 1.986 g., $X=0.889$ cm; (2) Cotton sample No. 1, $X=1.016$ cm; (3) cotton sample No. 2, weight = 1.979 g, $X=1.270$ cm; (4) cotton sample No. 2, $X=2.032$ cm.

Equation (13) and Eq. (14), introduced into Eq. (12), give

$$\frac{Q_0}{A}=\frac{k}{\mu}\left(\frac{\tau}{\sigma}\right)^2\frac{(1-c)^3}{c^2}\frac{(p_2+0.50\Delta p)}{(p_2+0.74\Delta p)}\left(\frac{\Delta p}{\Delta X}\right). \qquad (15)$$

For relatively small pressure drops, Δp, the variation in the factor $(p_2+0.50\Delta p)/(p_2+0.74\Delta p)$ is so slight that it can be replaced by its average value in the range of Δp used.

In the experimental apparatus, therefore, the relationship,

$$\frac{Q_0}{A}=\frac{0.99k}{\mu}\left(\frac{\tau}{\sigma}\right)^2\frac{(1-c)^3}{c^2}\left(\frac{\Delta p}{\Delta X}\right), \qquad (16)$$

should hold. A complete experimental verification of this equation would require the study of the effect on any one of the variables of an independent variation of all the rest. Since it was convenient to choose Δp as this variable, its dependence was checked on: (a) Q_0, (b) ΔX (c remaining constant), (c) $(1-c)^3/c^2$, (d) $(\tau/\sigma)^2$, and (e) $0.99k/\mu$.

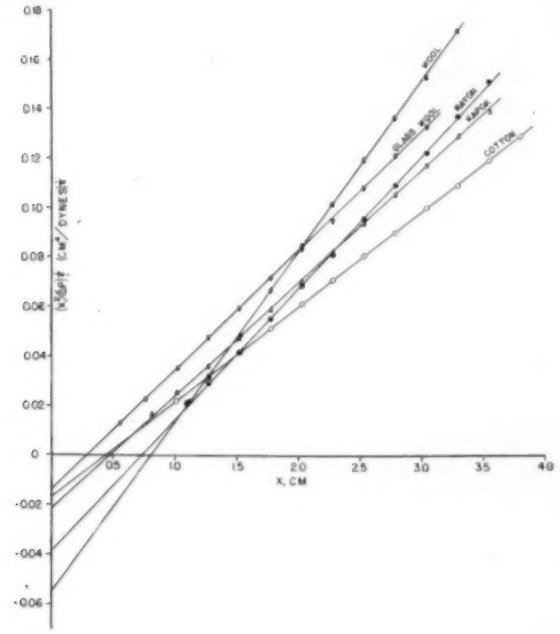

FIG. 3. Variation of pressure drop across weighed samples of fibers as a function of the length of the samples, the quantity of air flowing being constant.

(a) Figure 2 gives the results of holding all the independent factors constant except Q_0, the rate of volume flow reduced to atmospheric pressure. Δp was found to be directly proportional to Q_0 as Eq. (16) indicates it should be.

(b) Curves showing directly the dependence of the pressure drop Δp on the length of the plug ΔX are omitted. The curves which were straight lines through the origin were in agreement with the theoretical formula and with the work of other investigators. Moreover, the verification of the factor $(1-c)^3/c^2$ involves the verification of the proper length dependence indirectly.

(c) In the experiments adopted to check the variation of Δp with c, a prepared weighed sample of fibers was placed in the apparatus. With the quantity of air flowing through the fibers constant as shown by the manometer tube D (Fig. 1), the pressure drop across the wad of fibers was taken at regular length intervals as the fibers were compressed by the movable plunger. Eq. (16) can be written as

$$K^2=\left(\frac{\tau}{\sigma}\right)^2\frac{(1-c)^3}{c^2}\frac{\Delta p}{X}, \qquad (17)$$

where

$$K^2=\frac{\mu}{0.99k}\frac{Q_0}{A}$$

and Δx is replaced by X. Since μ, Q_0 and A are constant, K will be constant if the form factor k is constant.

Let X_0 be the length of the sample of fibers for which $c=1$. From Eq. (16), with $c=1$ it is evident that X_0 is also the length of the sample for which an infinite pressure drop is required to maintain the flow Q_0. X_0 therefore represents the length of the wad compressed to such an extent that no passages are left open to the flow of the gas. X_0A then will be the volume of fiber in the wad. At any particular setting the total volume of the wad is XA. Thus the value of c is $X_0A/XA=X_0/X$. Eq. (17) can be written as

$$\left(\frac{X^2}{\Delta p}\right)^{\frac{1}{2}}=\left[\left(\frac{\tau}{\sigma K}\right)^2X_0\right]^{\frac{1}{2}}\frac{X}{X_0}-\left[\left(\frac{\tau}{\sigma K}\right)^2X_0\right]^{\frac{1}{2}}. \qquad (18)$$

TABLE II. *Comparison of densities determined from gas flow data with densities found by other methods.*

Fibers	Density by gas flow g per cc		Density by other methods g per cc	
	Range	Average	Range	Average
Glass Wool	2.19–2.50	2.40	2.41–2.43	2.42[1]
Textile Wool	1.26–1.37	—	1.28–1.33	—[2]
Cotton	1.25–1.59	—	1.21–1.58	—[3]
			1.50–1.55	—[2]
Rayon	—	1.44	—	—
Kapok	0.40–0.43	0.42	—	—
Cotton	1.25–1.50	1.36	1.21–1.58	1.32[3]

[1] Density determined by weighing glass wool No. 1 in alcohol and benzene. (K. L. Hertel)
[2] Data from *International Critical Tables*. (Vignon) Fibers weighed in benzene.
[3] Estimate of density determined for six cottons from linear density and average cross-sectional area.

If the factor $(X^2/\Delta p)^{\frac{1}{2}}$ (calculated from experimental data) were plotted as a function of X, Eq. (18) would indicate that a straight line should be obtained. In Fig. 3 representative graphs are plotted from experimental data taken on wool, cotton, rayon, kapok, and glass wool fibers. It is evident that the points fall rather accurately on the straight lines drawn through them and, therefore, the form factor k may be considered constant over this range. According to Eq. (18), the intercept on the horizontal axis is X_0. Since AX_0 is the volume of the fibers, then, if M is the mass of the sample, the density ρ of the fibers is given by

$$\rho = M/AX_0. \tag{19}$$

In Table II, values of densities obtained by use of Eq. (19) are compared with values obtained by other methods. While there is considerable random spread in the experimental values, in general, the agreement is enough to justify the assumptions leading to Eq. (19).

(d) Checking this point involved a measurement of τ/σ. In the case of cylindrical bodies the lengths of which are large compared with their effective diameters, the ratio of volume to surface τ/σ is the same as the ratio of cross-sectional area to cross-sectional perimeter, a/s. This last factor was determined independently by measuring a number of enlarged cross sections for each sample of fibers with a map measure and a planimeter. In the case of samples marked with a solid circle in Fig. 4, microscopic photographs of cross sections were made from slides prepared with the "Hardy thin cross section device."[7] In the case of the other textile fibers the enlarged drawings of the slides were made with the camera lucida. The magnification for both cases was determined by enlarging the image of an engraved scale the same amount the cross sections were enlarged. For the glass wool data, represented in Fig. 3, the average area divided by average perimeter was calculated from average diameter measurements taken with camera lucida. This was possible because the glass wool fibers were very nearly circular in cross section.

Equation (18) indicates that the vertical intercepts of the lines of Fig. 3 ought to be $-[(\tau/\sigma K)^2 X_0]^{\frac{1}{3}}$. If this intercept is $-y_0$, then substitution of a/s for τ/σ gives

$$\frac{a}{s} = \left[\frac{\mu Q}{0.99kA}\right]^{\frac{1}{3}} \left[\frac{y_0^3}{X_0}\right]^{\frac{1}{3}}, \tag{20}$$

where the value for K has been substituted also. The factor $(y_0^3/X_0)^{\frac{1}{3}}$, calculated from a number of experimental values of the intercepts, $-y_0$ and X_0, taken from curves similar to those in Fig. 3, is

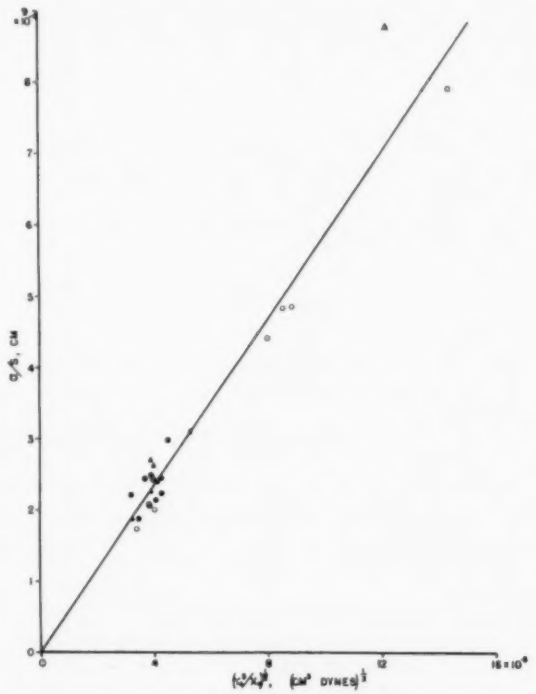

FIG. 4. Variation of ratio of average cross-sectional area to perimeter of fibers with a function of intercepts taken from curves of the type shown in Fig. 3. Points marked with ● represent samples the cross sections of which were obtained from microscopic photographs. The remaining points are for samples which had their cross sections determined from enlarged drawings made with the camera lucida. Points marked with △ are the average results of three or four separate gas flow determinations.

plotted against the measured values of a/s in Fig. 4. In the case of samples marked with Δ the average of three sets of intercepts is given. Although there is some scattering of the points, the line drawn through them gives satisfactory agreement with Eq. (20).

(e) The slope of the line in Fig. 4 is 5.8×10^{-2}, which, according to Eq. (20), should be equal to $(\mu Q_0/0.99kA)^{\frac{1}{3}}$. Since all the factors in this ex-

[7] J. I. Hardy, United States Department of Agriculture, Circular No. 378, November, 1935.

pression except k were measured, the value of k can be found from the experimental slope. From a calibration curve, Q_0 was 9.82 cc/sec. The area, A, of the cross section of the medium was 2.85 cm². At 25°C, the approximate temperature at which the work was done, μ, the viscosity of air, is about 1.78×10^{-4} c.g.s. unit. Using these values, one finds $k=0.18$, which is in fair agreement with the value obtained by other experimenters with data obtained from flow through media made up of sand grains, glass beads, and other small particles.

The hydrodynamical method using air seems to be well adapted to the determination of the surface per unit volume or per unit mass of fibrous materials.

After this work was completed a paper on liquid flow through fibers was published,[8] in which Carman's value of $k=0.20$ is used to find the surface area per cubic centimeter (σ/τ). The results are given in terms of the ratio of calculated value of (σ/τ) to measured value. The weighted mean of this ratio taken from the paper is about 1.07, which would be reduced to about 1.02 if the value of $k=0.18$ were used.

In conclusion, the authors wish to acknowledge their indebtedness to Dr. R. R. Sullivan, who, together with Mr. Robert Newton, Miss Beth Cheney, Miss Marguerite Taylor, Miss Louise McCamy, and Miss Elizabeth Cotter, obtained much of the microscopic data used in this work. Thanks are due also to Dr. W. G. Pollard for his interest in the problem and his helpful suggestions, and to Director C. A. Mooers, of the University of Tennessee Agricultural Experiment Station, who kindly placed at our disposal the necessary funds with which to carry on this work.

[8] E. J. Wiggins, W. B. Campbell and O. Maass, Can. J. Research **17**, 318–324 (1939).

Electronic Generation of Electromagnetic Oscillations

E. U. Condon
Westinghouse Research Laboratories, East Pittsburgh, Pennsylvania
(Received March 2, 1940)

A general formulation of the problem of transfer of power from the electron beam to an oscillating circuit by moving charged particles is given. The method is applied specifically to calculation of the behavior of the klystron oscillator in making approximations analogous to those made by Webster in his treatment of the same problem.

THE general problem of the electronic generation of electromagnetic oscillations is that of the construction of a system of conductors with or without auxiliary constant magnetic fields such that if electrons are emitted from one conductor, called the cathode, they are given energy by a source of steady electromotive force and in the course of their motion to one or more collecting conductors called anodes, they deliver some of this energy to oscillations of the electromagnetic field.

In the following discussion it will be supposed that the density of charge everywhere outside the conductors is small enough that space charge is negligible. Also, that whenever an electron strikes a conductor it sticks to it without emission of secondary electrons, its energy of motion at the moment of impact being dissipated as heat at the anode which it strikes. The method used here is familiar to students of quantum theory[1] but its use in this connection is believed to be new.

Neglecting the effect of the presence of the electrons, the electromagnetic field in the region where the electrons move can be represented as the superposition of the fields associated with normal modes of oscillation. The field is governed by Maxwell's equations

$$\text{div } E=0, \qquad \text{div } H=0,$$

[1] See e.g., W. Heitler, *The Quantum Theory of Radiation* (Oxford, 1936).

$$\text{curl } E=-\frac{1}{c}\frac{\partial H}{\partial t}, \quad \text{curl } H=\frac{1}{c}\frac{\partial E}{\partial t}, \tag{1}$$

where E is in electrostatic units (300 volt/cm) and H in gauss.

These fields can be derived from a vector potential A by the relations

$$H=\text{curl } A, \quad E=-\frac{1}{c}\frac{\partial A}{\partial t}. \tag{2}$$

The equation div $H=0$ is then satisfied automatically, the equation div $E=0$ requires that we impose on A the condition

$$\text{div } A=0.$$

Substituting in the first curl equation

$$-\frac{1}{c}\frac{\partial}{\partial t}\text{curl } A=-\frac{1}{c}\frac{\partial}{\partial t}\text{curl } A$$

and see that it is satisfied identically. The second curl equation gives

$$\text{curl curl } A=-\frac{1}{c^2}\frac{\partial^2 A}{\partial t^2}$$

or

$$\nabla^2 A=\frac{1}{c^2}\frac{\partial^2 A}{\partial t^2}.$$

Neglecting the finiteness of the conductivity of the conductors we must have E normal to the bounding surfaces which implies A normal to boundary surfaces. Hence the conditions on A are

$$\text{div } A=0, \quad \begin{matrix}A \text{ normal at}\\ \text{bounding}\\ \text{surfaces,}\end{matrix} \quad \nabla^2 A=\frac{1}{c^2}\frac{\partial^2 A}{\partial t^2}. \tag{3}$$

These equations determine a set of proper frequencies and normal modes for the field. If ν_λ is a proper frequency, then $A_\lambda(r,t)=A_\lambda(r)e^{2\pi i\nu_\lambda t}$ and the spatial dependence of A is determined by

$$\text{div } A_\lambda=0, \quad \begin{matrix}A_\lambda \text{ normal at}\\ \text{boundaries,}\end{matrix} \quad \nabla^2 A_\lambda+\left(\frac{2\pi\nu_\lambda}{c}\right)^2 A_\lambda=0.$$

The normal fields $A_\lambda(r)$ have the orthogonal property

$$\int A_\lambda(r)\cdot A_\mu(r)d\tau=\delta_{\lambda\mu}=\begin{cases}0 & \lambda\neq\mu\\ 1 & \lambda=\mu\end{cases} \tag{4}$$

if normalized to unit amplitude.[2] Here it is assumed that ν_λ and ν_μ are unequal. For the degenerate case in which ν_λ and ν_μ are equal, it is always possible to choose normal fields that are orthogonal, so it will be supposed in what follows that the normal fields are so chosen.

The general oscillating field determined by the conductors is then a superposition of these normal fields

$$A=\sum_\lambda q_\lambda(t)A_\lambda(r) \tag{5}$$

and the state of the field is completely specified by giving the $q_\lambda(t)$ which will be called the coordinates of the field.

The equation of motion of an electron moving in an electrostatic field described by the static potential φ and the static vector potential A_0 is

$$m\frac{d^2r}{dt^2}=e\left(E+\frac{1}{c}v\times H\right), \tag{6}$$

where the E and H include the field due to the coordinates q_λ and also the field due to the static potentials φ and A_0 and are to be evaluated at the position of the electron. The coupling of the electron's motion to the field coordinates thus comes from the fact that E and H here depend both on the field coordinates and on the electron's coordinates.

The vector potential must satisfy an altered equation of motion when an electron is present. For then we have

$$\text{curl } H=\frac{4\pi\rho v}{c}+\frac{1}{c}\frac{\partial E}{\partial t}, \tag{7}$$

which becomes

$$\text{curl curl } A+\frac{1}{c^2}\frac{\partial^2 A}{\partial t^2}=\frac{4\pi\rho v}{c}.$$

Inserting

$$A=\sum_\lambda q_\lambda A_\lambda(r),$$

we get

$$\sum_\lambda\left[-\nabla^2 A_\lambda q_\lambda+\frac{\ddot{q}_\lambda}{c^2}A_\lambda\right]=\frac{4\pi\rho v}{c}.$$

Multiplying by A_μ and integrating over all space outside conductors, using the equation

[2] Frenkel, *Elektrodynamik*, Vol. 2, p. 320.

$$\nabla^2 A_\lambda = -\left(\frac{2\pi\nu_\lambda}{c}\right)^2 A_\lambda$$

and the normal-orthogonal property (4) of the A_λ, we get

$$\frac{1}{c^2}\ddot{q}_\mu + \left(\frac{2\pi\nu_\mu}{c}\right)^2 q_\mu = \frac{4\pi}{c}\int \rho v \cdot A_\mu d\tau. \qquad (8)$$

In the applications we can neglect the variation of A_μ with position over the small volume of the electron and write

$$\int \rho v \cdot A_\mu d\tau = ev \cdot A_\mu(r),$$

where e is the charge on the electron and $A_\mu(r)$ is to be evaluated at the electron's position. Thus the equation of motion for any field coordinate becomes

$$\ddot{q}_\lambda + (2\pi\nu_\lambda)^2 q_\lambda = 4\pi e c v \cdot A_\lambda(r). \qquad (9)$$

We will now see that the rate of change of the electron's kinetic plus potential energy due to its coupling with the field is just equal to the rate of change of the field's energy. Multiply the electron's equation of motion through by v

$$mv \cdot \frac{dv}{dt} = -ev \cdot \text{grad}\ \varphi - \frac{e}{c}\sum_\lambda \dot{q}_\lambda(t) v \cdot A_\lambda(r)$$

or

$$\frac{d}{dt}(\tfrac{1}{2}mv^2 + e\varphi) = -\frac{e}{c}\sum_\lambda \dot{q}_\lambda(t) v \cdot A_\lambda(r).$$

The terms coming from the magnetic field vanish in the energy equation since $v \cdot (v \times H) = 0$. To complete the proof, we need the expression for the field energy in terms of the field coordinates. It is

$$U = \frac{1}{8\pi}\int (E^2 + H^2) d\tau = \frac{1}{8\pi}\int \frac{1}{c^2}(\dot{q}_\lambda A_\lambda)\cdot(\dot{q}_\mu A_\mu) d\tau + \frac{1}{8\pi}\int (q_\lambda \text{ curl } A_\lambda)\cdot(q_\mu \text{ curl } A_\mu) d\tau.$$

The electric terms reduce to

$$\frac{1}{8\pi c^2}\sum_\lambda \dot{q}_\lambda^2$$

by direct use of the normal orthogonal property of the A's. The magnetic terms can be reduced by using the formula

$$\int (\text{curl } a \cdot \text{curl } b + \text{div } a \text{ div } b + a\nabla^2 b) d\tau = \int [(a \times \text{curl } b)_n + a_n \text{ div } b] d\sigma,$$

where the second integral is over the bounding surfaces. If $a = A_\lambda$, $b = A_\mu$, we have

$$\int\int \left[\text{curl } A_\lambda \cdot \text{curl } A_\mu - \left(\frac{2\pi\nu_\mu}{c}\right)^2 A_\lambda \cdot A_\mu\right] d\tau = 0,$$

since the surface integral vanishes. Hence

$$\int \text{curl } A_\lambda \cdot \text{curl } A_\mu d\tau = \left(\frac{2\pi\nu_\mu}{c}\right)^2 \delta_{\lambda\mu}$$

and the magnetic energy terms reduce to

$$\frac{1}{8\pi}\sum_\lambda \left(\frac{2\pi\nu_\lambda}{c}\right)^2 q_\lambda^2,$$

so the whole field energy becomes

$$U = \sum_\lambda U_\lambda$$

where

$$U_\lambda = \frac{1}{8\pi c^2}[\dot{q}_\lambda^2 + (2\pi\nu_\lambda)^2 q_\lambda^2]. \qquad (10)$$

We can get an equation for dU_λ/dt from the equation of motion of the field coordinate q_λ:

$$\frac{d}{dt}\frac{1}{2}[\dot{q}_\lambda^2 + (2\pi\nu_\lambda)^2 q_\lambda^2] = 4\pi e c \dot{q}_\lambda v \cdot A_\lambda(r).$$

So, dividing by $4\pi c^2$

$$\frac{d}{dt}U_\lambda = \frac{e}{c}\dot{q}_\lambda v \cdot A_\lambda(r) = -ev \cdot E_\lambda(r). \qquad (11)$$

This is exactly the negative of the rate of increase of the electron's kinetic plus potential energy, when summed over all the field coordinates.

In the steady operation of an oscillation generator converting d.c. power into electromagnetic oscillations, we will suppose that electrons are emitted at a steady rate, and that

there is a load applied to the oscillating power such that the value of the amplitude of q_λ remains constant. Our problem is, then, to calculate the mean value of dU_λ/dt, the power flow from electron to field, averaged over a complete cycle of phase of motion of the electron and over a complete family of trajectories. This gives the useful power delivered by the generator. Likewise, if we calculate the energy with which the electron reaches an anode and average this over all phases of the motion, we will find the power wasted as heat at the anodes. Another source of power loss is that in the actual device, other field modes than the one to which the load is applied will be excited and, since they are all dissipative to some extent, this will represent an absorption of energy.

In what follows, we will assume these parasitic fields to be negligible in calculating the electron's trajectory.

As an illustration of the use of the formulation here presented, let us consider the operation of the "klystron"* recently developed by the group at Stanford University.[3] (During a recent visit to Stanford University I learned from Professor Hansen that he has also been using the method presented here for some time past.) Here the electronic motion is entirely one-dimensional. Electrons are emitted at a uniform rate from a cathode-ray gun entering the oscillating field at velocity v_0. In the work done at Stanford, the oscillating field is that of two "rhumbatrons" electromagnetically coupled and of the form shown in Fig. 1. Let us suppose that these or any other electrode structure are provided, which makes the electric force on an electron be entirely in the x direction and equal to

$$E_x = \frac{m}{e} F(x) \sin \omega t, \tag{12}$$

so the equation of motion of the electron is

$$\frac{d^2x}{dt^2} = F(x) \sin \omega t \tag{13}$$

and the initial condition defining the motion $x(t, \delta)$ of a particular electron entering at phase δ is

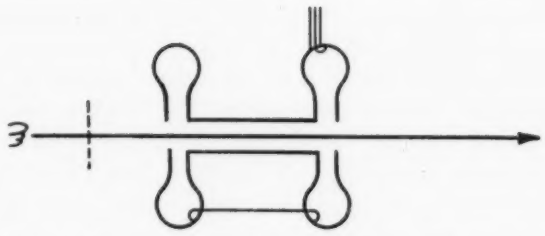

FIG. 1. Klystron recently developed by the group at Stanford University.

$$x\left(\frac{\delta}{\omega}, \delta\right) = 0,$$
$$\left[\frac{dx(t, \delta)}{dt}\right]_{t=\delta/\omega} = v_0. \tag{14}$$

Let it be supposed that $F(x)$ is zero beyond $x=a$ and that the field is weak enough that every electron gets through the apparatus, i.e., that $dx/dt>0$ for all $t>\delta/\omega$ and for all δ. Then the velocity of the electron entering at phase δ after it has gone through the apparatus will be $dx(t, \delta)/dt$ evaluated at a sufficiently large value of t that it is out of the field and so moving with constant velocity. Let us write $u(\delta)$ for this speed

$$u(\delta) = \frac{dx(t, \delta)}{dt} \text{ for large } t. \tag{15}$$

Then the mean energy of motion of the electrons after going through the field is

$$\frac{m}{2} \cdot \frac{1}{2\pi} \int_0^{2\pi} [u(\delta)]^2 d\delta. \tag{16}$$

If this is less than $mv_0^2/2$ it means that the electrons on the average lose energy to the oscillating field and the efficiency of the device as an oscillation generator, neglecting losses in the conductors which are used to produce the field, is

$$\mathcal{E} = 1 - \frac{1}{2\pi} \int_0^{2\pi} \left(\frac{u(\delta)}{v_0}\right)^2 d\delta. \tag{17}$$

If the quantity (16) comes out greater than $\frac{1}{2}mv_0^2$ it means that the average electron has gained energy from the oscillating field. Instead of operating as an oscillation generator, the device then operates as a means of accelerating electrons with a high frequency field.

This formulation of the problem brings out clearly that the descriptive language which has

* Trademark registered by Sperry Gyroscope Company.

[3] R. H. Varian and S. F. Varian, J. App. Phys. **10**, 321 (1939); W. W. Hansen, J. App. Phys. **9**, 654 (1938).

been used about "bunching" the electrons is not an essential part of the operation of such a device. "Bunching" in fact does occur with practical beam currents, but the device would operate as an oscillation generator even if operated at such a low electron beam current that only one electron were actually in the oscillating field at a time.

More specifically, we may illustrate this method of handling the problem of the klystron using the same approximations as those used by Webster[4] in his method.

Suppose the electron path in the first rhumbatron is h_1 and the field there is $E_1 \sin \omega t$, counting E_1 as positive when it is in the sense to accelerate the electron. Let e be the magnitude of the electronic charge. Neglecting the phase change in the oscillation which occurs in the electron's flight through the rhumbatron, the energy of an electron after going through the first rhumbatron is

$$e(V+h_1E_1 \sin \delta),$$

if V is the voltage used to give it its initial energy and δ the phase at which it enters. If d is the distance between the rhumbatrons, then the phase at which it arrives at the other rhumbatron is

$$\delta+\frac{\varphi}{(1+\alpha \sin \delta)^{\frac{1}{2}}} \quad \text{where} \quad \alpha=\frac{h_1E_1}{V} \quad \text{and} \quad \varphi=\frac{\omega d}{v_0}.$$

If the length of path in the second rhumbatron is h_2 and the field there is $E_2 \sin \omega t$, again counted positively in a direction to accelerate the electron, then the energy received by the electron in going through the second rhumbatron is

$$eh_2E_2 \sin\left(\delta+\frac{\varphi}{(1+\alpha \sin \delta)^{\frac{1}{2}}}\right).$$

The energy gained by an electron entering at phase δ is the sum of what it gains in each rhumbatron and the average energy is obtained by averaging over all values of δ. The average of $eh_1E_1 \sin \delta$ is zero, indicating that in this approximation no power is consumed by the action of the first rhumbatron on the electron beam. The whole effect arises from the average action of the second rhumbatron. This calls for calculation of

$$I(\varphi, \alpha)=\frac{1}{2\pi}\int_0^{2\pi} \sin\left(\delta+\frac{\varphi}{(1+\alpha \sin \delta)^{\frac{1}{2}}}\right)d\delta.$$

Now $\alpha<1$ is required to keep the first rhumbatron from throwing back some of the electrons that enter it. We may make an approximate calculation by supposing $\alpha \ll 1$ so that the radical may be approximated by $1-\alpha/2 \sin \delta$ giving

$$I(\varphi, \alpha)=\frac{1}{2\pi}\int_0^{2\pi} \sin\left(\delta+\varphi-\tfrac{1}{2}\alpha\varphi \sin \delta\right)d\delta$$
$$=\sin \varphi \cdot J_1(\tfrac{1}{2}\alpha\varphi),$$

where $J_1(x)$ is the Bessel function of order one usually denoted in this way.

In this approximation, therefore, the mean energy gained by an electron going through the apparatus is

$$eh_2E_2 \sin \varphi \cdot J_1(\tfrac{1}{2}\alpha\varphi).$$

For generation of oscillations, this should come out negative either by making E_2 negative or by making $\sin \varphi$ negative. By choosing $\varphi=\pi/2$, $3\pi/2\cdots$, etc. the $\sin \varphi$ factor can be made unity so that the efficiency of power conversion becomes

$$\mathcal{E}=-\frac{h_2|E_2|}{V}J_1(\tfrac{1}{2}\alpha\varphi).$$

The maximum value of the Bessel function is 0.58, and this value is attained when its argument is equal to 1.84. The factor $h_2|E_2|/V$ can be made quite close to unity but if it is made too large the formula will not be valid because some of the electrons would not go through the second rhumbatron. It also has to be remembered that the formula is not valid except for $\alpha \ll 1$. Some relevant values of the Bessel function are those given in Table I. This indicates that efficiencies

TABLE I.

α	$\varphi=\pi/2$	$\varphi=3\pi/2$
0.1	0.040	0.117
.2	.077	.230
.4	.155	.421
.6	.230	.544

of the order of 50 percent might be attainable, perhaps even higher if the errors introduced by the approximations are in the direction to underestimate the efficiency.

[4] D. L. Webster, J. App. Phys. **10**, 501 (1939).

Letter to the Editor

Backfiring in Mercury Arc Rectifiers

The reviving interest shown in this country recently in the question of rectifier backfiring, and opposing theories as to the prevailing causes of the phenomenon[1-3] make it seem desirable to introduce some evidence from another source[4] into the discussion.

Paper (1) systematically does away with all other proposed backfire causes in favor of the idea that most backfires are caused by bursts of gas from the electrodes (anodes) bearing negative voltage. Paper (2) supports this idea, and attempts to justify the assumption by calculation of the quantity of gas apparently necessary to cause a backfire. Arguments are brought forth in paper (3), that certain experimental results can best be explained by supposing the most active backfire cause to be the presence on the anode of tiny insulating patches, which are charged by incoming positive ions.

In spite of the opinion of authors[2] that their experimental results "seem conclusive" in proving gas emission the major backfire instigator in their tests, there still seems room for argument. It must be emphasized, that the experimental data upon which the contentions supporting the gas-burst theory are based, consist in essence of these facts: The backfire susceptibility of an electrode becomes less as its time under ion bombardment increases; and, backfire susceptibility rises when an electrode is left in a high vacuum for a period of 15 hours or more, without bombardment. These effects have been observed elsewhere[3,4] without the necessity of postulating gas bursts as a breakdown source. Kingdon and Lawton[3] assume that their insulated patches are destroyed by backfires, and, presumably, reestablish themselves—by any of a number of mechanisms which might operate most effectively when the electrode is cold and unbombarded.

The theoretical evidence for gas bursts in paper (2) consists primarily of a demonstration that a very small quantity of gas is necessary for the maintenance of an arc cathode spot; the mechanism proposed for initiating the spot, however (emission of electrons from the cathode by ion impact, and ionization of the gas in turn by collisions of these electrons) is nothing more than the familiar Thomson breakdown theory, which follows the Paschen curve. From the Paschen curve for mercury vapor,[6] however, the quantity of gas quoted in paper (2) will be far from giving breakdown at even 30 kv, and then the resulting discharge would be merely a glow discharge. The idea that an arc would form in a time less than 10^{-7} sec.[2] after these conditions are satisfied, contradicts experimental evidence. A stable self-maintaining glow has been held inmercury vapor at voltages as high as 60 kv.[4]

A possible source of insulating films for the patch theory can be found in the presence of minute quantities of organic vapor in the discharge space. Even the amount of such vapor coming from a greased stopcock through a liquid-air trap, has been observed to give films with a puncture strength of 4 to 14 volts.[5] Such films have been found to be formed by the vapors from rectifier seal rubber at normal operating temperatures,[4] and to be destroyed only by such intensive ion bombardment as to remove a layer of the anode material.

JOHN E. WHITE

Department of Electrical Engineering,
West Virginia University,
Morgantown, West Virginia,
May 2, 1940.

[1] Maxfield and Fredenhall, J. App. Phys. **9**, 600 (1938).
[2] Maxfield, Hegbar and Eaton, A.I.E.E. Tech. Paper 39-152, Aug. 1939.
[3] Kingdon and Lawton, Gen. Elec. Rev. **42**, 474 (1939).
[4] White and Rigrod, unpublished work at V. E. I., Moscow, U. S. S. R.
[5] Stewart, Phys. Rev. **45**, 488 (1934).
[6] Klarfeld and Gusjeva, Tech. Phys. U. S. S. R. [5], **6**, 425 (1939).

Innovations in Instruments

Instrument Bulletins Issued

Three new bulletins have been issued recently by the Shallcross Manufacturing Company, 10 Jackson Avenue, Collingdale, Pennsylvania. These bulletins describe products of the Company as follows: Bulletin No. 146–1, resistance standards, decade boxes, and special parts for electrical measurement; No. 146–2, bridges for measuring d.c. resistance, high and low resistance, conductivity and other special problems; No. 146–3, test sets and special apparatus used in electrical measuring, particularly in industrial work and electrical laboratories.

Extruded Tubing in Plastics

Extruded tubing in plastic materials, particularly fitted for use in automotive, aviation, marine, radio, and other fields in which flexible tubing plays an important part, has been developed recently and is manufactured by the Irvington Varnish and Insulator Company, 24 Argyle Terrace, Irvington, New Jersey. The tensile strength of this tubing in size No. 8 is reported 2150 pounds per square inch, and the material is fire resistant when tested in accordance with A.S.T.M. specification D350–39T. It has been found to remain intact when heated for 48 hours at 220°F in Wemco or other transformer oil. The tubing's dielectric strength when it is dry is 750 volts per mil up to 0.022 inch, and, when it is wet, 350 volts per mil up to 0.022 inch.

Tubes for Audio Work

"Sound X/tra," a special line of tubes for use in sound amplifiers, are being manufactured by the National Union Radio Corporation, Newark, New Jersey. The Corporation lists the following modifications in construction and details of engineering which have been incorporated into these tubes: emission limits are high to obtain uniformity, long life and adequate power handling capacity; gas and grid current are held to low limits to give minimum distortion, uniformity and stability; each tube is tested for hum and microphonics and, where necessary, changes have been made in construction such as the use of special micas, extra rugged supports, double helix heaters and special insulation for minimum hum.

Electric Stopwatch

An electric stopwatch with a direct-reading counter on which time intervals up to 2 hours 46 minutes can be read to $\frac{1}{10}$ of a second, is announced by the Precision Scientific Company, 1751 North Springfield Avenue, Chicago, Illinois. Like an electric clock, this stopwatch is controlled by the power house master clock which governs the cycle constancy of alternating current. The counter can be reset to zero from any reading. The electric stopwatch cannot be carried in the pocket, but it can be used wherever there is a 110-volt a.c. line.

Variable-Frequency Stimulator

For stimulation of the cortex in neuro-surgery or for use in research where it is desirable to supply a stimulating current accurately controlled in both frequency and amplitude, a variable-frequency stimulator has been developed and is now made available by the Allen B. DuMont Laboratories, Inc., of Passaic, New Jersey. The instrument is said to be characterized by the following features: continuously-variable frequency range from 1 stimulus every 2 seconds to 1500 stimuli per second; independent stimulus-amplitude and stimulus-frequency control; full protection for the patient in event of accidental contact between stimulator and high voltages; completely self-contained power supply for operation from 115-volt (or 230-volt), 40-60-cycle a.c. power line; circuit design to minimize frequency drift; convenient electrode sterilization, and simplified control.

Low Thermal Expansion Glassware

A new Pyrex glassware with a linear coefficient of expansion of 0.0000008 per °C, as compared with 0.0000032 per °C for the regular Pyrex brand chemical glass, has been recently fabricated by the Corning Glass Works, Corning New York. The new Pyrex Vycor glassware is made from 96 percent silica glass No. 790, and is said to have exceptional chemical stability and a high softening point, rendering it important for laboratory work.

Pyrex Vycor glass is produced from a glass of apparently normal characteristics from which practically all the constituents other than silica are removed by leaching in hot chemical solutions. The silica residue, after being washed, dried slowly, and finally fired at carefully controlled high temperatures, becomes a transparent vitreous glass of simple chemical composition.

Photoelectric Hole Detector

Spotting holes as small as one-hundredth of an inch in a steel sheet moving as fast as 1000 feet per minute, a Westinghouse photoelectric hole detector contributes to quality production in a steel mill shearing line. The steel sheets, trimmed to uniform width, move between guides and hold-down blocks. Two light sources are mounted in the enclosing cabinet overhead, and the photo-tube housing is mounted below the moving stream of metal sheet on a separate foundation to avoid vibration. If there is a hole in the steel strip, light passing through the hole actuates the photo-tube and a marking device that scores the strip alongside the hole. The strip is then cut into shorter lengths and these pass to a classifier which has a gate timed with the hole detector to open and discharge all defective sheets to a pit below. This photoelectric hole detector is announced by the Westinghouse Electric and Manufacturing Company of East Pittsburgh, Pennsylvania.

"WRATTEN LIGHT FILTERS"

NEW, REVISED EDITION

THE SIXTEENTH EDITION of this well-known book, just off the press, contains spectrophotometric and other data concerning the more than one hundred filters that now comprise the Wratten series.

Wratten Light Filters are universally employed in widely separated fields of scientific research. They are made according to rigid standards, for use in photography, photomicrography, spectroscopy, photometry, and astronomy.

The Sixteenth Edition of the book, *Wratten Light Filters*, is available at dealers in photographic supplies; the price is 50 cents. A booklet containing prices of filters, as well as other information, accompanies each volume and will also be furnished free upon request.

Be sure to visit the Kodak Building at the New York World's Fair

EASTMAN KODAK COMPANY

Research Laboratories **ROCHESTER, N. Y.**

EPPLEY STANDARD CELLS

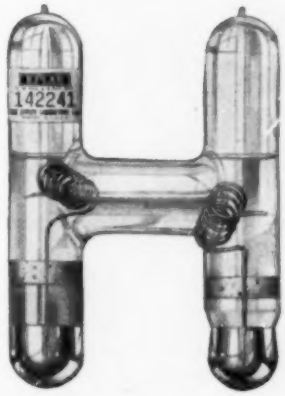

For more than 20 years the leading American manufacturers of industrial temperature control apparatus have used Eppley Standard Cells in their recorders, pyrometers and other instruments utilizing the potentiometric system of measurement.

We feel that this almost universal adoption of the Eppley Standard Cell is the result of high standards of quality and reliability, achieved and maintained through years of painstaking research, which still continues in an endeavor to render American industry a service of ever-increasing value.

When you purchase an instrument containing an Eppley Standard Cell you are obtaining maximum standard cell efficiency and reliability. The best testimonial to this fact is 20 years acceptance by American manufacturers.

EPLAB

THE EPPLEY LABORATORY, INC.

SCIENTIFIC INSTRUMENTS

NEWPORT, R.I.

U. S. A.

—MICO—
ENGRAVER

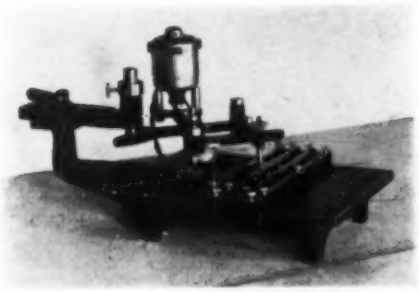

For lettering panels of steel, aluminum, brass, or bakelite, or for marking finished apparatus

Attachments adapt it to small or large work on flat or curved surfaces.

Excellent engraving can be produced by an inexperienced operator.

Widely used for production as well as occasional engraving.

Samples of work and catalogues on request

Price with Type—$113.50

MICO INSTRUMENT CO.

12 Arrow Street Cambridge, Mass.

FIRST SURFACE MIRRORS

by High Vacuum Deposition

EVAPCO first surface are excellent for projection mirrors and other uses that require an opaque mirror of high reflectivity that does not tarnish or give double image.

DUOLUX semi-transparent for one exposure three color cameras, range finders, or wherever an accurate beam-splitter is needed. Made to order for all practical transmission —reflection ratios.

EVAPORATED METAL FILMS CORP.

ITHACA, N. Y.

MEASURE R. P. M.

without even seeing the rotating element!

THE "FRAHM" TACHOMETER operates merely by being held against or mounted on the machine under test and imposes no load. There are no belts, gears or electrical connections—simply a set of accurately tuned steel reeds which operate by resonance. Various ranges from 900 up to 30,000 r.p.m. Unique also for measuring vibrations per minute.

Write for descriptive Bulletin 1590-R.

JAMES G. BIDDLE CO.

ELECTRICAL AND SCIENTIFIC INSTRUMENTS

1211-13 ARCH STREET. PHILADELPHIA, PA.

FOR MODERN, COMPLEX RECEIVERS!

New RCA Test Oscillator #167 $34.50

Let this new RCA Test Oscillator make your tough servicing jobs simpler! It has the range you want—6 bands: 100 to 30,000 KC. in fundamentals . . . with harmonics of 6th band for U-H-F applications. AC operated. High output, for single-stage alignment work, or for sets misaligned altogether—plus a new, precision, easy-reading dial-scale, trim appearance and RCA engineering—make it a real buy at only $34.50. Ask your RCA Distributor to show you all its features.

Over 335 million RCA Radio Tubes have been purchased by radio users . . . in tubes, as in parts and test equipment, it pays to go RCA ALL THE WAY.

RCA Test Equipment

RCA Manufacturing Company, Inc., Camden, New Jersey

A Service of the Radio Corporation of America

• AN IMPORTANT TWO-VOLUME TEXT •

Introduction to Electricity and Optics

By NATHANIEL H. FRANK, Massachusetts Institute of Technology. 395 pages, 6 x 9. $3.50

The publication of this long-awaited book completes the author's two-volume text in physics for the introductory technical course, the first half of which has been so successfully covered by *Introduction to Mechanics and Heat*. *Introduction to Electricity and Optics* gives a logical exposition of the fundamental principles, emphasizing field theory and the elementary application of these principles to circuits and to the electrical, magnetic, and optical properties of matter. The treatment is quantitative throughout and modern atomic ideas are stressed along with the more classical modes of presentation.

Introduction to Mechanics and Heat

By NATHANIEL H. FRANK. Second edition. 384 pages, 6 x 9. $3.00

Send for copies on approval

McGRAW-HILL BOOK COMPANY, Inc.

330 West 42nd Street New York, N. Y.

LIPPICH TRIPLE FIELD POLARIMETER

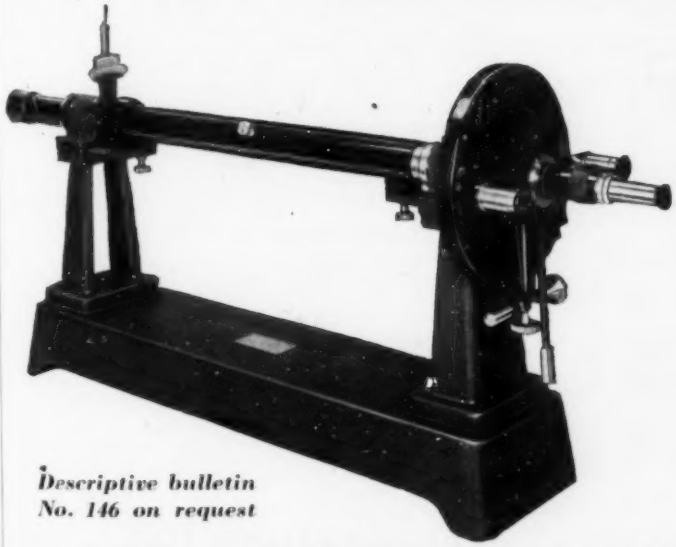

Descriptive bulletin No. 146 on request

The *GAERTNER* polarimeter is designed to permit repeated readings to 0.01 degree. This **accuracy** is assured by the amply large precision circle and the high grade quality of the optical parts. Tubes up to 400 mm in length can be accommodated.

The instrument is designed for greatest permanence and the rugged construction gives long and trustworthy service.

THE GAERTNER SCIENTIFIC CORPORATION

1212 Wrightwood Ave. Chicago, Illinois

IMPROVED "SPOTLIGHT" GALVANOMETERS

Rubicon MULTIPLE REFLECTION galvanometers have recently been improved through a redesign of the optical system. The definition of the line-image is now so sharp that readings can be estimated to .1 of a millimeter division.

These sturdy, self-contained galvanometers are available with sensitivities as high as .0006 microampere per millimeter. The scales, which are 100 mm. long, are remarkably proportional. Send for Bulletin 320.

RUBICON COMPANY

ELECTRICAL INSTRUMENT MAKERS

29 North Sixth Street Philadelphia, Pa.

STABILIZED A-C VOLTAGE

INPUT 95-130 volts
Instantaneous action
A magnetic unit

OUTPUT
115 volts ±½%
Stabilizes at any load within rating

No moving parts. Nothing to wear out.

RAYTHEON Voltage Stabilizer

APPLICATIONS **Broadly it insures stable operation of all precision apparatus obtaining its power from an A.C. source, for example:—**

- **Insures constant brilliancy from all types of lamps.**
- **Improves the operation of X-ray equipment.**
- **Stabilizes all electronic apparatus.**

Write for Bulletin 48-71JP.

RAYTHEON MFG. CO. WALTHAM, MASS.

INDEX TO ADVERTISERS

The following firms have shown their interest in the advancement of physics through their support of the journals and other services of the American Institute of Physics and its Founder Societies. This should entitle them to consideration by physicists whenever possible.

Name — *Page*

BAUSCH & LOMB OPTICAL COMPANY ii
Makers of Microscopes, Microtomes, Colorimeters, Refractometers, Spectrometers, Balopticons, Photomicrographic and Microprojection Apparatus and related instruments. Also makers of Orthogon Eyeglass Lenses for Better Vision.

JAMES G. BIDDLE COMPANY iv
"Jagabi" Rheostats; Adam Hilger and Kipp & Zonen Optical Instruments; "Pointolite" Lamps; Electrical Testing and Speed-measuring Instruments.

CENTRAL SCIENTIFIC COMPANY .....Cover 4
Manufacturers of Cenco Physical Apparatus and Instruments to meet all requirements of University, College and High School Physics Laboratories. Specializing in high vacuum pumps and development of instruments and apparatus for various sciences.

EASTMAN KODAK COMPANY iii
Purified Organic Chemicals for research purposes; Plates for Photography, Photomicrography, Spectroscopy, Photometry, Astronomy; Wratten Light Filters; Cameras and Films.

THE EPPLEY LABORATORY, INC. iii
Standard Cells, thermopiles, pyrheliometers and temperature bridges.

EVAPORATED METAL FILMS CORPORATION iv
First surface and semi-transparent mirrors by high vacuum deposition.

GAERTNER SCIENTIFIC CORPORATION v
Spectroscopes, Spectrometers, Spectrographs, Spectrophotometers, Heliostats, Measuring Microscopes, Comparators, Cathetometers, Reading Telescopes, Interferometers, Chronographs, Dividing Machines, etc.

GENERAL RADIO COMPANY .....Cover 3
Manufacturers of electronic measuring instruments; vacuum-tube voltmeters, amplifiers and oscillators; wave analyzers, noise meters and analyzers, stroboscopes; laboratory standards of capacitance, inductance and frequency; impedance bridges, decade resistors and condensers; air condensers and variable inductors; rheostats, Variacs, transformers; other laboratory accessories.

LEEDS & NORTHRUP COMPANY i
Manufacturers of Galvanometers, Resistors, Bridges, Condensers, Inductances, Potentiometers, Testing Sets; Temperature Measuring, Recording and Controlling Apparatus; Instruments for Measuring and Controlling Conductivity of Electrolytes and Hydrogen Ion Concentrations.

MCGRAW-HILL BOOK COMPANY, INC. v

MICO INSTRUMENT COMPANY iv
Manufacturers of precision mechanical and optical devices for general scientific and industrial uses.

RAYTHEON MFG. COMPANY vi
Voltage stabilizers and regulators. Electrical measurement and control instruments.

RCA MANUFACTURING COMPANY, INC. iv
RCA Oscillators and Oscillographs, RCA Test Equipment, RCA Ultra-Sensitive DC Meter.

RUBICON COMPANY vi
Galvanometers, electrometers, potentiometers, Wheatstone and Kelvin bridges, resistance boxes, hydrogen ion and conductivity apparatus.

SITUATIONS OPEN

Engineer: Experienced in the manufacture of glow discharge devices using hot cathodes. Excellent opportunity with growing concern in Chicago. State education and experience in detail. All correspondence strictly confidential. Address Box G3–13. Rm. 1502, 175 Fifth Ave., New York, N. Y.

PRECISION RESISTANCE BOXES

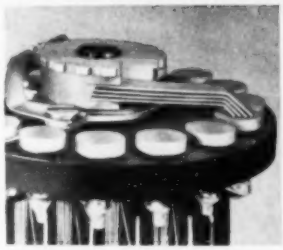

Quadruple-leaf, phosphor-bronze switches with wiping contact. Contact surfaces ground flat. Contact resistance only 0.002 ohm. Cam-type positive detent mechanism. Entire unit shielded behind panel

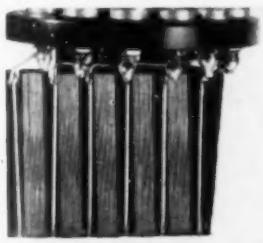

Aryton-Perry windings of the 1-, 10-, and 100-ohm decades on bakelite cards

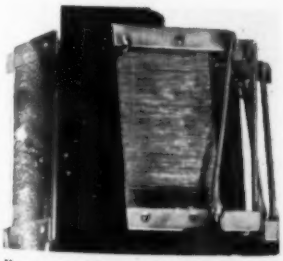

Unifilar windings of the 1,000- and 10,000-ohm decades on mica cards

- The General Radio Type 602 Decade-Resistance Boxes are universally accepted as the adjustable standards of resistance in laboratories where a wide range of resistance values is required.

FEATURES

- PERMANENT CALIBRATION
- THOROUGH AGING
- ACCURATELY ADJUSTED RESISTANCE VALUES
- LOW TEMPERATURE COEFFICIENT
- LOW INDUCTANCE AND CAPACITANCE WINDINGS
- NO APPRECIABLE FREQUENCY ERROR BELOW 50 KC
- LOW AND CONSTANT CONTACT RESISTANCE
- PROTECTED WINDINGS AND SWITCHES
- POSITIVE DETENT MECHANISMS
- SHIELDED CABINETS—NO BODY CAPACITANCE
- CURRENT-CARRYING CAPACITY ENGRAVED ON EACH DECADE
- NINE SIZES BETWEEN 0.1 TO 111 OHMS AND 1 TO 111,110 OHMS
- MODERATELY PRICED BETWEEN $25 AND $70

Write for Bulletin 608 for Complete Information

GENERAL RADIO COMPANY

30 STATE STREET . . . . . CAMBRIDGE, MASSACHUSETTS

BRANCHES: New York and Los Angeles

Simple—Practical

PHOTOELECTRIC DEMONSTRATION UNIT

With Infrared Control Lamp

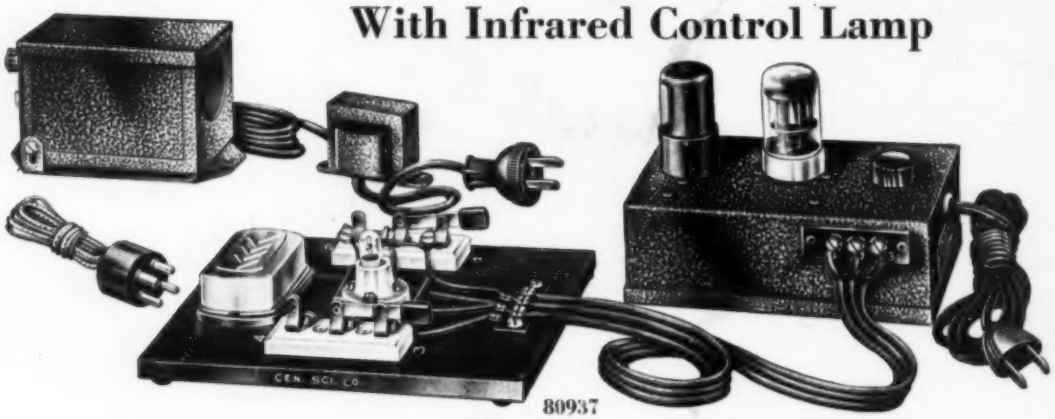

80937

FOR demonstrating photocell principles and photoelectric equipment used in such practical applications as open or closed circuit burglar alarms, fire alarms, illumination control, liquid level control, turbidity control, smoke indication, etc. Through the use of additional equipment, such as magnetic counters, power relays, etc., the demonstrations may be extended to an unlimited number. The set is so simple that an extensive knowledge of electronics is not required for performing the demonstrations.

The set consists of an amplifier-relay control unit, a demonstration panel, a light source with invisible infrared beam filter, and instructions for performing a number of demonstrations. An emissive type photocell of high sensitivity and long life and a type 7E6 amplifying tube with loctal base are provided. The base plate of control unit case is detachable to permit examination of the transformer, relay, condenser, resistors, photocell and amplifier sockets, and potentiometer. An adapter plug with lead wires is furnished for use in place of the photocell on the amplifier-relay control unit for demonstrations of other means of electrical control than that of the photocell. Two single-pole, double-throw knife switches, a buzzer, and a miniature screw base lamp socket with 1½ candlepower lamp are mounted on the demonstration panel. By proper manipulation of the switches, either audible or visual signals can be given in either open or closed circuit demonstrations. The light source will control the amplifier-relay control unit from a distance of approximately 20 feet.

80937 PHOTOELECTRIC DEMONSTRATION SET, Cenco, complete with amplifier-relay control unit, demonstration panel, and infrared light source, for operation from 115 volts, 60 cycles A.C. only, but *without* magnetic counter, etc.. *Each* $17.50

Ask for Circular 1103

CENTRAL SCIENTIFIC COMPANY

SCIENTIFIC INSTRUMENTS & LABORATORY APPARATUS

CHICAGO
1700 Irving Park Blvd.,
Lakeview Station

TRADE MARK CENCO REG. U.S. PAT. OFF.

BOSTON
79 Amherst St.,
Cambridge A Station

LANCASTER PRESS, INC., LANCASTER, PA.